AZAMACROCYCLIC COBALT CATALYSTS.

By

Simon J. Grant.

Submitted for the degree of Doctor of Philosophy

Department of Chemistry

University of Warwick

September 1991.

TO FRANCINE

Summary.

Ten azamacrocyclic ligands were synthesised and characterised. The coordination chemistry of these ligands was evaluated by the study of their Ni(II), Cu(II) and Zn(II) complexes in the development of azamacrocyclic cobalt catalysts.

Co(II) complexes of ligands L^3 and L^4 were evaluated as potential auto-oxidation catalysts for aqueous gloss paint systems. These compounds act as catalysts, producing through dry paint films in a shorter time than commercially available catalysts. This surprising result could indicate the presence of a different drying mechanism for these complexes when compared to the commercial catalysts.

Ligands L^5 and L^6 were designed to activate dioxygen when coordinated to Co(II). The X-ray crystal structure of $\{Zn(L^5)\}(BF_4)_2$ and n.O.e. experiments on $\{Zn(L^6)\}(BF_4)_2$ prove that the correct theoretical geometry is adopted by the ligands on coordination to metals. The Co(II) complexes of ligands L^5 and L^6 were not isolated as a result of their high reactivity towards dioxygen. The products obtained were the μ-peroxo-bridged dimer species - a result of a bimolecular reaction. The Co(II) compounds were considered too reactive to be used as auto-oxidation catalysts.

Azamacrocyclic organocobalt(III) complexes have been shown to act as photopolymerisation catalysts in the polymerisation of alkenes. In water a free radical mechanism occurs. In t.h.f. a metal centred polymerisation is proposed. Diode array gel permeation chromatography of polymeric solutions shows the presence of dimeric and trimeric species which could react to form high molecular weight species.

A novel hydridocobalt(III) complex of L^8 was prepared by reaction of hydrogen with $\{Co(L^8)\}^{2+}$. The presence of the Co-H bond was established by chemical means. A similar reaction was attempted for $\{Co(L^7)\}(BF_4)_2$ but the compound was unstable in solution, reductively eliminating H_2.

Acknowledgements.
I would like to express my thanks to:

Dr P. Moore for his enthusiasm, advice and good humour throughout.

Dr. P. Taylor and Dr. J. Mathews for helpful discussions .

My "fellow macrocyclists", Simon Rawle, Hadi Omar, Andi Wynn, Andy Benniston, Adam Clarke and Pauli Kofod for many helpful discussions (on cricket!) and numerous bad jokes.

Dr. N.W. Alcock and Dr. W. Errington for crystal structure determinations.

Mr. I. Katyal for running the mass spectra, and Dr. O. W. Howarth, Dr.J. Lall and Mr. J. Hastings for running the NMR spectra

Dr. D.W. Hutchinson and Dr. A.F. Hill for the kind use of computing facilities.

Jane Hanrahan for her invaluable assistance in the production of this thesis.

S.E.R.C. and I.C.I. plc (Paints) for their generous financial support.

My family and friends for their support over the years in ways too many to mention.

Finally, a special "thank you" to my wife Francine. Thanks for everything.

Declaration.

The work described in this thesis is the original of the author, except when acknowledgement has been made to results and ideas previously published. The work was carried out at the Department of Chemistry, University of Warwick, between October 1st, 1988 and September 27th, 1991 and has not been submitted for a degree at any institution.

I would like to make it known that the azamacrocyclic organocobalt(III) compound used in studies I undertook was prepared by Dr. H.A.A. Omar.

Publications.

A part of the work reported in this thesis has been accepted for publication in the scientific literature with the following reference:-

Alcock, N. W., Benniston, A. C., Grant, S. J., Moore, P. and Omar, H. A. A., *J. Chem. Soc., Chem. Commun.*, in press.

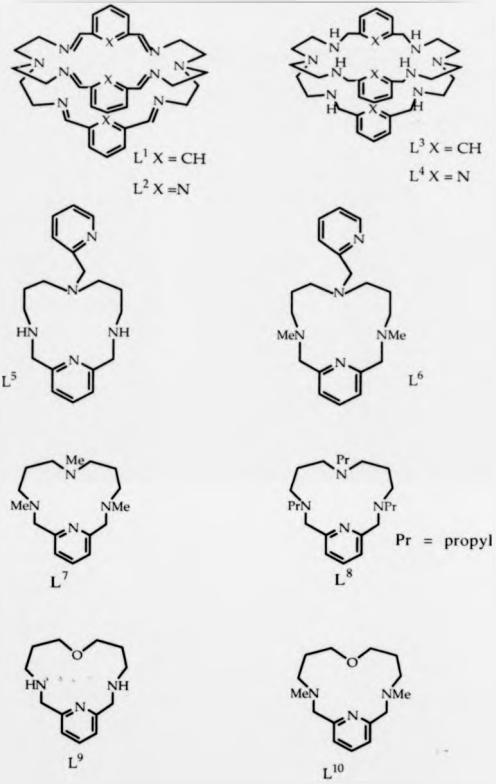

Ligands described in this thesis.

Abbreviations.

n.m.r.	Nuclear magnetic resonance spectroscopy.
ppm	Parts per million.
TMS	Tetramethylsilane.
m.p.	Melting point.
b.p.	Boiling point.
min.	Minutes.
DMF	Dimethylformamide.
dmso	Dimethylsulphoxide.
thf	Tetrahydrofuran
R	Alkyl.
Me	Methyl.
Et	Ethyl.
en	Ethylenediamine

INTRODUCTION.

MACROCYCLIC CHEMISTRY.

1.Introduction.

Macrocycles are polydentate ligands with donor atoms (often N, O, S, or P) incorporated in or connected to a cyclic backbone. The ligands consist of a minimum of three donor atoms within a ring of at least nine atoms.

Naturally occurring macrocyclic ligand complexes are essential to the function of several biological systems e.g. photosynthesis and dioxygen transport in respiratory systems.

The number of synthetic macrocycles has increased rapidly since the late 1960's. This has been the result of research directed towards the preparation of model compounds for naturally occurring macrocycles. This work has led to a great expansion of the field, and research now impinges on the areas of metal ion catalysis, metal ion discrimination and organic synthesis as well as numerous industrial applications.

The thesis will describe work carried out in the development of azamacrocyclic cobalt catalysts. This involved the study of macrocyclic complexes of a number of first row transition metals, and relating the properties of these compounds to those of the desired catalysts. Macrocyclic ligands have properties which make them attractive for the preparation of new catalysts. The introduction will describe general methods for the synthesis of azamacrocycles, properties of the macrocycles and discuss some of the rich chemistry of macrocyclic ligand complexes.

1.1. Synthesis of Azamacrocycles.

There exist numerous procedures for the preparation of azamacrocyclic ligands. These can be divided into two broad categories: (a) direct organic synthetic methods and (b) template methods. Direct methods utilise conventional organic reactions to achieve cyclisation. In

template syntheses, metal ions act as "templates" for the cyclisation reactions. The overall strategy of both methods is to maximise the yields of the desired cyclic products, and reduce the polymerisation reactions which are commonplace during these preparations.

1.1.1. Direct Methods

1.1.1.1. High Dilution

In this procedure equimolar concentrations of the two reactants which incorporate the fragments of the desired macrocycle are mixed in a large exess of solvent. This enhances the likelihood of a 1+1 reaction and reduces the tendency for competing polymerization. An example of a macrocycle which can be prepared by this technique is shown below (1.1).

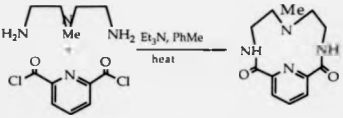

(1.1)

Here, a linear diamine and a diacid chloride are condensed in toluene. This procedure is facilitated by using syringe pumps which dispense equal quantities of reactant into the reaction medium at a slow rate, and hence at any time the concentration of reactants is extremely small. This method gives moderate to small yields. An improvement to this procedure was developed by Tabushi[1,2]. A linear diamine is condensed with dimethyl esters of α,ω–dicarboxylic acids to yield the cyclic amide (1.2). The cyclic amides of equations 1.1 and 1.2 can be reduced to give the amine using borane-tetrahydrofuran.

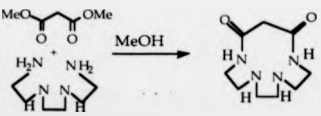

(1.2)

1.1.1.2. The Richman and Atkins procedure.

Richman and Atkins[3] reported a method which can be used in the preparation of saturated polyazamacrocycles. Deprotonated tosylated amines can be ring closed in dimethylformamide at 100°C without the need for high dilution. The bulky tosyl groups enhance cyclisation by reducing the number of conformational degrees of freedom of the reactants and intermediates. The tosyl groups also increase the acidity of the N-H groups towards the formation of the dinucleophile (A) (1.3). Hydrolysis of the tosylate using concentrated sulphuric acid or hydrobromic acid/acetic acid/phenol mixture yields the saturated polyaza macrocycle.

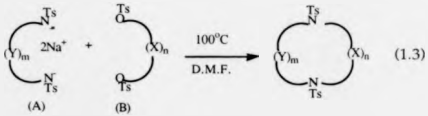

X, Y = O, NTs. m = n = 1 - 3.
Ts = toluene - p - sulphonate.

1.1.2. Metal ion template syntheses.

Metal ions can be used *in situ* in the preparation of polyaza macrocycles. The role of the metal ion in this type of synthesis has been described by Thompson and Busch[4]. Firstly the metal ion can act by shifting the equilibrium of the reaction mixture by complexation with the macrocycle as it forms (the "thermodynamic template" effect). The metal ion can also control the steric course of a sequence of stepwise reactions by bringing the reactants into a favourable postion to complete cyclisation- the "kinetic template effect".The first synthetic macrocycle obtained by a template reaction was the preparation of an Fe(II) complex of a phthalocyanin. This method has now been extended to produce a range of phthalocyanin complexes.[5] Curtis[6] reported a novel template reaction,

a result of the reaction between $[Ni(1,2\text{-diaminoethane})_3]^{2+}$ and dry acetone. Analysis[7] proved that the product was a mixture of two isomeric compounds shown in (1.4).

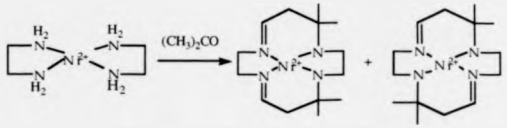

(1.4)

There exists a large number of template reactions in the literature which can be subdivided into two groups (a) non-Schiff's-base and (b) Schiff's base template reactions.

1.1.2.1. Non Schiff's-base template reactions.

Ring closing reactions can take place at:

(a) atoms which are not donor atoms.

This was demonstrated by the reaction of the Ni(II) complex of the psuedo macrocycle formed by dimethylglyoxime with BF_3[8] in which a BF_2 moiety has replaced the proton of the bridging oxime (1.5)

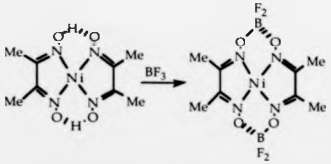

(1.5)

(b) atoms which are donor atoms.

Cyclisation can occur between functional groups which are in a *cis*-conformation when coordinated to a metal. Ansell and co-workers[9] have

used this in the synthesis of a novel phosphorous containing macrocycle (1.6).

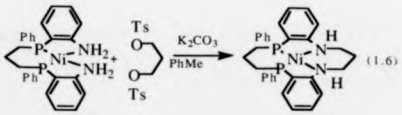

1.1.2.2. Schiff's-base template reactions.

The condensation reaction between amines and aldehydes or ketones has played a major role in metal ion template syntheses. The Schiff's-base condensation produces an imine link which can be readily reduced to give a more stable product. Formation of the imine bond is shown below (1.7).

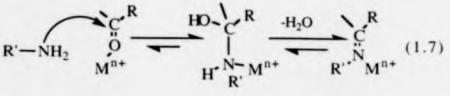

The range of cyclidene ligands developed by Busch and Cairns[10] has utilised this method (1.8).

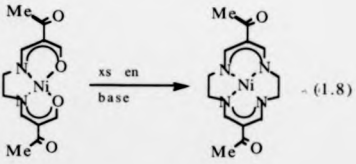

Nelson[11] *et al* have prepared a range of tetra and pentaaza Schiff's-base macrocycles from 2,6-diacetylpyridine. It has been postulated that the

presence of a good donor atom (the pyridine nitrogen) is important as this promotes the coordination of the carbonyls to the template ion. This effect activates the carbonyls to nucleophilic attack.

The size of the template ion has a effect on the macrocycle produced. Condensation of 2,6-diacetylpyridine with bis-(3-aminopropyl)amine in the presence of small metal ions (Ni(II), Cu(II)) give the 14 membered macrocycle. When Ag(I) is used a 28 membered macrocycle is formed (scheme 1.1).

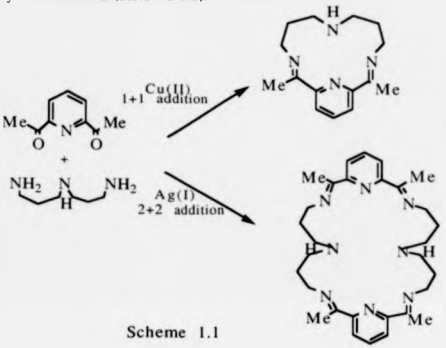

Scheme 1.1

1.2. The properties of macrocyclic ligand complexes.

Macrocyclic ligand complexes have a range of different applications from ion selective electrodes[12] to the oxidation of substrates catalysed by Fe(II)[13]. This versatility is a result of the properties of macrocycles which will be discussed in the following sections.

1.2.1. The Macrocyclic Effect.

The "macrocyclic effect" is the term used to describe the enhanced stability of macrocyclic complexes in comparison to their acyclic analogues. This effect was first identified by Cabbiness and Margerum[14,15] who

determined the stability of the Ni(II) complexes of 1,4,8,11-teraazacyclotetradecane(cyclam) and its acyclic analogue 2,3,2-tet.(fig.1.1).

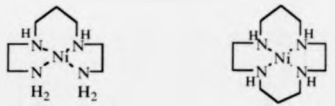

log K =15.8 log K = 22.2

Figure 1.1 Stability constants of Ni(II) complexes of 2,3,2-tet and cyclam.

The macrocyclic effect is defined as the ratio of stability constants for the macrocyclic complex and its closest linear analogue.

$$\text{Macrocyclic Effect} = \frac{K_M n+ \text{ (mac)}}{K_M n+ \text{ (linear)}}$$

The origins of this effect has been a cause of confusion and conflicting results. Early studies of tetraazamacrocycles indicated the extra stability was a result of favourable entropy factors[16]. This argument was based on the observation that a linear ligand will lose configurational entropy on coordination to a metal ion, whilst a macrocycle will lose little as it already exists as a constrained cyclic system. On the other hand Hinz and Margerum[17] stated that the macrocyclic effect was wholly a result of enthalpic factors.

The state of uncertainty continues when solvation effects are considered. Assuming that similar desolvation of the metal ion occurs on complexation to either a macrocycle or a linear chelator, then desolvation of the ligand should have a contribution to the macrocyclic effect. Macrocycles should be solvated to a lesser degree in comparison to linear ligands, as they can be considered to be more compact. Hence, the

macrocyclic ligand desolvation enthalpy should be less than that of a linear ligand, thus making a contribution to the thermodynamic stability of the macrocyclic system.

The variation in the enthalpic term reflects a number of influences including changes in ligand conformation, the nature and strength of the metal to ligand bonds and the match of the macrocyclic hole size for the metal ion. This range of inter-related factors must be considered during the determination of the enthalpic contribution to the macrocyclic effect.

The entropic contribution is also similarly difficult to interpret. Contributions from changes in the total number of species present and the translational entropy must be considered as well as the solvation effects mentioned earlier.

Detailed analysis of a particular macrocyclic effect can only be considered in cases where the macrocycle and linear ligand adopt similar coordination geometries. The conclusion of these studies is that the macrocyclic effect cannot be defined simply, and different systems will respond in different ways to stabilising factors

1.2.2. Metal ion selectivity.

One of the most important ideas in macrocyclic chemistry is that of size-match selectivity i.e. the metal ion will form the most stable complex with the macrocycle whose cavity is the closest in size[18,19]. This argument was illustrated by consideration of the stability of the complexes of 18-crown-6 (for nomenclature see section 1.3.1) with alkali metals.

Using molecular mechanics calculations Hancock[20] found that this concept was somewhat flawed. Hancock determined the stability constants of metal complexes of a series of related tetraazamacrocycles. He found that the chelate ring size was an important factor in the stability of a macrocyclic complex. Five membered chelate rings were found to increase the stability of complexes of macrocycles and large metal ions, whilst six membered chelate rings increased the stability of complexes of macrocycles

and small metal ions. This effect was shown to be independent of the conformation that the macrocycle adopts on complexation. This effeect was demonstrated by the results obtained from a study of the formation constants for a range of metal ions of various sizes with a series of tetraaza macrocycles. This revealed that complexes of very large metal ions (*e.g.* Pb^{2+}) show a steady decrease in stability as the size of the macrocyclic ring is increased[20].

1.2.3. Electrochemistry.

The electrochemistry of macrocyclic ligand complexes has been studied widely. There are many reasons for this:

(a): The inertness of macrocyclic systems makes the competing reactions of ligand dissociation unlikely, hence any redox potential changes are not influenced by this type of reaction.

(b): Many synthetic macrocycles were prepared as models for naturally occurring macrocycles which are essential in catalysing *in vivo* redox reactions.

(c): Macrocyclic ligands provide well defined environments with preorganised donor sets. These geometric constraints mean that the environment, which effects the electron transfer kinetics, can be carefully controlled during the design of macrocycles. This control enables "tuning" of the redox reaction.

The manifestation of these properties has led to the development of macrocyclic ligands which can stabilise unusual oxidation states. This is useful for the development of catalysts as the accessability of unusual oxidation states of metal ions may play a crucial role in a catalytic cycle.

1.2.3.1. Stabilisation of high oxidation states.

Tetraazamacrocyclic ligands have shown the ability to stabilise uncommon oxidation states such as Cu(III) and Ni(III). This was first illustrated by Olsen and Valsilevkis[21,22] who reported the electrochemical generation of these species. Lovecchio *et al* [23] tried to

determine the factors which influence the stabilisation of unusual oxidation states. They found that the structure of the macrocycle was critical. The redox properties were found to be linked to a number of factors which were:-

(a) macrocyclic ring size

(b) nature of the ligand substituents

(c) extent of conjugation in the ligand

(d) charge of the ligand.

Fabrizzi[24] compared the electrochemical oxidation of Ni(II) and Cu(II) with ligands cyclam and dioxocyclam. Dioxocyclam contains two amide protons which on coordination of a metal ion are lost thus producing a dinegatively charged ligand. It was argued that this negative charge on the ligand should stabilise the higher positive oxidation state, making oxidation more facile. This was proved to be the case.

1.2.3.2. Stabilisation of low oxidation states.

Tetraazamacrocycles have also found favour for stabilising Cu(I) and Ni(I) species. These species were found to be stable only in dioxygen free aprotic solvents[25]. In aqueous media, Cu(I) species of this type decompose by loss of ligand[26]. Modification of the ligand by extensive alkylation has led to the stabilisation of Cu(I) by a tetraazamacrocycle in aqueous solution[27].

The reduction of Cu(II) to Cu(I) changes the nature of the metal ion from d^9 to d^{10}. This change is the main reason why tetraaza macrocycles with their enhanced ligand field properties are not as effective for the stabilisation of Cu(I). Decreasing the σ-donor ability of the ligand by ,for example, increasing the unsaturation of the ligand combined with increasing the π- acceptor ability of the ligand will aid the stabilisation of Cu(I). This entails designing the ligand specifically for destabilisation of Cu(II). An example of this type of approach is the work of Rorabacher[28] who utilised sulphur donors to stabilise Cu(I).

1.3. Comparison of different types of macrocycles.

The methods outlined in section (1.1) for the synthesis of azamacrocycles have been used to prepare a wide range of macrocycles with varying ring sizes and various donor atoms. The following sections will dicuss the properties of various macrocycles classed by their donor atom type.

1.3.1. Macrocyclic Crown Ethers.

Cyclic crown ethers were first synthesised by Pedersen[29]. These compounds are simple monocyclic ring compounds which form stable complexes with alkali and alkaline earth metal cations. The interaction between these two species is believed to be essentially electrostatic. They are known as "crown ethers" because of the observations of Pedersen who noted from models that on complexation the ligands tended to form a "crown" about a metal ion. Prior to the discovery of crown ethers, the coordination chemistry of alkali and alkaline earth metals was scant, but the discovery that Na, K ,Mg and Ca play a vital role in biological systems stimulated extensive research.

1.3.1.1. Nomenclature.

A typical crown ether is shown below (fig.1.2).

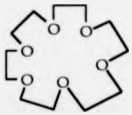

Figure 1.2. 18-crown-6

Throughout the introduction the nomenclature of Pedersen[29] will be used. In figure 1.2, the numbers 18 and 6 refer to the number of atoms in the ring and the number of oxygen donors. The word "crown" will be used to describe ligands with only oxygen donors. In later sections,

the word "crown" will be substituted by "N" or "S" when describing ligands with only nitrogen or sulphur donors.

1.3.1.2. Crown ether synthesis.

Crown ethers are prepared by the high dilution technique mentioned in section (1.1). Crown ethers usually have an ethylene link between oxygen donors. This structural feature leads to metal complex formation which contain the more stable five membered chelate ring. Cyclisation usually involves the nucleophilic displacement of a halide or good leaving group by an alkoxide in a Williamson Ether synthesis[30] (1.9).

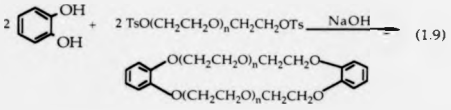

(1.9)

Alkali metal ions have been shown to promote the formation of crown ethers as illustrated in the synthesis of 18-crown-6 (1.10).

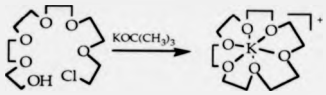

(1.10)

1.3.1.3. Properties of Crown Ethers.

Crown ethers have the ability to form complexes with alkali metal ions which, in some cases, are stable in aqueous solution. They tend to form less stable complexes with transition metals. Since Pedersen's original work many new crown ethers have been prepared containing numerous donors, and their coordination chemistry has been studied extensively[32,33].

Crown ethers form a number of crystalline complexes of varying stoichiometry with metal to ligand ratios of 1:1, 1:2, and 2:3. An example of a 1:1 complex is shown by the crystal structure of dibenzo 18-crown-6 RbNCS[34] (fig 1.3).

Figure 1.3 The crystal structure of dibenzo 18 crown 6 RbNCS.

Here the crown ether provides an approximately planar array of six oxygen donors with nearly equal Rb-O bond lengths. A second type of structure can occur when the cavity of the crown ether is much larger than the metal ion. In this instant the crown ether can either "wrap up" the metal ion[35] (fig.1.4) or coordinate two metal ions[36].

Figure 1.4 Folding of the ligand dibenzo 30-crown-10 on complexation of K^+

In figure 1.4, folding of the ligand, dibenzo-30-crown-10, has produced a smaller cavity which is suited for coordination of K^+. When

the metal is too large for the cavity, stoichiometries in excess of 1:1 can occur. A "sandwich" type structure occurs on complexation of two moles of benzo 15-crown-5 with K^{+}[37] which lies at the centre of symmetry (fig 1.5).

Figure 1.5 The "sandwich" type structure of benzo 15-crown-5 with K^{+}

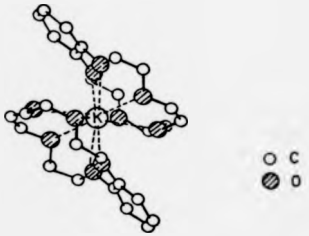

Crown ethers exhibit remarkable selectivity for particular ions. The factors which are believed to be important to selectivity are cavity size, number of oxygen donors, crown ether conformation and the solvation energy of the species involved. For small crown ring systems, enhanced complex stability occurs when the ionic radius of the cation matches the cavity size of the crown in a planar conformation. This was the explanation given by Lamb and co-workers[38] of the observation of the enhanced stability of the K complex of 18-crown-6 over the remaining alkali metals (fig.1.6).

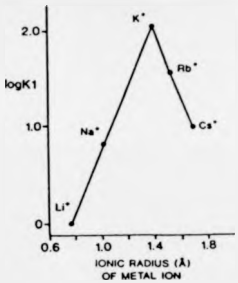

Figure 1.6 Enhanced stability of the K complex of 18-crown-6 over the remaining alkali metals.

Consideration of the crystal structures of the 18-crown-6 complexes of the alkali metals gives credence to this view. The crystal structure of the thiocyanate adduct of K 18-crown-6 shows K^+ occupying the macrocyclic cavity with minimal strain in the crown ether. The crystal structure of the thiocyanate adduct of Na 18-crown-6 shows a folded macrocycle which does not allow coordination of all the donor atoms in one plane. Although this is good evidence to explain the relative strengths of the complexes Izatt[39] has shown evidence that solvation has a large effect on the stability of the complexes of these ions.

The above discussion is of lesser importance in consideration of the complex stability of the larger crown ethers. Here, full participation of all oxygen donors may be a crucial factor. Full participation results in the maximum electrostatic interaction between the crown and the metal cation hence a more favourable enthalpy term for complex formation.

1.3.2. Azamacrocyclic ligands.

Azamacrocyclic ligands have been studied widely as a result of their similarity to the biologically important porphyrins. The following discussion will focus on the chemistry of two azamacrocycles undergoing

active research 1,4,7-triazacyclononane (9N3) and 1,4,8,11-tetraazacyclotetradecane (14N4 or cyclam).

9N3 is too small to encapsulate a metal ion, and in most instances it occupies a triangular face of the octahedral coordination sphere of a six-coordinate metal ion. The stability of the complexes is enhanced by the macrocyclic effect.

Complexes of 9N3 are often kinetically inert. This property was used by Chaurdhuri and Wieghart[40]. 9N3 will react with either $Mo(CO)_6$ or $W(CO)_6$ to give $[Mo(9N3)(CO)_3]$ and $[W(9N3)(CO)_3]$, which are air stable. The oxidation states of the metals are zero. These complexes react with 30% H_2O_2 to give good yields of $[Mo(9N3)O_3]$ and $[W(9N3)O_3]$ with the oxidation state of the metal centres now +6. This example shows that it is possible to use the thermodynamic and kinetic inertness of the coordinated 9N3 to utilise the redox activity of the transition metal centre. Thus 9N3 can act as an effective blocking group for three coordination sites and, in this respect, resembles other facially coordinating ligands (*e.g.* cyclopentadiene) used in organometallic chemistry[41].

Functionalisation of 9N3 can be achieved by reaction at the secondary amine groups. Introduction of additional donors modifies the behaviour of 9N3, allowing the formation of more stable complexes. This area of chemistry has recently been reviewed[42,43].

9N3 forms complexes with heavier main group elements such as Ga(III)[44], In(III)[45] and Tl(I)/(III)[46]. Monomeric 1:1 complexes are formed by the reaction of MX_3 (X=Cl or Br) with 9N3 in a range of solvents. Bis(octahedral) complexes of In^{3+} and Tl^{3+} are prepared by the reaction of $In(NO_3)_3$ or $Tl(NO_3)_3$ with excess 9N3.

Although there have been many reports of the complexes of transition metals and 9N3, surprisingly few of these are complexes of Co(II). Nonoyama[47] prepared a series of triazacycxloalkane thiocyanato complexes of Co(II) which, depending on the macrocyclic ring size, were

monomeric five coordinate species or binuclear six coodinate species. Similar results were obtained for Ni(II)[48].

There has been no other azamacrocycle that has been studied to a greater extent than 14N4. Reports of the complexes of 14N4 with transition metal ions are numerous[49-51]. This ligand shows flexibility on coordination to metal ions and exhibits both *cis* and *trans* coordination geometries. Zuckman and co-workers[52] report the *trans* planar coordination of 14N4 to a range of transition metal ions which include Ni(II), Co(II), Cu(II) and Tc(V). 14N4 has also been reported to form a folded complex in *cis* $[Co(14N4)(ethylenediamine)]Cl_3$[53]. 14N4 contains four secondary nitrogen donors, thus there exists five possible conformations. (fig.1.7).

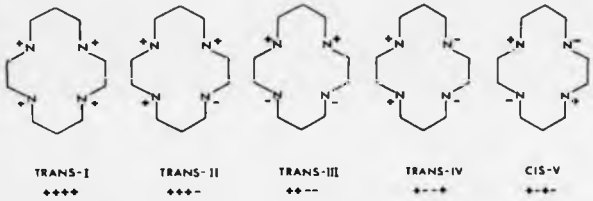

Figure 1.7 Five possible conformations of cyclam(14N4).

The comformations are not of equal energy: a result of the overall strain energy being dependent on the conformations available to the five and six membered chelate rings. For coordination in a plane the structure

of lowest energy results when the five and six membered chelate rings have gauche and chair conformations (conformer 5).

N functionalisation of 14N4 has also been widely reported[54,55]. In these reports functionalisation provides extra ligating groups capable of coordination to eight coordination sites; not necessarily on the same metal ion.

N-alkyl derivatives of 14N4 have been known for some time. The development of a simple two step synthesis to N-alkyl derivatives of 14N4 has been reported recently[56]. The secondary amines are reacted with excess acid chloride, and the product amide reduced to give good yields of N-alkylated 14N4.

1.3.3. Thioether Macrocycles.

The coordination chemistry of macrocyclic thioethers has blossomed over recent years. This is a result of the observation that macrocyclic thioethers can coordinate a range of transition metal ions to form stable metal complexes[57]. A second impetus to the study of macrocyclic thioether complexes is the role which thioether complexes play in nature, for example, in blue copper proteins (plastocyanin and azurin)[58].

Unlike crown ethers and azamacrocycles, the macrocyclic effect of certain thioethers is much reduced because of the reorganisation energy which needs to be used on chelation. This can be shown by consideration of the crystal structure of the free ligand 14S4. This ligand adopts a conformation in which the lone pairs of the sulphur donors are directed out of the ring[59]. Thus on complexation this ligand readily chelates metal ions outside the macrocyclic cavity, illustrated by the bridging 14S4 group in the complex $Cl_2Hg(14S4)HgCl_2$[60,61].

The study of the coordination chemistry of thioethers was hindered initially by the inability to prepare the cyclic thioethers in good yields. 9S3 was first reported in 1977 by Ochrymowycz[62] in 0.04% yield by the

reaction of 3-thiapentane-1,5-dithiolate with 1,2-dichloroethane. Improvement of the yield was obtained by Glass *et al* [63] who used the high dilution technique and changed the counter-cation from sodium to benzyltrimethylammonium. A biproduct of this route was the 2+2 addition product, 18S6, in 32% yield[64]. A high yield synthesis of 9S3 was developed by Sellman and Zapf[65] who used $MoCO_3$ as a template around which the cyclisation of the dithiolate and 1,2-dibromoethane can occur (yield 60%) (1.11).

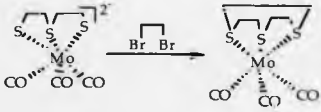

(1.11)

The synthesis of 12S4, 13S4 and 14S4 are now possible in good yields by utilising the methods of Ochrymowycz *et al* [66] (which involves the use of mustard gas or its derivatives) and the high dilution Cs_2CO_3 / DMF cyclisation techniques of Butler and Kellogg[67,68].

The Ni(II), Co(II) and Cu(II) complexes of 9S3 were reported by Glass in 1983[63]. In each complex the metal ion occupies a slightly distorted octahedral environment of sulphur donors provided by two facially coordinating 9S3 ligands. The electrochemistry of the Co(II) complex was compared to that of the 9N3 complex. These studies showed that the low spin Co(II) state was stabilised by the S donors[69]. Other thioether ligands have been used to stabilise low spin Co(II) species.[70]

The first cage thioether has been recently reported[71]. This ligand shows remarkable stabilisation of Co(II) when compared to its nitrogen analogue. The Co(II) cage thioether can be oxidised to the Co(III) species using $AgCF_3SO_3$. The authors argue that the Co(III) species could be used as a mild oxidant.

1.4. Macrobicyclic Ligands.

Macrobicyclic ligands or cryptands are a group of macrocycles whose properties are such that they merit special mention. Cryptands are a range of three-dimensional polycyclic ligands which were developed by Lehn and collaborators[72]. The design of these systems was a major breakthrough in polyether chemistry. A series of cryptands are represented in figure 1.8. These types of cryptands are prepared by high dilution techniques (1.12).

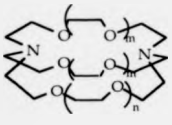

[1.1.1] m=n=0
[2.1.1] m=0, n=1
[2.2.1] m=1, n=0
[2.2.2] m=n=1

Figure 1.8 Cryptands and their nomenclature.

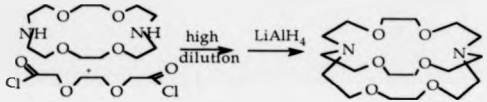

(1.12)

Cryptands of the type shown in figure 1.8 can exist in three isomeric forms since each of the bridgehead nitrogens can be orientated to face inwards or outwards with respest to the macrocyclic cavity.

These cryptands readily form metal complexes with a range of metal ions provided that the metal ion is not too large for the cavity. Encapsulation of a metal ion has been proved crystallographically by Moras *et al* (fig.1.9)[74].

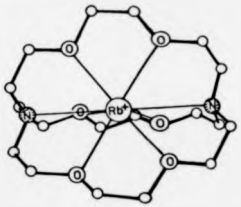

Figure 1.9. Rb^+ complex of cyptand [2.2.2][74]

The "cage-like" structure of these complexes results in considerably enhanced stability when compared to crown ethers. This enhancement was termed the "cryptate effect"[75] and can be considered a special case of the macrocyclic effect discussed in section(1.2.1.)

1.4.1 Binucleating Macrocycles.

Cyclic or macrobicyclic ligands which are capable of coordinating two metal ions are of considerable interest. These compounds have good prospects of generating unique chemical and electronic properties resulting from the close proximity of the metal ions.

The cryptand below (fig 1.10) was synthesised by Lehn and co workers[76]. This ligand contains two N subunits in a large cage capable of coordinating two metal ions simultaneously. Each of the N subunits is related to the tripodal ligand "tren" (2,2',2"-tris(2-aminoethyl)amine) and this ligand has been called "bis-tren".

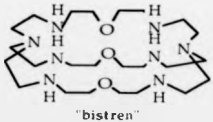

"bistren"

Figure 1.10 "bistren"

There exist a number of "bis-tren" type ligands. The metal complexes are of special interest not only because they can coordinate two metal ions within a cage but have the ability to coordinate small ions or solvent molecules between the metal centres. Lehn has called this type of compound "cascade complexes".

1.5. Novel Macrocyclic systems.

In this section novel macrocyclic systems will be highlighted.

1.5.1. Catenands.

Catenands are cyclic ligands which contain interlocking macrocyclic rings. Sauvage and collaborators[78] have developed a simple procedure for preparing such compounds. This method uses the ability of Cu(I) to coordinate two 2,9-substituted 1,10-phenanthroline molecules in a tetrahedral fashion. Hence, coordination of functionalised phenanthroline ligands to Cu(I) enables cyclisation to occur by reaction of the functionality in a novel template reaction (scheme 1.2).

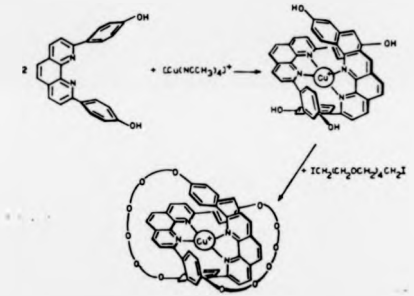

Scheme 1.2 Sythesis of a catenand by template technique.

Demetallation of the Cu(I) using tetramethylammonium cyanide gives free catenand. Surprisingly the catenand shows the ability to stabilise

Cu(0). The Cu(0) species can be electrochemically generated in DMF. The stability of the Cu(0) compound is a result of the interlocking rings.

1.5.2. Polyphosphorous and polyarsenic macrocycles.

Phosphorous donors are well known for their ability to stabilise low oxidation states of metal ions. When this ability is combined with the macrocyclic effect, the study of polyphosphorous macrocycles has unrivalled potential. The majority of the reported phosphorous containing macrocycles also contain other donors such as N, O and S[79,80].

Kyba and co-workers[81] have reported the synthesis of tri and tetraphosphorous donor macrocyles using high dilution techniques (scheme 1.3).

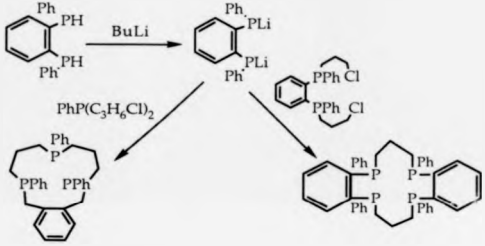

Scheme 1.3 Synthesis of polyphosphorous macrocycles.

Deldonno and Rosen[82] reported the template synthesis of polyphosphorous macrocycles using Ni(II) as a template (1.13).

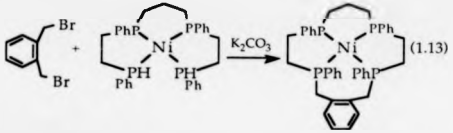

Polyarsenic macrocycles have not been investigated as widely as other types of macrocycles as a result of their difficult synthesis and the toxic nature of these compounds. The ability of arsenic to act as a donor to transition metals was described by Barnard[83]. The synthesis of polyarsenic macrocycles was reported by Kauffmann and Ennen[84-86]. No complexes of the ligands were described. The ligands were prepared using a similar strategy to that of polyphosphorous macrocycles shown in scheme 1.3.

PART TWO.

THE DEVELOPMENT OF AUTO-OXIDATION CATALYSTS. FOR AQUEOUS PAINT SYSTEMS.

2.1. Introduction.

Part two will describe the development of auto-oxidation catalysts for aqueous paint systems. The coordination chemistry of Ni(II), Cu(II) and Zn(II) complexes of azamacrocyclic ligands will be described and the information obtained used in the evaluation of the Co(II) auto-oxidation catalysts.

2.1.1. The drying of paint films.

The majority of current paint driers are cobalt compounds, typically cobalt acetate and cobalt octanoate. These compounds act as catalysts for the oxidative drying of paint films. They are believed to act by initial coordination of dioxygen from air to give cobalt-superoxo complexes. The superoxo complex (activated dioxygen species) reacts with unsaturation in the paint (tung oil, linseed oil etc). This leads to polymerisation and cross-linking in the formation of paint films.

The oxidative drying of paint is a very complex process, and even though much research has been done it has not been possible to elucidate the mechanism by which drying occurs. The postulated mechanism outlined previously is based on the following observations[87]:

(1). During the drying process, dioxygen uptake from air occurs.

(2). The rate of drying is increased by the addition of metal catalysts. Organic solvent based paints without catalysts are observed to dry over a 48-72 hour period. Addition of catalyst brings the drying time down to 105 minutes.

Paint driers can be classed as either primary or secondary. Primary catalysts are termed "through driers" and catalyse the drying of paint throughout the film. Secondary driers assist the drying of the lower layers of paint films by, as yet, unknown mechanisms. The secondary driers are

compounds based on Zr, Ca and Ce, and may act by interacting with carboxyl and hydroxyl groups within the paint.

2.1.2. Activation of dioxygen.

The reaction of an organic compound with dioxygen is themodynamically favoured, but there are significant barriers to this process.

Processes which involve reaction of dioxygen in its ground state (a triplet state) involves electron transfer from the singlet state of the substrate (organic molecule to be oxidised) to dioxygen. This would result in the formation of a diradical product, which is energetically unfavourable.

Metals which serve as catalysts for the oxidation of organic compounds must be catalysts for the reduction of dioxygen. Dioxygen is a potenial four electron acceptor. Its interaction with metals of varying oxidation state is complex. The stages of metal to oxygen electron transfer are shown in figure (2.1)[88]. The associated metal-dioxygen complexes are given in figure (2.2).

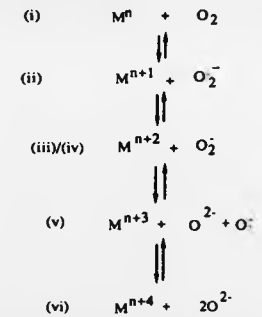

Figure 2.1. The formal stages of metal to dioxygen electron transfer.

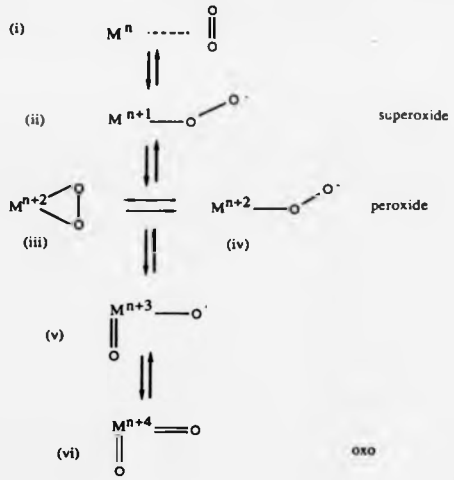

Figure 2.2. Metal-dioxygen complexes relating to the scheme in figure 2.1.

In (i) there has been no transfer of electrons. One and two electron transfer to dioxygen give superoxide(ii) and two types of peroxo complexes ((iii) + (iv)) (fig 2.2). Transfer of a third electron requires rupture of the dioxygen bond to give a metal-oxy radical species (v). Species (vi) is the result of the transfer of a fourth electron. In principle, any of the species (i) to (vi) can be oxidants.

2.1.3. Ideal auto-oxidation catalyst properties.

(1). The catalyst must show reversible uptake of dioxygen from the air.

(2). The catalyst must provide the correct environment to coordinatively activate dioxygen without the metal or the ligand being irreversibly oxidised.

(3). The catalyst must be relatively easy to handle. This is because throughout the manufacture of paint, ingress of dioxygen is highly likely.

(4)The catalyst must be completely soluble in aqueous paint mixtures to the level of 1% by weight of cobalt metal.

Thus the ideal catalytic cycle would be as follows (fig.2.3)

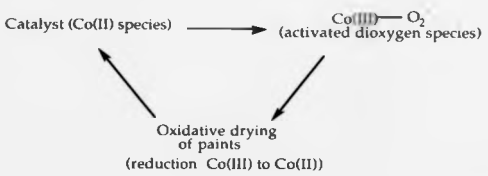

Figure 2.3 Ideal catalytic cycle for the oxidative drying of paints.

2.1.4. The nature of the cobalt-dioxygen bond.

The coordination of dioxygen to a metal complex is not a simple substitution process, such as that involved in the ligation of neutral or anionic ligands such as ammonia or chloride ion. The addition of dioxygen also involves a formal oxidation of the metal, and associated reduction of coordinated dioxygen. To occur the metal ion must have a sufficiently reducing lower oxidation state, and a thermodynamically accessible higher oxidation state.

Depending on the stoichiometry of the oxidation reaction and the nature of the metal, it is possible to envisage transfer of between zero and two electrons from metal to dioxygen.

A comparison of the O-O stretching frequencies from metal-dioxygen complexes with those observed for compounds containing ionic superoxide or peroxide indicate that the metal-dioxygen complexes have O-O stretching frequencies similar to those of ionic superoxide or peroxide species. This suggests significant transfer of electron density from the metal centre to the coordinated dioxygen moiety

This evidence has been further supported by electron spin resonance studies of low spin Co(II) Schiff's-base adducts of dioxygen. These studies[89] suggest that the majority of the unpaired electron density (>80%) resides on dioxygen. Getz and co-workers[90] carried out further electron spin resonance studies with O labelled dioxygen. Their work confirmed the previous findings, determining the electron spin density of dioxygen to be close to 100%.

On the basis of this evidence, in cobalt-superoxo complexes, cobalt is properly represented as having a +III oxidation state, while the coordinated dioxygen can be considered as having an oxidation state of -I.

2.2. The synthesis and coordination chemistry of four macrobicyclic ligands.

Work in this area began from recent reports by Martell[91-93]. He prepared the cryptand, O-bistren, shown below by a tripode-coupling technique.

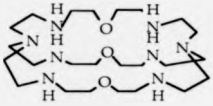

O-bistren

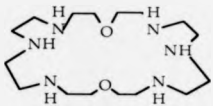

bisdien

This ligand forms a dinuclear cryptate with two Co(II) ions. This compound possessed remarkable properties. Martell[92,93] reported that the compound can reversibly coordinate dioxygen and that this can be used as a reversible dioxygen carrier for oxygen separation and transport. He also reported that this compound can coordinate oxalate anion, whilst coordinated to dioxygen (cascade complex) and facilitate the oxidation of oxalate to carbon dioxide. The proposed mechanism for this is given in figure (2.4).

More recently Martell and Motekaitis[94] have reported the oxidation of mesoxalate anions to carbon dioxide using a dicobalt(II) complex of bisdien.

An important feature of the mechanism (fig 2.4) is the formation of free radical species. This type of chemistry could be useful in the oxidative drying of aqueous paints. Ligands of this type were prepared and their coordination chemistry investigated.

Figure 2.4 The proposed mechanism for the oxidation of oxalate anion by dioxygen catalysed by the dicobalt complex of O-bistren.

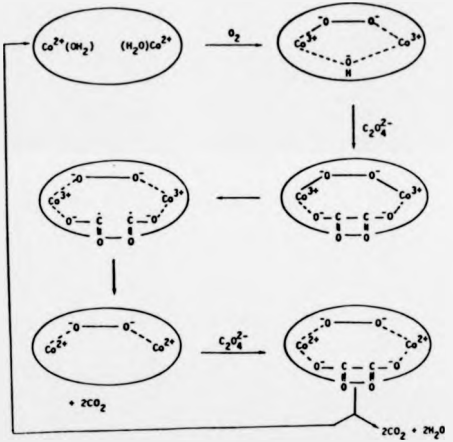

2.2.1.Synthesis of macrobicyclic Schiff's-base ligands L^1 and L^2. Characterisation of their Ni(II), Cu(II) and Zn(II) dinuclear cryptates.

2.2.1.1. Introduction.

Since their discovery by Lehn[95], the synthesis of macrobicyclic ligands has been a major hurdle to their study. Two strategies for their preparation are as follows:

(a).A stepwise process requiring two cyclisation reactions, each forming two bonds, which generate an intermediate macrocycle. The yield in this type of synthesis is typically around 4%.

(b). Direct macrobicyclisation *via* tripode coupling which requires the formation of three bonds in a single condensation step. An example of this synthetic technique is the preparation of O-bistren in 11% yield[96].

The approach used in this work was first described by Jazwinski[97] and co-workers and subsequently by Nelson and McDowell[98]. This involves the formation of six bonds in a single condensation step.

The dinuclear cryptates were studied by infra-red and u.v-visible spectroscopy, magnetic susceptibility, conductivity, and elemental analyses.

2.2.1.2. Experimental.

Materials: commercially avaidable materials were used without further purification. Purity was determined spectroscopically.

Solvents: Solvents were obtained from commercial sources. Acetonitrile and dichloromethane were dried by refluxing over CaH_2 under dry N_2 and stored over activated A4 molecular sieves prior to use. Nitromethane was dried by refluxing over anhydrous $CaCl_2$ under dry N_2 and stored over activated A4 molecular sieves in a dark glass bottle. Diethylether was distilled from Na/benzophenone before use.

Spectroscopy. ^1H. n.m.r. spectra were recorded at 220MHz using a Perkin-Elmer continuous wave spectrometer or at 40MHz using a Bruker

WH400 Fourier Transform(FT) spectrometer. Proton decoupled ^{13}C n.m.r. spectra were obtained at 45.28 MHz using a Bruker WH180 FT spectrometer or at 100.25 MHz with a Bruker WH400 FT spectrometer. Chemical shifts are reported on a scale relative to tetramethylsilane (TMS) at δ=0ppm. Mass spectra were obtained with a Kratos MS80 spectrometer. U.V-visible and infra-red spectra were obtaied using a Shimadzu 365 and Perkin-Elmer 1720X Fourier Transform spectrometers respectively. Conductivity measurements were obtained with a Philips PW9527 digital conductivity meter, and elemental analyses were carried out commercially.

Synthesis of L^1.

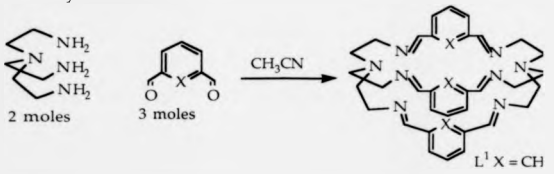

The reaction scheme is shown in equation (2.1). 2,2',2''-Tris(2-aminoethyl) amine (tren) (0.476g, 3.26mmol) is dissolved in acetonitrile (100cm^3) and the solution placed in a 500cm^3 round-bottomed flask fitted with a pressure equilising addition funnel and dry nitrogen inlet. Isophthalaldehyde (0.655g, 4.89mmol) is dissolved in acetonitrile (100cm^3) and the solution placed in the addition funnel. This solution is added with vigorous stirring to the solution of tren over a period of 30 minutes. Stirring is continued over 3 hours during which a pale green precipitate forms. The precipitate is collected and recrystallised from dichloromethane/acetonitrile (1:4) to give L^1 as a white solid (0.726g, 76% yield). Electron impact mass spectrum M^+ at m/z 586 (calc. 586). ^1H. n.m.r.

($CDCl_3$ solution, relative populations in parentheses): δ 8.2 (2H, d), 7.61 (2H, s), 7.52 (1H, t), 5.43 (1H, s), 3.79 (1H, br), 3.30 (1H, br), 2.94 (1H, br), 2.71 (1H, br) ppm. ^{13}C n.m.r. ($CDCl_3$):δ 160.63(2), 136.87(2), 132,36(1), 128.91(1), 127.33(2), 59.93(2), 56.02(2) ppm.

Synthesis of L^2

The above synthetic procedure was followed substituting 2,6-pyridinedi-carboxaldehyde[99] (0.66g, 4.89mmol) in place of isophthalaldehyde. The product is obtained as a pale yellow solid (0.672g, 70% yield). Electron impact mass spectrum M^+ at m/z 589 (calc. 589). ^1H n.m.r. ($CDCl_3$) δ 8.15 (2H, d), 7.85 (1H, t), 7.63 (2H, br), 2.86 (2H, br) ppm. ^{13}C n.m.r. ($CDCl_3$) δ 162.63(2), 158.98(2), 136.38(1), 121.26(2), 59.73(2), 56.39(2) ppm.

Synthesis of dinuclear cryptates.

Solid dinuclear cryptates of ligands L^1 and L^2 were prepared in good yields (> 60%) by mixing a dichloromethane solution of each ligand (0.60g, 1.02mmol) with two molar equivalents of $[M(dmso)_n][BF_4]_2$[100] (M=Ni, Cu, n=6; M=Zn, n=4) in ethanol. The solid precipitates were collected by suction filtration under dry nitrogen and were recrystallised from acetonitrile/ethanol/diethylether (1:2:2).

2.2.1.3. Results and Discussion.

Ligand Synthesis.

The Schiff's-base ligands containing six imine bonds are readily synthesised by the reactions of tren with dialdehydes in remarkably good yields, without the use of template metal ions. There could be two reasons for this:

(1) Tren is intramolecularly hydrogen bonded in acetonitrile solution and adopts a preferred conformation which facilitates the formation of the macrobicycle. The reaction could be considered as a "template reaction", using a hydrogen bond as the template.

(2). The macrobicycle is insoluble in acetonitrile and precipitates as formed. This has the effect of moving the equilibrium of the reaction mixture towards that of the product.

There have been recent reports by Hunter *et al* of the synthesis of two related Schiff's-base cryptands from the reaction of glyoxal with tren in the presence of alkaline earth metal ions[101]. The cryptate formed is unstable and decomposes on demetallation. Martell and co-workers[102] report the reaction of 2,2'2"-(3-aminopropyl)amine with isophthalaldehyde gives a cryptand similar to L^1,but which has propyl groups between the apical tertiary nitrogens and the imine bonds. This synthesis is facilitated by use of Ag(1) ion as a template. The ^1H n.m.r. spectra of the ligands L^1 and L^2 show interesting features (fig. 2.5).

Figure 2.5. The ^1H n.m.r. spectrum of L^1 in $CDCl_3$.

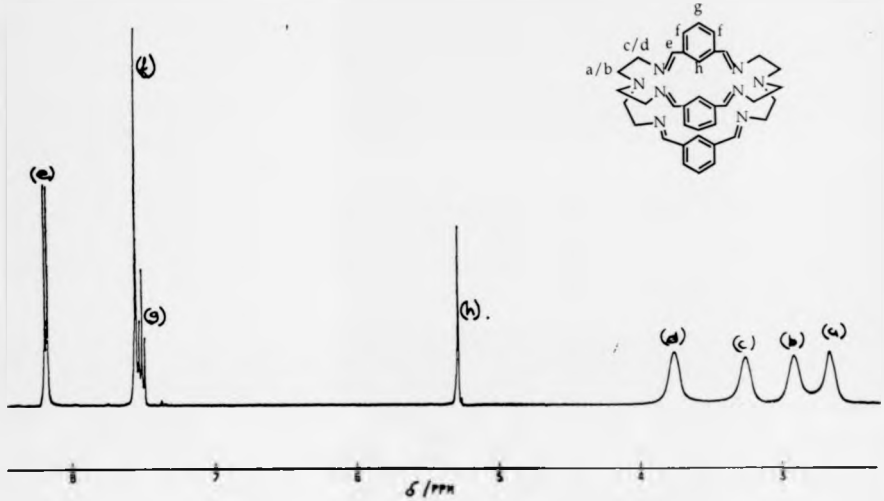

The tren moieties show fluctionality at room temperature (resonances (a)-(d)). Also of note is the unusual high field resonance of the aromatic proton (h), and the unusual low field resonance of the aromatic proton (f). The reason for these features can be explained by consideration of the crystal structure of the ligand L^1 [103].

[The crystal structure was determined independently from Nelson *et al* [103] who reported the structure]. The unusual high field resonance is the result of the proton lying above a neighbouring phenyl ring (distance 2.75 Å). Thus the ring current associated with the ring has caused the observed shift. The low field resonance (f) is a result of the close proximity of the proton at (e)[103]. The observed fluctionality of the tren moieties suggest that alternative conformations of the macrobicycle exist in solution. This fluctionality could result from the interconversion of axial and equatorial protons and a lowering of the temperature would cause a sharpening of these resonances. This observation was made[103].

Figure 2.6. The crystal structure of ligand L^1.

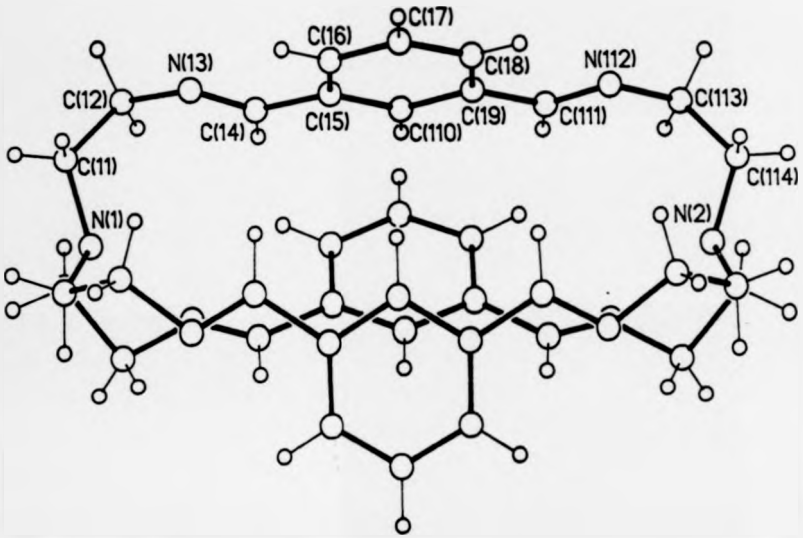

Figure 2.7. A view of the crystal structure of L^1 along the N1-N2 axis showing the high symmetry of the ligand.

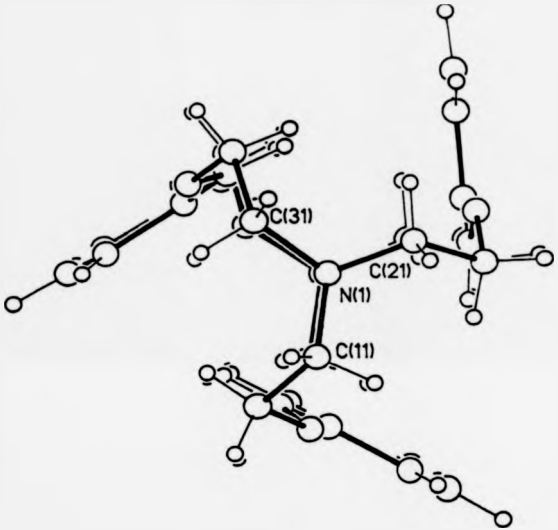

Dinuclear Cryptates.

The cryptates formed have the general formula $[M_2L(OH)][BF_4]_3$. This is confirmed by analysis and by conductivity measurements (Table 2.1). Nelson and co-workers[103] reported the unsuccessful preparation of the dinuclear $Zn(II)L^1$ complex, and that the dinuclear $Cu(II)L^1$ complex caused ligand modification. In this work, no ligand modification was observed during the characterisation of the dinuclear Cu(II) complex of L^1. Ligand modification could occur by copper mediated hydroxylation of the phenyl ring.[104] The dinuclear Zn(II) complexes were investigated by n.m.r. spectroscopy

Figure 2.8. The ^1H. n.m.r. of $[Zn_2(L^1)(OH)][BF_4]_3$ in CD_3NO_2.

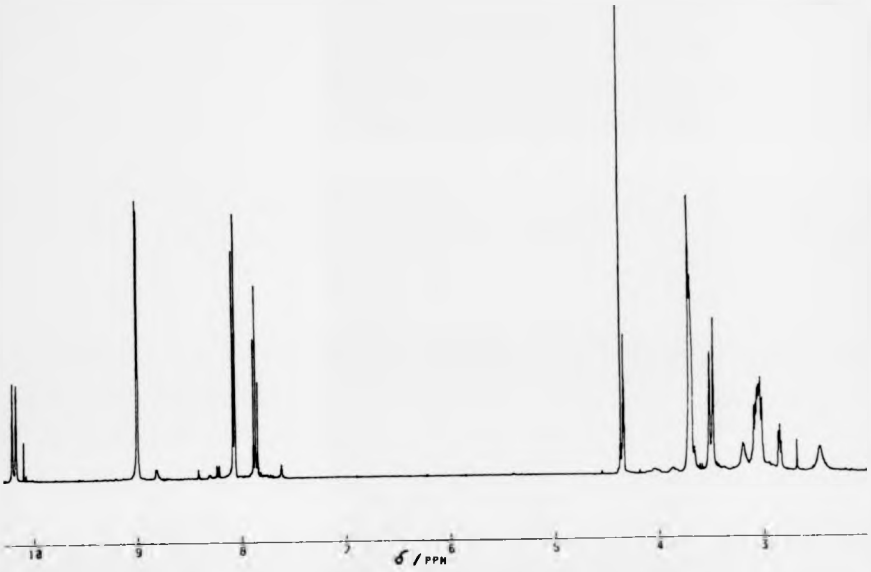

Figure 2.9. The ^{13}C n.m.r. of $[Zn_2(L^1)(OH)][BF_4]_3$ in CD_3NO_2.

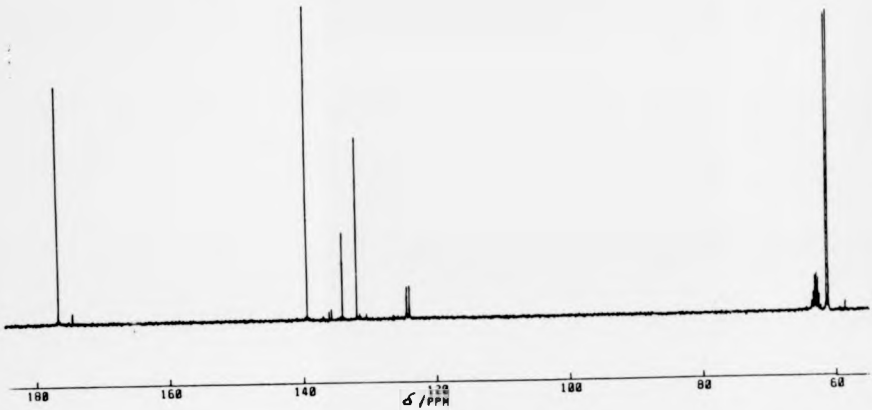

N.m.r. studies of $[Zn_2L(OH)][BF_4]_3$

The ^1H and ^{13}C n.m.r. spectra of the Zn(II) dinuclear cryptates are shown in figures 2.8 and 2.9.

Comparison of the ^1H n.m.r. spectra of the free ligand and the Zn(II) dinuclear cryptate shows a number of interesting features. There is less fluctionality of the tren moiety of the ligand on complexation and the high field resonance has shifted to more normal values. This evidence supports the view that on complexation, the conformation of the macrobicycle has changed to incorporate metal ions. The rigidity of the ligand is indicated by the sharp resonances and the fact that only a single bridging hydroxyl group can be incorporated between the metal centres. The OH resonance can clearly be seen at δ=4.5. This type of ligand conformation change on coordination was first reported by Jazwinski.

No satisfactory n.m.r. data was obtained for $[Zn_2L(OH)][BF_4]_3$ as this compound was unstable in solution. This could be a result of hydrogen bond formation between the bridging hydroxyl group and a pyridine nitrogen from the ligand. This would result in the formation of an unstable bridging oxygen group which readily decomposes.

U.V.-visible spectra.

The data for the u.v.-visible spectra of the dinuclear cryptates of Ni(II) and Cu(II) are given in table 2.1. The spectra are typical of five coordinate trigonal bipyramidal Ni(II) and Cu(II) ions.[105] A comparison of the u.v.-visible spectra of the Ni(II) dinuclear cryptates is shown in figure 2.10.

The spectra show the effect on the u.v.-visible spectrum of the hydrogen bond between the bridging hyroxyl group and the pyridine nitrogen of the ligand L^2.

Figure 2.10. The u.v.-visible spectra of $[Ni_2(L^1)(OH)][BF_4]_3$ (a) and $[Ni_2(L^2)(OH)][BF_4]_3$ in CH_3NO_2.

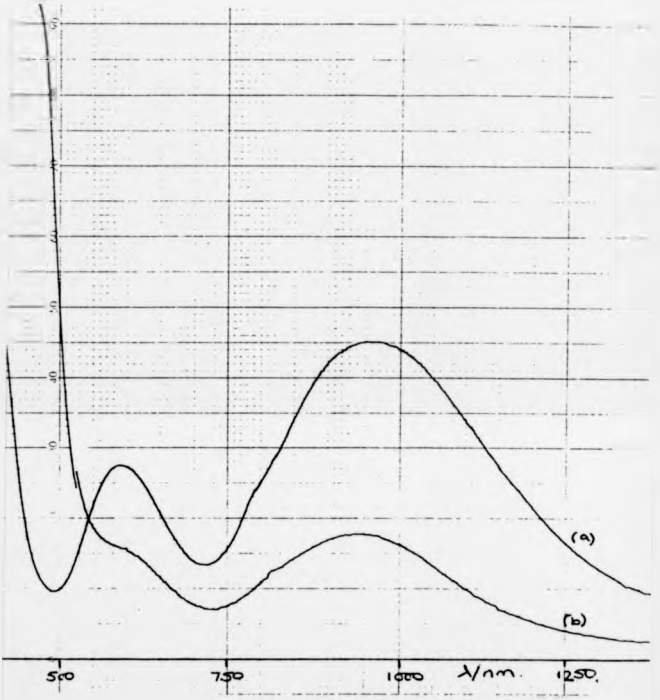

2.2.1.4. Conclusions.

The ligands L^1 and L^2 form dinuclear cryptates of general formula $[M_2L(OH)][BF_4]_3$. The structural characterisation support the assignment of five coordination about the metal ion. The rigidity of the ligands is indicated by the n.m.r. spectra of the dizinc(II) complex of L^1. The ligands undergo a large conformational change on chelation of metal ions, as shown by the n.m.r. spectra of the dizinc(II) cryptate of L^1. Hydrogen bond formation between the bridging hydroxyl group and a pyridine nitrogen is suggested by the change in the u.v.-visible spectra of the dinickel(II) species.

Table 2.1 Characterisation of the dinuclear cryptates of L^1 and L^2.

Dinuclear Cryptate	Colour	U.V. Visible (CH_3NO_2) λ_{max} (ε / $dm^3mol^{-1}cm^{-1}$)	Analysis			Conductivity $\Omega^{-1}cm^{-1}mol^{-1}$ (CH_3NO_2)	Magnetic suscept. μeff/BM
			% C	% H	% N		
$[Ni_2(OH)L^1](BF_4)_3.5H_2O$	blue/green	1404 (5) 960 (20) 780sh(10) 580 (12) 384 (23)	40.66 (40.34)	5.04 (4.98)	10.47 (10.45)	214.08	1.71
$[Cu_2(OH)L^1](BF_4)_3$	Green	940 (290) 796 (297)	42.05 (42.08)	4.72 (4.61)	10.83 (10.91)	239.80	1.15
$[Zn_2(OH)L^1](BF_4)_3.H_2O$	White		42.41 (42.21)	4.78 4.63)	11.12 (10.95)	248.41	
$[Ni_2(OH)L^2](BF_4)_3$ CH_3CN	yellow/green	1410 (4) 950 (20) 610 (17)	40.80 (40.99)	4.68 (4.22)	16.10 (16.39)	207.263	1.865
$[Cu_2(OH)L^2](BF_4)_3$	green	948 (275) 752 (280)	39.85 (39.86)	4.50 (4.50)	15.50 (15.32)	228.92	1.250
$[Zn_2(OH)L^2](BF_4)_3$ C_2H_5OH/CH_3CN	yellow		40.91 (40.95)	4.55 (4.55)	15.86 (15.49)	254.36	

magnetic susceptibilities determined using a Johnson Mathey balance.

2.2.2. Synthesis of macrobicyclic ligands L^3 and L^4. Characterisation of their Ni(II), Cu(II) and Zn(II) dinuclear cryptates.

2.2.2.1. Introduction.

The properties of the Schiff's-base macrobicycles L^1 and L^2 were greatly influenced by the nature and rigidity of the imine bonds. In this section, reduction of the imine bonds is described, and the effect on the chemistry of the ligands investigated.

2.2.2.2. Experimental.

The materials, solvents and equipment used were as described in section 2.2.1.2.

Synthesis of L^3.

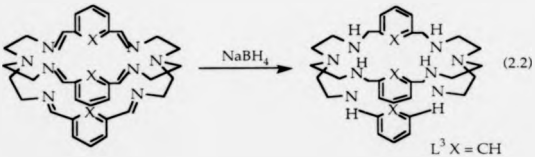

(2.2)

L^3 X = CH

L^4 X = N

The Schiff's-base ligand L^1 (1g, 1.7mmol) is slurried in methanol ($100cm^3$) in a $250cm^3$ round bottomed flask and cooled to 0°C using an ice bath. $NaBH_4$ (1g, 26.3mmol) is added slowly over a 90 minute period with vigorous stirring. After addition was complete the resulting solution was allowed to warm to room temperature and stirred for a further 2 hours. This solution is refluxed overnight. 1 $moldm^{-3}$ HCl ($40cm^3$) is added to the cooled solution to destroy exess $NaBH_4$. The solution is basified to pH 12 using NaOH and extracted with dichloromethane ($5x50cm^3$). The combined extracts are dried (anhydrous $MgSO_4$), filtered, and solvent removed to give a colourless oil which solidified on standing (0.843g,

83%). Electron impact mass spectrum (M+1) m/z 599 (calc 599). ^{1}H n.m.r. ($CDCl_3$): δ 7.41 (4H, br), 3.61 (4H, s), 3.50 (2H, br), 2.63 (4H, br), 2.55 (4H, br) ppm. ^{13}C n.m.r. ($CDCl_3$): δ 139.79 (2), 127.91 (1), 126.92 (1), 126.65 (1), 54.67 (2), 53.10 (2), 47.26 (2).

Synthesis of L^4.

The above procedure was used to reduce L^2 (1g) to L^4 (0.908, 89% yield). Electron impact mass spectrum (M+1) m/z 602 (calc.602) ^{1}H n.m.r. ($CDCl_3$): δ 7.61 (1H, t), 7.18 (2H, d), 4.22 (4H, s), 3.90 (2H, br), 2.74 (4H, br), 2.69 (4H, br) ppm. ^{13}C n.m.r. ($CDCl_3$):δ 158.76 (2), 136.76 (1), 120.98 (2), 55.26 (2), 54.57 (2), 47.50 (2) ppm.

Synthesis of the dinuclear cryptates of L^3 and L^4

Solid dinuclear cryptates of the ligands of L^3 and L^4 were prepared in good yield (>75%) by mixing ethanolic solutions of each ligand (0.6g, 1mmol) with two molar equivalents of $[M(dmso)_n][BF_4]_2$ (100) (M=Ni, Cu n=6, M=Zn, n=4). The solid precipitates were collected by suction filtration under nitrogen and were recrystallised from acetonitrile/ethanol/diethylether (1:2:2).

2.2.2.3. Results and Discussion.

Ligand Synthesis.

The reduced cryptands L^3 and L^4 were obtained in excellent yield by reduction using $NaBH_4$. The overall synthesis is an improved method of preparing macrobicyclic ligands in high yields in two steps. Figure 2.11 shows the proton decoupled ^{13}C n.m.r. spectrum of ligand L^4.

Dinuclear Cryptates.

The complexes formed have the general formula $[M_2L(OH)_2][BF_4]_2$, as confirmed by conductivity measurements and analyses (table 2.2). The room temperature magnetic susceptibilities of the Ni(II) and Cu(II) complexes indicate significant interaction between the metal centres. As

Figure 2.11. ^{13}C n.m.r. of ligand L^4 in $CDCl_3$.

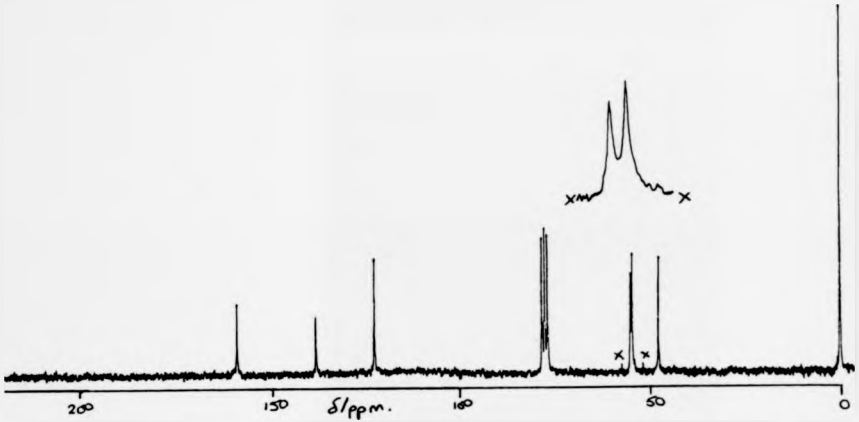

Figure 2.12. The ^{13}C n.m.r. of $[Zn_2(L^3)(OH)][BF_4]_2$ in CD_3NO_2 at 15°C.

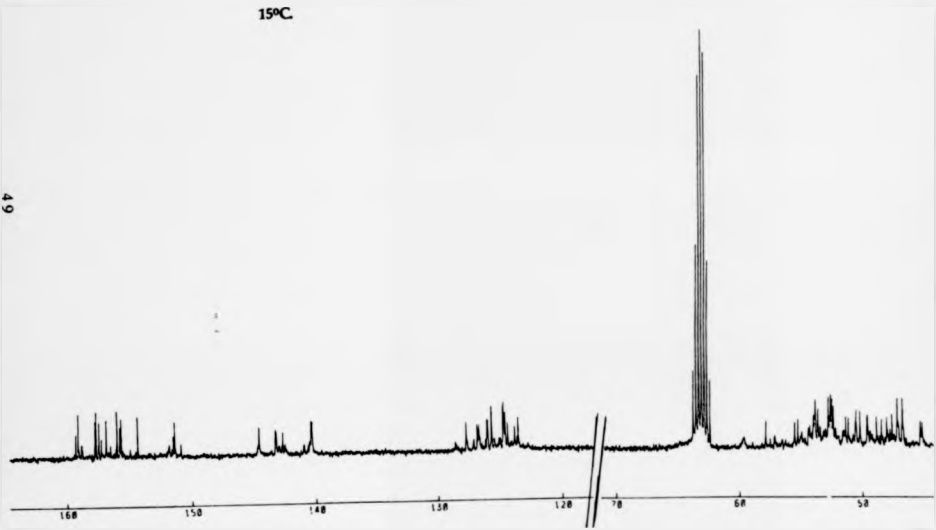

with the ligands L^1 and L^2, the dinuclear Zn(II) cryptates were studied by n.m.r. spectroscopy.

N.m.r. studies of $[Zn_2L(OH)_2][BF_4]_2$

At room temperature the proton decoupled ^{13}C n.m.r. spectrum of $[Zn_2L(OH)_2][BF_4]_2$ (L=L^3 and L^4) shows signs of fluctionality. This was investigated by recording the ^{13}C n.m.r. spectrum at reduced temperatures. On cooling to 15°C the ^{13}C n.m.r. spectrum collapses to give 83 separate resonances! This evidence shows that the compounds are highly fluctional. At room temperature, an average of all the different possible geometries is observed, but on cooling a number of preferred geometries can be seen. No attempt was made to interpret the low temperature spectrum.

U.V.-Visible Spectra.

The u.v.-visible spectral data are given in table 2.2. This data suggests six coordination about the metal ions. Unlike the cryptates of L^1 and L^2, these complexes are soluble in water without decomposition.

Cu(II) and Zn(II) dinuclear cryptates of L^3 and L^4 as model compounds for hydrolytic metalloenzymes.

A number of recent reports[106,107] suggest that simple Cu(II) and Zn(II) complexes could be used as models for hydrolytic metalloenzymes. Kimura[108] has reported that a Zn(II) complex of 12N3, which has proved to be a good model for the active site of carbonic anhydrase. The feature which characterises these models is coordination of either water or hydroxyl to the metal ion. This species is important as it is believed that the coordinated hydroxyl group is the reactive species in the hydrolysis of many substrates. The Cu(II) and Zn(II) dinuclear cryptates of L^3 and L^4 could act as models as these compounds contain bridging hydroxyl groups which could be utilised in this type of mechanism. The compounds can be used for models of metalloenzymes which have two metal centres in close proximity within the active site.

2.2.2.4. Conclusions.

The cryptands L^3 and L^4 display many superior properties when compared to the properties of L^1 and L^2.

(1). L^3 and L^4 form more robust complexes which are water soluble without decomposition.

(2). The complexes of ligands L^3 and L^4 display fluctionality in solution.

(3).The dinuclear Cu(II) and Zn(II) complexes could be used as potential model compounds for hydrolytic metalloenzymes.

The Co(II) dinuclear cryptates of ligands L^3 and L^4 were investigated as possible auto-oxidation driers for aqueous paint systems.

Table 2.2 Characterisation of the dinuclear cryptates of L^3 and L^4.

Dinuclear Cryptate	Colour	U.V. Visible (CH_3NO_2) λ_{max} (ε / $dm^3mol^{-1}cm^{-1}$)	Analysis			Conductivity $\Omega^{-1}cm^{-1}mol^{-1}$ (CH_3NO_2)	Magnetic suscept. μeff/BM
			% C	% H	% N		
$[Ni(OH)_2L^3](BF_4)_2$	Green	988 (15) 612 (14) 388 (35)	46.55 (46.80)	6.06 (6.11)	11.95 (12.13)	172.59	1.69
$[Cu_2(OH)_2L^3](BF_4)_2$	Green	844 (238) 696 (204)	46.21 (42.08)	5.96 (4.61)	11.95 (10.91)	165.62	1.20
$[Zn_2(OH)_2L^3](BF_4)_2$	White		46.01 (46.14)	5.89 (6.02)	11.88 (11.96)	160.7	
$[Ni_2(OH)_2L^4(BF_4)_2$	Green	970 (12) 596 (13)	42.55 (40.99)	5.62 (4.22)	16.44 (16.39)	155.9	1.82
$[Cu_2(OH)_2L^4(BF_4)_2$	Blue	704 (212)	42.11 (39.86)	5.62 (4.50)	16.28 (15.32)	162.5	1.35
$[Zn_2(OH)_2L^4](BF_4)_2$	White		42.09 (42.16)	5.55 (5.68)	16.11 (16.39)	169.2	

Magnetic susceptibilities determined using a Johnson Mathey balance.

2.3. Synthesis and coordination chemistry of two pentaaza macrocyclic ligands containing single pendant coordinating 2-pyridylmethyl arms.

2.3.1. Introduction.

There are many metal complexes which have been shown to coordinate dioxygen reversibly. Jones and collaborators[109] have proved that a coordinating axial base such as pyridine or imadazole is required before reversible dioxygen coordination is observed. In this type of complex the metal ion is coordinated in a planar fashion to four nitrogen donors of a cyclic ligand. Dioxygen then coordinates trans to the axial base (fig. 2.13).

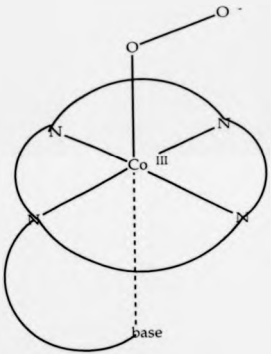

Figure 2.13. The proposed coordination of dioxygen to a metal complex with activating coordinating axial base.

The presence of sterically hindering groups on the ligand prevent irreversible oxidation to μ-peroxy bridged dimer species by a bimolecular reaction. In this section, the synthesis of two such ligands is described and their coordination chemistry explored by u.v.-visible spectroscopy, magnetic susceptibility, conductivity, ^{1}H and ^{13}C n.m.r. spectroscopy, elemental analyses and X-ray crystallography.

2.3.2. Experimental.

The materials, solvents and equipment used were as described in section 2.2.1.2.

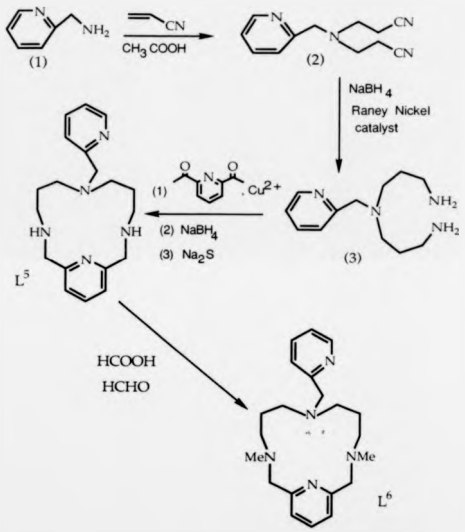

Scheme 2.1 Synthetic route to ligands L^5 and L^6.

Synthesis of 4-(2'-pyridylmethyl)4-amino-1,7-heptanedinitrile (2).

2-Aminomethylpyridine(1) (8g, 0.08 moles) is dissolved in acrylonitrile (92g 1.72 moles). Glacial ethanoic acid (7.2g, 0.16 moles) is added to the solution which shows signs of polymerisation on its addition. The resulting slurry is stirred and heated at reflux under nitrogen for 24 hours after which the solid dissolves and the solution changes to a deep yellow colour. Exess acrylonitrile is removed under reduced pressure, and dichloromethane (150cm^3) added. The organic solution is washed with 0.88 ammonia solution (125cm^3), distilled water (3x100cm^3) and dried (anhydrous $MgSO_4$). After filtration, the solvent is removed to give the product as a yellow oil (9.76g, 57% yield). Electron impact mass spectrum M^+ 214 (calc. 214), infra-red CN 2248cm^{-1}. ^{1}H. n.m.r. ($CDCl_3$ relative populations in parentheses). δ 8.56 (1H, d), 7.75 (1H, t), 7.58 (1H, d), 7.24 (1H, t), 3.90 (2H, s), 2.95 (4H, t), 2.60 (4H, t) ppm. ^{13}C. n.m.r. ($CDCl_3$): δ 158.07 (1), 149.03 (1), 136.83 (1), 123.09 (1), 122.53 (1), 118.75 (2), 59.73 (1), 49.57 (2), 16.70 (2) ppm.

Synthesis of 5-(2,-pyridylmethyl)-1,5,9-triazanonane (3).

This procedure was first described by Egli[111]. To a 50% suspension of active Raney nickel (7.10g) in water is added a solution of dinitrile(2) (9.83g, 0.046 moles) in methanol (200cm^3). Whilst vigorously stirring, a solution of $NaBH_4$ (3.55g, 0.093 moles) in 8 moldm^{-3} NaOH (50cm^3) is added at such a rate as to maintain the temperature at 60^{0}C. After addition the reaction mixture is stirred at room temperature overnight. Raney nickel catalyst is removed by filtration through celite and methanol removed under reduced pressure. A 50cm^3 portion of 8 moldm^{-3} NaOH solution is added to the residue which is extracted with dichloromethane (5x50cm^3). The organic washings were combined, dried (anhydrous Na_2SO_4) and the solvent removed. The impure product is passed down a neutral alumina column (2x20cm long) and eluted with 20% methanol in dichloromethane to give the product (6.43g, 63% yield) Electron impact

mass spectrum: M^+ 222 (calc 222). ^1H n.m.r. ($CDCl_3$):δ 8.55 (1H, d), 7.70 (1H, t), 7.45 (1H, d), 7.17 (1H, t), 3.72 (2H, s), 2.70 (4H, t), 2.55 (4H, t), 1.75 (4H, br), 1.60 (4H, pent) ppm. ^{13}C .n.m.r. ($CDCl_3$): δ 159.45 (1), 148.28 (1), 135.79 (1), 121.26 (1), 59.72 (1), 51.34 (2), 39.62 (2), 29.60 (2) ppm.

Synthesis of L^5. 7-(2'-pyridylmethyl)-3,7,11,17-tetraazabicyclo[11.3.1]heptadeca-1(17),13,15 triene.

$Cu(NO_3)_2.3H_2O$ (6.04g, 0.025 moles) is dissolved in 1:1 ethanol/water (300cm) in a 500cm^3 round bottomed flask. The amine (3) (5.57g, 0.025 moles) is added to the solution which immediately turns royal blue indicating coordination of the amine to Cu(II). Pyridine-2,6-dicarboxaldehyde (3.38g, 0.025 moles) is added and the resulting solution heated on a steam bath for 3 hours. During this time the solution turns deep blue/violet. The solution is transferred to a 2 litre beaker and cooled to 0°C using an ice bath. $NaBH_4$ (4.18g, 0.11 moles) is added slowly over an hour, and the resulting solution stirred at room temperature for 2 hours. After heating on a steam bath for 2 hours, $Na_2S.9H_2O$ (32.42g, 0.135 moles) is added to the cooled solution which is heated for a further hour. The black precipitate (CuS) is removed by filtration through celite. The filtrate is extracted with dichloromethane (6x50cm^3), extracts dried (anhydrous Na_2SO_4), filtered and the solvent removed to give a brown oil. The oil is passed through a neutral alumina column (2x20 cm long), eluted with 2% methanol in dichloromethane. Pure L^5 is obtained by synthesis and recystallisation of the Zn(II) salt (nitromethane/diethylether 1:1) and demetallation of the complex (7.90g) with NaCN (1.75g, 0.035 moles), to give 4.631g of L^5 in 57% yield. Electron impact mass spectrum $(M+1)^+$ m/z 326 (calc. 326). ^1H n.m.r. ($CDCl_3$): δ 8.50 (1H, d), 7.65 (1H, t), 7.55 (1H, t), 7.28 (1H, d), 7.12 (1H, t), 7.08 (2H, d), 3.91 (4H, s), 3.65 (2H, s), 3.41 (2H, br), 2.52 (4H, t), 2.48 (4H, t), 1.75 (4H, pent) ppm. ^{13}C n.m.r. ($CDCl_3$): δ 157.78 (1), 156.09 (1), 147.21 (1), 135.53 (1), 134.87 (1), 121.73 (1), 120.52 (1), 119.40 (2), 57.56 (1), 51.99 (2), 50.54 (2), 44.63 (2), 24.84 (2) ppm

Synthesis of L^6. 3,11-dimethyl-7-(2'-pyridylmethyl)-3,7,11,17-tetraazabicyclo[11.3.1]heptadeca-1(17),13,15 triene.

The ligand L^5 (0.43g, 1.323mmol) is dissolved in 98% formic acid (0.46g, 0.01 moles) in a 50cm^3 round bottomed flask and cooled in an ice bath. Formaldehyde solution (37%,0.1g, 3.17mmol) is added and the resulting solution heated at 90°C for 24 hours. The solvent is removed and the residue co-evaporated twice with concentrated HCl (this converts acid impurities to the acid chloride which are more volatile). The residue is basified to pH>12 with NaOH and extracted with dichloromethane (5x50cm^3). The combined extracts are dried (anhydrous $MgSO_4$), filtered and solvent removed to give the product as a pale yellow oil (0.42g. 90% yield). Electron impact mass spectrum: $(M+1)^+$ m/z 354 (calc 354). ^{1}H. n.m.r. ($CDCl_3$): δ 8.42 (1H, d), 7.75 (1H, t), 7.40 (1H, t), 7.25 (2H, d), 7.06 (1H, t), 6,67 (1H, d), 3.70 (4H, s), 3.50 (2H, s), 2.40 (6H, s), 2.30 (4H, t), 2.22 (4H, t), 1.49 (4H, pent) ppm. ^{13}C. n.m.r. ($CDCl_3$): δ 160.20 (1), 157.52 (1), 147.63 (1), 135.92 (1), 135.27 (1), 122.30 (1), 122.07 (2), 120.95 (1), 64.01 (2), 61.11 (1), 52.55 (2), 51.66 (2), 43.47 (2), 25.11 (2) ppm.

Preparation of the metal complexes of L^5 and L^6.

Solid complexes of L^5 and L^6 were obtained in good yields (>70%) by mixing ethanolic solutions of each ligand with molar equivalents of $[M(dmso)_n][BF_4]_2$[100] (M=Ni, Cu, n=6. M=Zn, n=4). The solid precipitates were isolated by suction filtration under nitrogen and recrystallised from nitromethane/ethanol/diethylether (1:2:2).

X-ray crystallography of $[Zn(L^5)][BF_4]_2$; {7-(2'-pyridylmethyl)-3,7,11,17-tetraazabicyclo[11.3.1]-heptadeca-1(17),13,15 triene}zinc(II) tetrafluoroborate.

The x-ray structural determination of the Zn(II) complex of L^5 was carried out by N.W. Alcock to determine the coordination geometry about the metal ion.

A colourless crystal of 7-(2'-pyridylmethyl)-3,7,11,17-tetraazabicyclo[11.3.1.]-heptadeca-1(17),13,15 triene zinc(II) tetrafluoroborate $C_{19}H_{27}B_2F_8N_5Zn$, M =564.4 orthorhomic space group $P\,2_12_12_1$, a =11.017(9), b =14.515(13), c =14.902(13), U=2383.8(3)A, Z =4, T =290K, Mo-K_α radiation, λ=0.71069A, μ(Mo-K_α)=11.3cm^{-1}. Data were collected with a Nicolet $P\,2_1$ four circle diffractometer in ω-2ϑ mode. Maximum 2ϑ was 45°, with scan range 1.1(2ϑ) around$K_{\alpha1}$-$K_{\alpha2}$ angles, scan speed 4-29° min^{-1} depending on the intensity of a 2-s pre-scan; backgrounds were measured at the end of each scan for 0.25 of the scan time. *hkl* ranges were 0/13; 0/15; 0/15. Three standard reflections were monitored every 200 reflections and showed no changes during data collection. Unit cell dimensions and standard deviations were obtained by least squares fit to 15 reflections (18<2ϑ<22°).

Reflections were processed using profile analysis to give 2672 unique reflections; 2051 were considered observed ($I/\sigma(I)$>2.0) and used in refinement, they were corrected for Lorentz polarisation and absorption effects, the last by the Gaussian method; maximum and minimum transmission factors were 0.86 and 0.79. The crystal dimensions were 0.13 x 0.36 x 0.60mm. Systematic absences h OO,h =2n, Ok O, k =2n, OOl, l =2n indicate space group $P\,2_12_12_1$. The zinc atom was located by the Patterson interpretation section of SHELXTL and light atoms then found on successive Fourier syntheses. Anisotropic temperature factors were used

Figure 2.14. The crystal structure of the cation $[Zn(L^5)]^{2+}$. Hydrogen atoms are omitted for clarity.

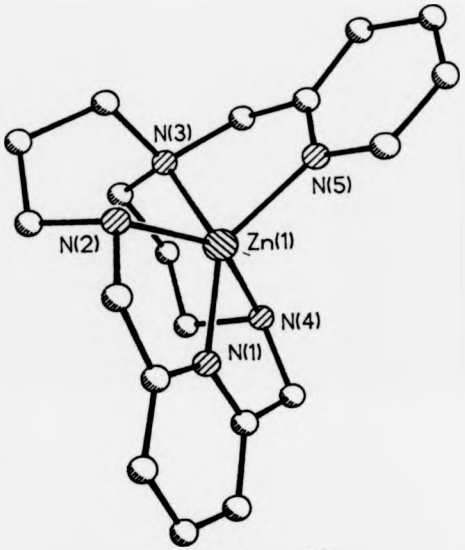

Figure 2.15. The crystal structure of the cation $[Zn(L^5)]^{2+}$ showing atomic numbering.

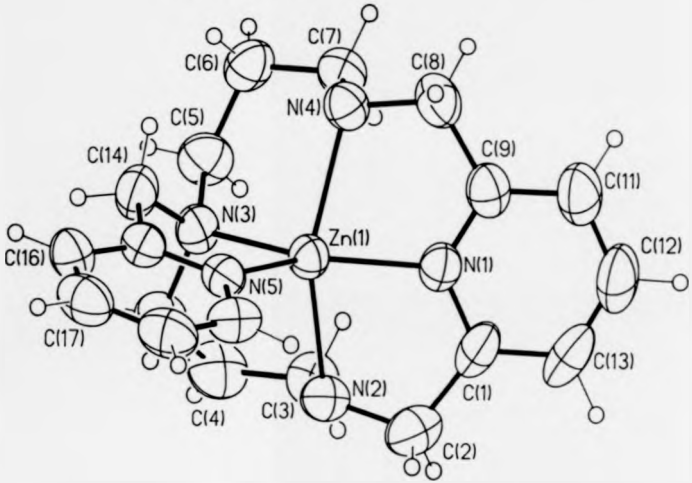

for all non hydrogen atoms. Hydrogen atoms were given fixed isotropic temperature factors, U =0.08A. They were inserted in calculated positions and not refined; their initial orientation taken from the strongest hydrogen atom peaks on a difference Fourier synthesis. The absolute structure of the individual crystal chosen was checked by refinement of ($\delta f''$) multiplier. Final refinement was on F by least square method refining 316 parameters including an isotropic extinction parameter. Largest positive and negative peaks on a final difference Fourier synthesis were of height 0.5 eA^{-3}. A weighting scheme of the form $W=1/((F)+gF^2)$ with g =0.0027 was used and shown to be satisfactory by weight analysis. Final R =0.050 (R_w =0.066). Maximum shift/error in the final cycle was 0.10. Computing with SHELXTL PLUS[112] on a DEC Microvax-II. Scattering factors in the analtyical form and anomalous dispersion factors were taken from reference 113. Final atomic coordinates are given in the appendix. Selected bond lengths and angles are given in table 2.3. The molecular geometry of the cation is shown in figure 2.14.

2.3.3. Results and Discussion.

Ligand Syntheses.

The Michael Addition of acrylonitrile to 2-aminopyridine was facilitated by the use of ethanoic acid as a catalyst. This ensured the addition of two moles of acrylonitrile and also produces a product of higher purity with reduced reaction times.

Previous attempts of the reduction of the dinitrile (2) were unsuccessful as other methods led to unwanted reduction of the pyridine moiety[114]. The method of Egli was used and gave good yields. This method of reduction can be used to reduce nitrile groups in the presence of aromatic groups. The isolation of the amine (3) could lead to the synthesis of a wide range of macrocycles with pendant 2-pyridylmethyl arms.

The ligand L^5 was prepared by the template method on Cu(II). Cu(II) was preferred to Ni(II), which had been used to prepare similar macrocycles[115], as this gave better yields. This short, three step synthesis is an improved method for the preparation of simple pendant pyridyl arm macrocycles. The method also allows subsequent modification of the ligand by reaction at the secondary amine functionality, as illustrated by the synthesis of L^6.

Metal complexes of L^5 and L^6.

The metal complexes have the general formula $[M(L)(OH_2)][BF_4]_2$ except for the Zn(II) complexes which analyses as $[Zn(L)][BF_4]_2$. The diamagnetic Zn(II) complexes of L^5 and L^6 were studied by ^1H and ^{13}C n.m.r. spectroscopy and x-ray crystallography.

Crystal structure of $[Zn(L^5)][BF_4]_2$.

The geometry about zinc can be best described as distorted square pyramidal. The bond lengths between Zn and the pyridine donors are approximately 0.1Å shorter than the remaining Zn-N bond lengths. Zn lies 0.59Å above the plane of the macrocyclic ring towards the pendant pyridyl group. This structure compares favourably with the idealised geometry illustrated in figure 2.13. The structure of the cation (3,11-dibenzyl-7-(2'-pyridylmethyl)-3,7,11,17-tetraazabicyclo[11.3.1]heptadeca-1(17),13,15 triene) zinc(II) has been determined[116] and is shown in figure 2.16. In this structure the geometry is best described as distorted trigonal bipyramidal. The difference between the structures shown in figures 2.14 and 2.16 is the result of the presence of the bulky benzyl groups. In figure 2.15, the ligand has adopted a geometry in which the benzyl groups are as far apart as possible but lying on the same side of the macrocyclic plane hence acquiring the geometry with minimum steric interaction of the pendant groups. The Co(II) complex of this ligand has been shown to be air stable[116]. The benzyl groups do not act as a steric barrier to hinder the formation of μ-peroxy bridged species

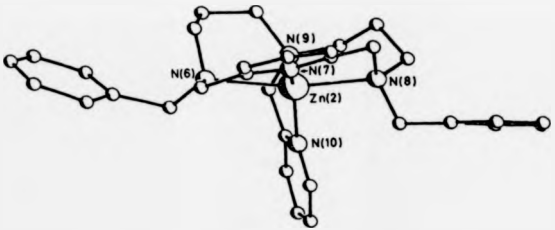

Figure 2.16. The structure of the cation(3,11-dibenzyl-7-(2'-pyridylmethyl)-3,7,11,17-tetraazabicyclo[11.3.1]heptadeca-1(17),13,15-triene zinc(II) from reference 116.

^{13}C n.m.r. spectroscopy of the Zn(II) complexes of L^5 and L^6.

The substituents of the nitrogen donors can protrude above or below the macrocyclic ligand plane. This gives four possible isomers for the metal complexes, shown in figure 2.17. The proton decoupled ^{13}C n.m.r. spectrum of $\{Zn(L^6)\}[BF_4]_2$ is shown in figure 2.18. The spectrum shows the presence of only one symmetric isomer in solution (either (α) or (β)). The x-ray structure of $\{Zn(L^5)\}[BF_4]_2$ establishes the N-H protons to be on the same side as the pendant 2-pyridylmethyl arm.

N.O.E. difference spectra of $[Zn(L^6)][BF_4]_2$.

N.O.E. experiments were undertaken to establish the geometry of $[Zn(L^6)][BF_4]_2$ in solution. The N.O.E. difference ^1H. n.m.r. spectra conclusively show that the pendant arm lies on the same side of the macrocyclic plane as the N-methyl groups. For example, irradiation of the N-methyl protons produced significant N.O.E. enhancements of the ortho hydrogen of the pendant pyridyl group as well as the methylene protons of the pendent arm. This indicates that the solution structure is the same as that found in the crystal of $[Zn(L^5)][BF_4]_2$.

U.V.-Visible spectra of $[M(L)(OH_2)][BF_4]_2$

The u.v.-visible spectral data for the Ni(II) and Cu(II) complexes of ligands L^5 and L^6 are given in table 2.3. It is possible to protonate the pendant pyridyl group in nitromethane solution by addition of triflic acid. This type of behaviour has been reported previously[116]. Again, as reported, the protonated compounds were unstable and accurate absorption coefficients could not be determined.

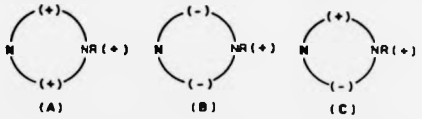

Figure 2.17 Schematic representation of the four possible isomers of complexes of ligands L^5 and L^6 ions (+) and (-) represent the positions of either macrocyclic NH groups, NMe groups or N pendant arm(R), either above or below the macrocyclic ligand plane. The pyridine -N atom is in bold type. (C is enantiomeric.

Figure 2.18. The ^{13}C n.m.r. spectrum of $[Zn(L^6)]^{2+}$ showing one symmetric isomer in CD_3CN solution.

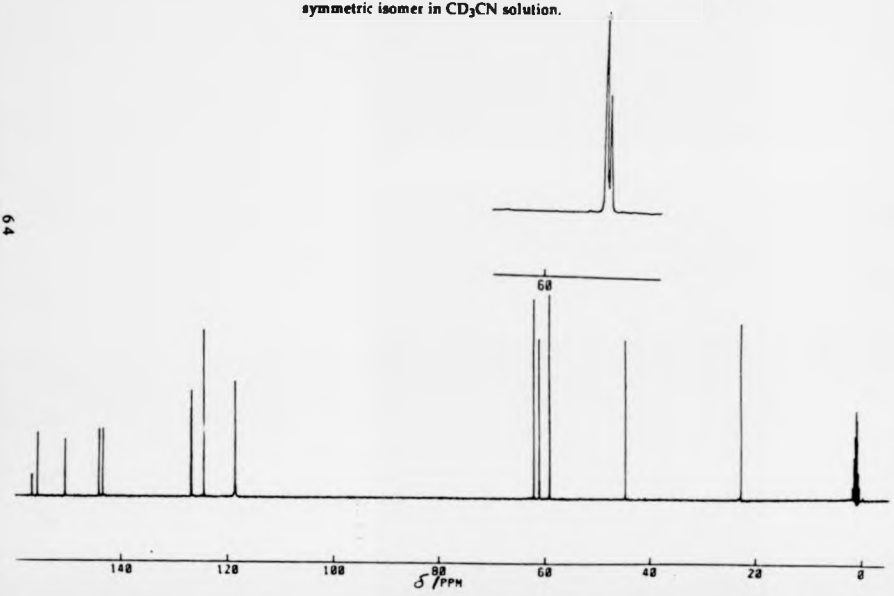

Figure 2.19. The u.v.-visible spectra of $[Ni(L^5)(OH_2)]^{2+}$ (a) and $[Ni(L^5H)]^+$ (b) in CH_3NO_2.

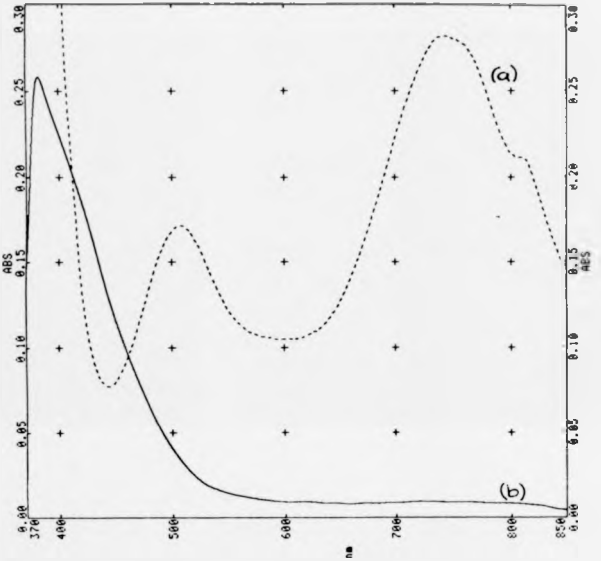

2.3.4. Conclusions.

The synthesis of the ligands L^5 and L^6 demonstrate an improved method of preparing simple pendant arm macrocycles. The x-ray crystal structure of $[Zn(L^5)][BF_4]_2$ shows a distorted square pyramidal geometry. A similar geometry is implied for $[Zn(L^6)][BF_4]_2$ from analogy to $Zn(L^5)][BF_4]_2$, and from n.O.e. difference spectra. Both ligands L^5 and L^6 provide the correct theroretical geometry on chelation to metal ions for the coordination of dioxygen activated by a coordinating axial base.

The Co(II) chemistry of the ligands L^5 and L^6 was investigated and the complexes evaluated as auto-oxidative driers for aqueous paint systems.

Table 2.3 Characterisation of the metal complexes of L^5 and L^6.

Complex	Colour	U.V. Visible (CH_3NO_2) λ_{max} (ϵ / $dm^3mol^{-1}cm^{-1}$)	Analysis			Conductivity $\Omega^{-1}cm^{-1}mol^{-1}$ (CH_3NO_2)	Magnetic suscept. μeff/BM
			%C	%H	%N		
$[NiL^5(OH_2)](BF_4)_2$	Pale blue/ purple	744 (16.6) 504(11)	39.25 (39.63)	5.22 (5.08)	12.06 (12.16)	152.61	3.13
$[CuL^5(OH_2)](BF_4)_2$	Blue	600 (172)	38.80 (39.30	4.76 (5.03)	11.74 (12.06)	149.52	1.95
$[ZnL^5](BF_4)_2$	White		40.20 (40.43)	4.72 (4.82)	12.30 (12.41)	160.17	
$[NiL^6(OH_2)](BF_4)_2$	Green	804 (27) 600 (11) 540 (10)	41.33 (41.77)	5.42 (5.51)	11.28 (11.60)	161.55	3.21
$[CuL^6(OH_2)](BF_4)_2$	Blue	615 (196)	41.29 (41.44)	5.33 (5.46)	11.27 (11.50)	171.42	2.04
$[Zn_2L^6](BF_4)_2$	White		42.17 (42.57)	5.19 (5.27)	11.61 (11.82)	169.2	

Magnetic susceptibilities determined using a Johnson Mathey balance.

2.4. The cobalt chemistry of macrobicyclic ligands L^3 and L^4 and pendant arm macrocycles L^5 and L^6.

In sections 2.2 and 2.3 are described the coordination chemistry of the macrobicyclic ligands L^3 and L^4, and pendant arm macrocycles L^5 and L^6. The following section will highlight the Co(II) chemistry of these ligands and determine their suitability as auto-oxidation catalysts for aqueous paint systems.

2.4.1. The cobalt chemistry of macrobicyclic ligands L^3 and L^4.

2.4.1.1. Introduction.

The cobalt chemistry of the macrobicyclic ligands L^3 and L^4 can be related to the cobalt chemistry of O-bistren which has been studied by Motekaitis and Martell[7]. This chemistry will be outlined briefly.

The dinuclear Co(II) complex of O-bistren was first prepared by Lehn and collaborators[118]. Motekaitis *et al* [119] have reported the dioxygen formation constants. Pontentiometric studies[93] indicate that the simple binuclear complex (A) (figure 2.20) was never more than a minor species in aqueous solution, but is further stabilised by hydroxide ion bridging to give the major species (B) and (C). The dioxygen complex formed from species (B) and (C) is the dibridged μ-hydroxo-μ-peroxo type (D). This species has an unexpectedly low oxygenation constant ($K_{O2}=[D]/([B]P_{O2}]=10^{12}$ atm^{-1}) when compared to those of cobalt complexes of related ligands such as tren[120]. This low stability was attributed to steric crowding of dioxygen within the cryptate cavity. U.V.-visible studies of this compound has demonstrated the reversibility of dioxygen coordination. The absorption at 380nm (peroxo-cobalt charge transfer band) was monitored

(a) over time on equilibriation with dioxygen in air

(b) over the temperature range 25-95ºC.

The charge transfer band was noted to increase with time and decrease with increasing temperature. These effects could be reversed by

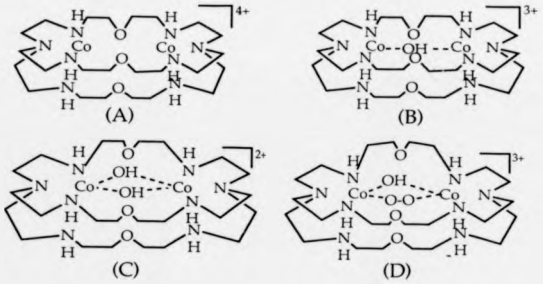

Co-N bonds omitted for clarity.

Figure 2.20. The various species of the binuclear Co O-bistren complex in aqueous solution.

(a) bubbling an inert gas (N_2) through the solution

(b) by decreasing the temperature.

The dicobalt cryptates of ligands L^3 and L^4 were prepared and studied using u.v.-visible spectroscopy.

2.4.1.2. Experimental.

All manipulations were carried out using standard Schlenk-line techniques and conditions. N_2 and Ar gases were bubbled through a deoxygenating solution which consisted of a basic solution of anthraquinone-2-sulphonate(Na salt) over zinc amalgam. U.V.-visible spectra were obtained using a Shimadzu 365 machine with a Churchill

variable control unit. Solutions under study were placed in 1.000cm path length quartz cells with tight fitting teflon stoppers.

Preparation of $[Co_2(L^3)(OH)_2][BF_4]_2$.

0.6g (1 mmol) of L^3 is dissolved in ethanol($10cm^3$) in a Schlenk tube with a magnetic stirrer bar fitted with a tight fitting subaseal. Dioxygen is removed by repeated evaporation/degassing cycles. In a separate Schlenk tube $[Co(dmso)_6][BF_4]_2$[100] (1.542g, 2.2 mmol) is dissolved in ethanol($10cm^3$) and subjected to the same deoxygenation treatment. The cobalt solution is added to the ligand solution using a transfer needle, applying a slightly lower pressure to the ligand Schlenk. On stirring for 20 minutes a pale green solid precipitated. This is collected with a N°3 porosity sinter filter stick and washed with dioxygen free diethylether. The solid was collected under an inert atmosphere and recrystallised from dioxygen free nitromethane/ethanol/diethylether (1:2:2). Yield 62%(0.572g).

Preparation of $[Co_2(L^4)(OH)_2][BF_4]_2$.

The procedure outlined above is used to prepare this compound in 60% yield (0.556g) as a pale purple solid.

2.4.1.2. Results and Discussion.

The formulae of the compounds was assumed from analogy with the dinuclear cryptates described in section 2.2.

U.V.-Visible spectroscopy of the dicobalt cryptates of L^3 and L^4 in water.

(1). Variation of the u.v.-visible spectrum with pH.

The u.v.-visible spectra of the dicobalt cryptates of L^3 and L^4 were recorded at room temperature at different pH values between 8.6 and 10.6. The solutions had been equilibriated in air overnight prior to recording the spectra. The spectra shown in figure 2.21 are for the dicobalt cryptate of L^3. The spectra indicate that the equilibrium concentration of the μ-hydroxo-μ-peroxo bridged dicobalt cascade complex is greatest at pH 8.6. This result is in good agreement with that of Motekaitis[93] who found potentiometrically that the concentration of the μ-hydroxo-μ-peroxo bridged dicobalt cascade complex of O-bistren occurred between pH 7.8 and 8.8.

(2) Variation of the u.v.-visible spectrum with time at pH 8.6.

The previous spectra suggested that the greatest equilibrium concentration of the μ-hydroxo-μ-peroxo bridged dicobalt complex of L^3 and L^4 occurred at pH 8.6. The equilibrium process (O_2 uptake) was followed by recording the u.v.-visible spectrum of a solution of complex at pH 8.6 without pre-equilibration over a period of time. The spectra were recorded at 30 minute intervals. Results obtained are shown in figure 2.22. The figure shows a significant increase in the peroxo-cobalt charge transfer band at 350nm with time. This shows that the complexes $[Co_2(L)(OH)_2][BF_4]_2$ (L= L^3 or L^4) will coordinate dioxygen over a period of

Figure 2.21. The u.v.-visible absorbance spectra showing the equilibration of the dicobalt(L)-dioxygen complex as a function of pH. A=pH 8.6, B=pH 9, C= pH 9.4, D= pH 10, E= pH 10.6.

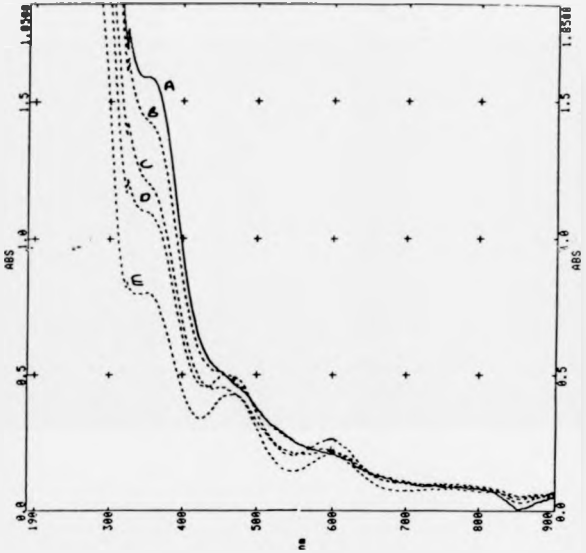

The pH dependence of the species shown in fig. 2.21 are illustrated in equations 2.3 and 2.4 below. (A), (B), (C) and (D) refer to species in fig 2.20.

$$\text{(A)} \overset{OH^-}{\rightleftharpoons} \text{(B)} \qquad 2.3$$

$$\text{(B)} \overset{OH^-}{\rightleftharpoons} \text{(C)} \qquad 2.4$$

Figure 2.22. The equilibration of $[Co_2(L^3)(OH)_2][BF_4]_2$ with dioxygen at pH 8.6 followed by u.v.-visible spectroscopy.

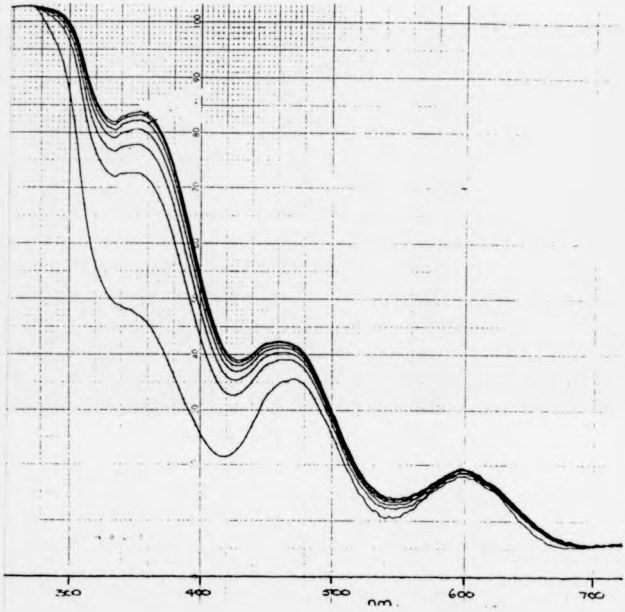

Figure 2.23. U.V.-visible spectra showing the extent of oxygenation of $[Co_2(L^3)(OH)_2][BF_4]_2$ as a function of temperature at pH 8.6.

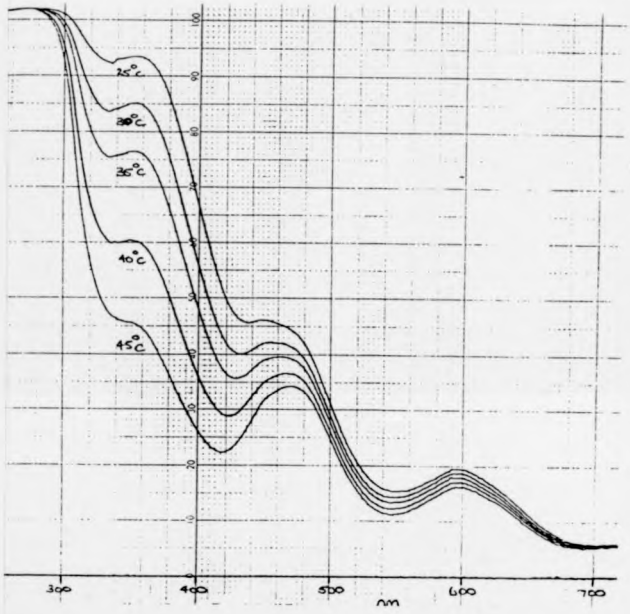

time until the maximum equilibrium concentration of the dioxygen species has been achieved.

Variation of the u.v.-visible spectrum with temperature at pH 8.6.

The u.v.-visible spectra of air equilibriated solutions of $[Co_2(L^3)(OH)_2][BF_4]_2$ and $[Co_2(L^4)(OH)_2][BF_4]_2$ at pH 8.6 were recorded at temperatures between 25 and 45°C. Steady temperature conditions occurred after approximately 45 minutes at each set temperature. The results of this study are shown in figure 2.21. The peroxo-cobalt charge transfer band at 350nm decreases with increasing temperature. This shows that the coordination of dioxygen to cobalt in the cascade complexes of ligands L^3 and L^4 is a reversible process.

2.4.1.4. Conclusions.

The u.v.-visible studies show that the dicobalt complexes of ligands L^3 and L^4 reversibly uptake dioxygen. This is an important property of the desired catalyst. The compounds are relatively easy to handle and manipulate which is of prime importance during paint manufacture. The properties exhibited by these compounds merit evaluation of their ability to act as auto-oxidation catalysts.

2.4.2. The cobalt chemistry of the pendant arm macrocycles L^5 and L^6.

2.4.2.1. Introduction.

The ligands L^5 and L^6 were designed specifically for activation of dioxygen on their coordination to cobalt. Activation was to be achieved by the axial coordination of the pendant pyridyl group to cobalt which destabilises the dz^2 orbital of Co(II). The single electron in this orbital should be of sufficient energy to reduce dioxygen. This approach was investigated and the results obtained compared to those of a related dibenzylated pendant pyridyl containing macrocycle[116].

2.4.2.2. Experimental.

For conditions see section 2.4.1.2.

Preparation of $[Co(L^5)\text{-}\mu(O_2)\text{-}Co(L^5)][BF_4]_4$.

The ligand L^5 (0.325g 1 mmol) is dissolved in ethanol (10cm^3) in a Schlenk tube with a magmetic stirrer bar and tightly fitting subaseal. Dioxygen is removed by repeated evaporation/degassing cycles. $[Co(dmso)_6][BF_4]_2$[100] (0.771g, 1.1mmol) is dissolved in a separate Schlenk tube and subjected to the same deoxygenation treatment. The ethanolic $[Co(dmso)_6][BF_4]_2$ solution is added to the ligand solution using a transfer needle, applying a slightly lower pressure to the ligand Schlenk. Immediately on addition the solution turned brown and on stirring for 10 minutes a brown solid precipitated. This was collected with a N^{o}3 porosity sinter filter stick and washed with dioxygen free diethylether. The solid was recrystallised from dioxygen free nitromethane/ethanol/diethylether (1:2:2). Yield 69% (0.396g).

Preparation of $[Co(L^6)\text{-}\mu(O_2)\text{-}Co(L^6)][BF_4]_4$.

This was prepared following the procedure outlined above. This compound was isolated as a brown solid in 70% yield (0.421g).

Synthesis of $[Co(L)][BF_4]_2$. L=L^5 and L^6.

The isolation of these compounds has been unsuccessful as a result of the presence of dioxygen impurities. Use of different techniques of dioxygen removal from the system (freeze-thaw cycles, exhaustive bubbling of dioxygen free N_2 or Ar gas through the solutions) did not improve the results.

The coordination geometry of the ligands L^5 and L^6 can be assumed to be similar to the square pyramidal geometry exhibited by the Zn(II) complexes of L^5 and L^6. This geometry facilitates the coordination of dioxygen to cobalt as a result of axial coordination of the pendant pyridyl group. Dioxygen coordination is trans to the axial base. Unfortunately, this structure does not hinder the bimolecular reaction which leads to the formation of m-peroxo bridged dimers. Modification of the ligand by the addition of bulky substituents at the secondary amine functionality gives oxygen stable Co(II) complexes[116]. The addition of bulky groups was an attempt to produce a "picket fence" type steric barrier to the bimolecular reaction. The intrinsic flexibility of the macrocycle has allowed the adoption of a geometry which has reduced steric interaction to a minimum. The addition of methyl groups in ligand L^6 does not provide a sufficient steric barrier to the bimolecular reaction.

2.4.2.4. Conclusions.

It proved impossible to isolate the Co(II) complexes of ligands L^5 and L^6. This indicates that the compounds are too reactive to be used as auto-oxidation catalysts for aqueous paint systems. Ensuring a completely dioxygen free environment during paint manufacture is most unlikely. The Co(II) complexes of L^5 and L^6 do not appear to reversibly coordinate dioxygen, one of the required properties of the catalyst.

2.5. The evaluation of the dicobalt complexes of L^3 and L^4 as auto-oxidation catalysts for aqueous paint systems.

2.5.1. Introduction.

This section will describe the evaluation of the dicobalt complexes of L^3 and L^4 as auto-oxidation catalysts in aqueous paint films and compare their ability to that of cobalt(II) acetate, a commercially used catalyst. The chemistry and physical properties of paints will be described.

2.5.1.1. The constituents of paint.

Paint is the most versatile of the many different surface coatings which are used to minimise damage to surfaces. Paints consist of three main ingredients:

(1) **Pigment:** pigments have both decorative and protective properties. The simplest form of paint is whitewash. When dry, this is nothing more than pigment ($CaCO_3$) spread over a surface. This decorates and protects to some extent, but it rubs off.

(2). **Film Former or Binder**: these are polymer resins which bind the pigment particles together and hold them to a surface. If there is no pigment, the film former covers and protects the surface, decorating by giving gloss.

(3). **Vehicle**: the fluidity of paint permits its penetration into the most intricate crevices. Fluidity is achieved by dissolution of the film former or binder in a solvent or by the colloidal suspension of both pigment and film former in a diluent. This diluent or, in some cases, a film former/diluent mixture is the vehicle for the paint.

2.5.1.2. Dry paint film properties.

Once the paint is applied, the properties of the dry paint film must be considered as this influences the choice of the method of drying.

Adhesion: adhesion of the paint to the surface is a critical property. Adhesion is a result of physical forces of attraction between molecules on the surface and the paint. These forces are very short range and at

distances of 1 x 10^{-9}m and above become negligible. The paint must "wet" the surface, displacing air or other adsorbed material. The critical surface tension (γ_c) of a smooth solid surface is a measure of its ease of wetting. It is equal to the surface tension of a liquid that will spread over it immediately when placed on it. For a paint to wet the surface, it must have a surface tension equal or lower than the critical surface tension of the solid.

Hardness, toughness and durability: these properties are connected with the film former. Generally, cross-linked films are tougher and more durable than those polymers that are not cross-linked. However, high molecular weight linear polymers can produce tougher, harder and more durable films than low molecular weight polymers.

Flexibility: hard films tend to be brittle and brittle films fail by cracking and falling off if adhesion is poor. Flexibility is achieved into cross-linked films by increasing the spacing beween the cross-links. Linear polymers are made more flexible by mixing in smaller molecules which act as lubricant allowing the polymer molecules to slide past each other. The small molecules are called plasticisers.

2.5.1.3. The drying of paints.

The mixture of compounds which make up paint must remain stable for long periods so these compounds must not react with each other chemically. But the paint must dry when applied to a surface. There are three mechanisms for the drying of paint, two of which involve chemical reaction.

Drying without chemical reaction: here film formation is facilitated by the evaporation of solvent. The polymer is fully formed in the can and when free of solvent, is relatively hard and non sticky. During drying, there is no chemical change to the polymer. Decorative emulsion paints dry by this mechanism.

Drying by chemical reaction between components within the paint: This type of paint must remain chemically stable when stored and the reactants must react on the application of the paint. Yet the reactants must be held within the paint. This paradox is resolved by either separating the reactants and mixing them prior to application or by choosing reactants that require higher temperatures or exposure to radiation to react.

Chemical reaction beween paint and air: dioxygen is a reactive component of air and is kept separate from paint by a tight fitting can lid. If air is not excluded, reaction at the surface can cause skin formation which can prevent further reaction by forming a barrier between the air and the paint below the skin. Assuming air is excluded, no reactions begin until the paint is applied. As the solvent evaporates, cross-linking begins and low molecular weight polymer is converted to a cross-linked film. This process is relatively slow at room temperature as dioxygen must penetrate into the film before full hardening can occur. Cobalt compounds are used as auto-oxidative paint driers to accelerate the drying process by uptaking dioxygen from the air and forming more reactive oxidising species.

2.5.2. Experimental.

Materials. All materials were prepared at I.C.I. plc (Paints). Dimethyl sulphoxide (dmso) was obtained commercially and used without further purification.

Apparatus. Sand dry and B.K. testers were supplied by I.C.I. plc (Paints). Dioxygen uptake measurements were taken using apparatus designed by I.C.I. plc (Paints).

Techniques. Where applicable, all manipulations were carried out under standard Schlenk conditions. The complexes $[Co_2(L)(OH)_2][BF_4]_2$ ($L=L^3$ and L^4) were prepared as in section 2.4.1.2.

Preparation of a waterborne gloss paint system without cobalt catalyst.

Millbase (250g) was placed in a 500cm^3 paint can. To this was added neutralised polymer solution (199.4g), N.I.A.D. (95.2g) and distilled water (220g). (For the definition of millbase and N.I.A.D. see section 2.5.3.). The components were thoroughly mixed using a palette knife. The viscosity of the resulting paint was measured using a cone and plate viscometer and water added until the viscosity was 3 poise. This required the addition of further water (17g).

Preparation of a waterborne gloss paint system incorporating cobalt(II) acetate as catalyst.

The cobalt(II) acetate catalyst was added at a level to give 0.2% by weight cobalt metal. Cobalt(II) acetate tetrahydrate (0.844g, 3.39mmol) was dissolved in dmso (3g). This solution was added to 96.156g of the waterborne gloss paint previously prepared and shaken to ensure complete mixing.

Preparation of waterborne gloss paints containing $[Co_2(L)(OH)_2][BF_4]_2$ (L=L^3 and L^4) as catalysts.

The procedure outlined above was used to prepare the test paint samples. The catalysts were added to give 0.2% by weight cobalt metal. $[Co_2(L^3)(OH)_2][BF_4]_2$ (1.566g,1.69mmol) was dissolved in dmso (3g) and added to paint (95.434g). $[Co_2(L^4)(OH)_2][BF_4]_2$ (1.571g, 1.69mmol) was dissolved in dmso (3g) and added to paint (95.429g).

Measurement of dioxygen uptake of waterborne gloss paint systems.

Dioxygen uptake of the aqueous paint samples were determined using apparatus designed at I.C.I. plc (Paints). This consisted of a glass apparatus, comprised of two chambers which are connected by a glass tube. A three way tap was positioned in the tube that connected the two chambers. A differential pressure transducer was used to determine the

difference in pressure between the two chambers, one which contained the test sample and the second which was empty (reference) (figure 2.24).

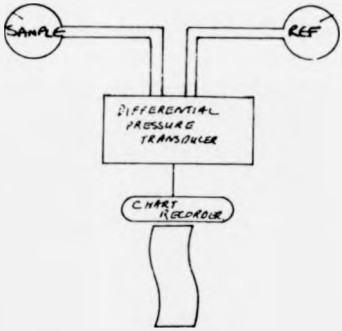

Figure 2.24. A schematic diagram of the dioxygen uptake apparatus.

NaOH (10g) was placed in each of the chambers to absorb CO_2 from the air. Two glass slides were washed with acetone and wiped dry. One slide was weighed and a sample of the paint under test was drawn along the slide to give a film thickness of 100µm. The slide was left to stand at room temperature for 30 minutes to allow the solvent to evaporate. The slide was reweighed to determine the weight of the paint film and placed in the sample chamber. The second glass slide was placed in the reference chamber. The glass apparatus was suspended in a constant temperature bath at 25°C in a constant temperature room at 25°C. Dioxygen uptake was monitored over 8 hours by feeding the output of the pressure transducer directly to an XY chart recorder.

Determination of the drying properties of the paint films

(1). Sand Dry.

This is a very simple test which determines the speed at which the paint films become surface dry. A large glass panel was copiously cleaned using acetone to remove all traces of grease from the surface. The paint samples were spread (37μm thickness) along the length of the panel and placed in the sand drier. This consists of a small hopper containing sand which falls on to the surface of the panel. The hopper moves over the surface of the panel at a fixed rate (1 inch $hour^{-1}$). At the end of the test, the panel is removed from the sand dry tester and excess sand removed. The time of surface drying was indicated by the point at which the sand did not stick to the paint films.

(2). B.K. Dry.

Another simple test which allows the determination of both surface and through drying times. A large glass panel was washed with acetone to remove grease. The paint samples were spread (37μm film thickness) along the lengh of the panel and the panel placed in the B.K. drier. This consists of a small needle which is pulled at a fixed rate (2 inches $hour^{-1}$) through the paint films. When the paint is wet, the needle scratches the paint film to the glass. On surface dryness the needle breaks the surface of the film. On through drying the needle does not break the paint film. Sand dry and B.K. dry tests were carried out at 25°C in a constant temperature room.

Optical microscopy of the paints.

The morphology of the paints prepared was investigated using an optical microscope. The paint samples were diluted with water (x 20) and a small drop placed on a clean microscope slide. The drop was covered by a small cover plate and a drop of oil placed on the plate to ensure that the lens of the microscope was not damaged. Photographs of the images seen were recorded.

2.5.3. Results and Discussion.

The paint consisted of the following components:

Millbase: essentially a dispersion of TiO_2 in water, sterically stabilised.

Neutralised polymer solution: An acrylic polymer that has been neurtralised by NaOH solution (9.5% by weight) to improve its solubility in water.

N.I.A.D.: A non ionic aqueous dispersion of an acrylic emulsion polymer stabilised by steric means.

The vehicle for the paint was water. The paint consists of the three components contained in most paints but also a very small quantity of N.I.A.D. This acrylic polymer has a glass transition temperature (T_g) of approximately 30°C. At this temperature the polymer undergoes the transition from displaying properties of a glassy material to displaying properties associated with rubbers. The N.I.A.D. is added to give the paint film added strength (glass-like property) and added flexibility (rubber-like property) at room temperature. Addition of the N.I.A.D. has the added side effect of improving the glossof the paint film[121].

The paint mixtures became unstable on addition of the catalysts which were dissolved in dmso. As this was a feature common to all of the paint samples, it was concluded that the problem arose as a result of the incorrect mixing of the paints. On spreading, the paints formed very poor quality films as a result of the flocculation of the pigment. As this was observed for all of the paints, the film properties could be investigated and compared. The morphology of the paint systems were investigated to determine the cause of flocculation.

Figure 2.25. Optical microscopy of the paint sample prior to the addition of any catalyst. Scale 1 cm = 20μm.

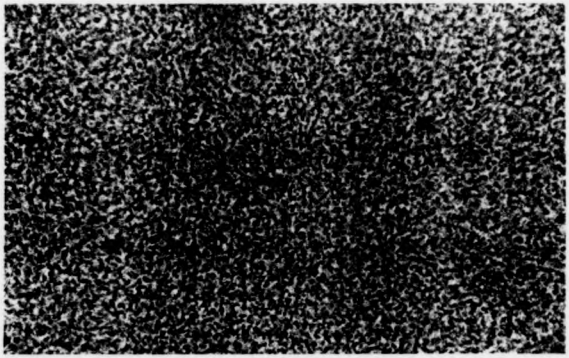

Figure 2.26. Optical microscopy of the paint sample on addition of Co acetate catalyst in dmso. Scale 1cm = 20μm.

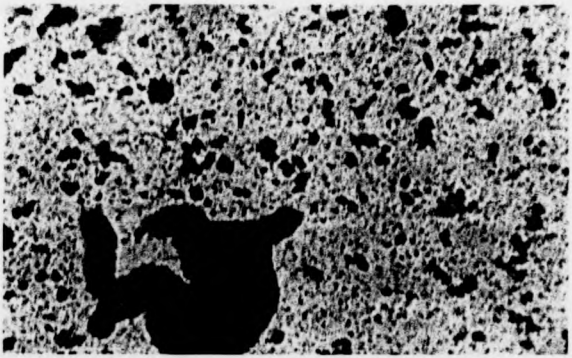

Optical Microscopy of paint samples.

The paint prepared without added catalyst was shown to consist of TiO_2 particles (2μm diameter) uniformly dispersed throughout the sample (figure 2.25). Addition of the catalyst dissolved in dmso has caused aggregation of the TiO_2 particles (figure 2.26) observed as large floccs within the paint. Agitation of the paint will cause some breakdown of the floccs but a stable paint cannot be formed. The results indicate that the addition of dmso has caused flocculation. To check this, dmso was added to the millbase and the N.I.A.D. The N.I.A.D. immediately flocculates and evolves heat on the addition of dmso. The destabilisation of the paint samples were caused by the flocculation of the N.I.A.D. on addition of dmso which results in the aggregation of TiO_2 particles.

Dioxygen uptake measurement of the paint films.

The results obtained from these measurements can only be considered qualitatively[122]. All the paint samples exhibited some uptake of dioxygen. Problems were encountered with the sensitivity of the chart recorder so measurements of the fall in pressure of the sample chamber were noted (table 2.4). The fall in pressure of the sample chamber was considered to be the result of dioxygen uptake of the sample.

Table 2.4 Dioxygen uptake measurements.

Complex	Weight paint film (g)	Pressure drop (mmH$_2$O) after 8 h.
Co(II) acetate	0.0416	5
$[Co_2(OH)_2(L^3)(BF_4)_2$	0.0522	7
$[Co_2(OH)_2(L^4)(BF_4)_2$	0.0472	7

Optical Microscopy of paint samples.

The paint prepared without added catalyst was shown to consist of TiO_2 particles (2μm diameter) uniformly dispersed throughout the sample (figure 2.25). Addition of the catalyst dissolved in dmso has caused aggregation of the TiO_2 particles (figure 2.26) observed as large floccs within the paint. Agitation of the paint will cause some breakdown of the floccs but a stable paint cannot be formed. The results indicate that the addition of dmso has caused flocculation. To check this, dmso was added to the millbase and the N.I.A.D The N I A.D. immediately flocculates and evolves heat on the addition of dmso. The destabilisation of the paint samples were caused by the flocculation of the N.I.A.D. on addition of dmso which results in the aggregation of TiO_2 particles.

Dioxygen uptake measurement of the paint films.

The results obtained from these measurements can only be considered qualitatively[122]. All the paint samples exhibited some uptake of dioxygen. Problems were encountered with the sensitivity of the chart recorder so measurements of the fall in pressure of the sample chamber were noted (table 2.4). The fall in pressure of the sample chamber was considered to be the result of dioxygen uptake of the sample.

Table 2.4 Dioxygen uptake measurements.

Complex	Weight paint film (g)	Pressure drop (mmHg(Torr)) after 6 h.
Co(II) acetate	0.0416	5
$[Co_2(OH)_2(L^3)(BF_4)_2$	0.0522	7
$[Co_2(OH)_2(L^4)(BF_4)_2$	0.0472	7

PAGE(S) MISSING
NOT AVAILABLE

TABLE 2.5

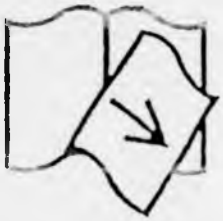

Drying properties of the paint films.

The results obtained from the sand dry and B.K. dry tests are recorded in table 2.6. The cobalt(II) acetate paint film was surface dry quickly in 1.25 hours. Through drying occurred after 5 hours; a result of the slow dioxygen permeation through the formed paint film. The dicobalt cryptates acted as auto-oxidative paint driers, producing dry paint films in 3 hours but surprisingly, through cure occurred 30 minutes later. The speed of through cure can only be a result of a different drying mechanism occurring within the paint film, i.e. at the surface, cross-linking occurs by uptake of dioxygen and in the body of the paint film by an hydroxide ion mechanism postulated for secondary paint driers[87].

Table 2.6 The drying times of the paint films as measured by sand and B.K. tests.;

Catalyst	Sand Dry (hr.)	B.K. Dry (hr)	
		Surface	Through
Co(II) acetate	1.25	1.25	5
$Co_2(OH)_2(L^3)(BF_4)_2$	3	3	3.5
$[Co_2(OH)_2(L^4)(BF_4)_2$	3	3	3.5

2.5.4. Conclusions.

The method used to prepare the paint samples gave problems with paint stability and poor paint film quality.

The dicobalt cryptates of L^3 and L^4 were active as auto-oxidation catalysts. Their surprising speed of through cure suggests a different drying mechanism occurs in the body of the paint film. This could be utilised in the development of secondary paint driers.

2.6 Further Work.

The work described in Part 2 could be extended to include the following:

The evaluation of the dicobalt cryptates of L^3 and L^4 as auto-oxidation catalysts for aqueous paint systems was hindered by the poor quality of the paint films and paint instability. This problem could be overcome by the addition of the catalyst to the millbase prior to the addition of the neutralised polymer solution, water and N.I.A.D.[123]

The cobalt(II) complexes of L^5 and L^6 proved too reactive to isolate. Use of the secondary amine functionality to attach L^5 to a polymer support (perhaps chloromethylated polystyrene) would reduce to a minimum the bimolecular reaction and allow easy handling of the compound. The properties of the polymer support can be modified to suit the properties required of the paint film.

Another approach to circumvent the problem of the bimolecular reaction which forms the μ-peroxo bridged dimer would be to use the method of Busch and co-workers[124] and prepare a vaulted complex by modification of the ligand L^5 at the secondary amine functionality.

The Fe(II) chemistry of L^5 and L^6 could be studied as a synthetic model system of iron in haemoglobin and myoglobin.

PART THREE

AZAMACROCYCLIC ORGANOCOBALT(III) COMPLEXES.

3.1. Introduction.

Part three is concerned with the preparation and use of azamacrocyclic organocobalt(III) complexes in living free radical polymerisation reactions. The mechanism of polymerisation will be discussed.

3.1.1. Organocobalt(III) compounds.

The discovery of the naturally occurring cobalt-carbon bond of Vitamin B_{12}[125] coenzyme has led to the study of many organocobalt(III) compounds. This introduction will present a brief overview of the chemistry of organocobalt(III) compounds. Work in this area has mainly centred on alkylcobaloximes and alkylcobalamins. The nature of the Co-C bond will be highlighted.

3.1.1.1. Preparation of organocobalt(III) compounds.

Several methods for the synthesis of organocobalt(III) compounds have been reported. These include the following methods:-

(1): Reactions of Grignard reagents with halocolbalt(III) compounds.

Generally this method has only been successfully applied to halocobalt(III) compounds which are soluble in organic media and which do not decompose the organometallic reagent[126]. For example

$$PhC{\equiv}CMgX + Co(dmgH)_2py \longrightarrow PhC{\equiv}CCo(dmgH)_2py + MgX_2 \quad (3.1)$$

(2): Reaction of Co(II) compounds with free radicals.

Co(II) species are paramagnetic and are capable of initiating and terminating free radical reactions. One of the earliest methods of synthesis of organocobalt(III) compounds involved the addition of an alkyl halide to a solution of pentacyanocobalt(II) ion under anaerobic conditions. The

Co(II) species acts as both halogen atom extractor and as a free radical trap for the free radical formed producing the relatively stable organopentacyanocobaltate(III) ion[127]. This reaction can be applied to

$$RHal + Co(CN)_5^{3-} \longrightarrow R + HalCo(CN)_5^{3-} \quad (3.2)$$

$$R + Co(CN)_5^{3-} \longrightarrow RCo(CN)_5^{3-} \quad (3.3)$$

other Co(II) compounds, but there are few examples of its application, and many require the use of fairly reactive halides[128]. For example

$$CCl_4 + 2\,Co(dmgH)_2py \longrightarrow Cl_3CCo(dmgH)_2py + ClCo(dmgH)_2py \quad (3.4)$$

(3): Nucleophilic attack by Co(I) species.

The most common route to an organocobalt(III) compound involves the reaction of a nucleophilic Co(I) species with an organic compound. A wide range of Co(I) species can be used (including anionic bis(dimethylglyoximato)pyridinecobaltate(I) ion). Co(I) species are among the most powerful nucleophiles known for attack of saturated carbon compounds, readily displacing halide, tosylate and phosphate[129] from their alkyl derivatives, e.g.

$$CHBr_3 + [Co(dmgH)_2py]^- \longrightarrow Br_2CHCo(dmgH)_2py + Br^- \quad (3.5)$$

(4): Addition of hydridocobalt compounds to alkenes and alkynes.

Co(I) species in basic media tend to form covalent hydrides[131] which can react with unsaturated compounds. Diazomethane has been reported to react with hydridocobalt compounds[129].

$$H_2CCHCN + HCo(dmgH)_2py \longrightarrow NCCHMeCo(dmgH)_2py \quad (3.6)$$

3.1.1.2. Properties of organocobalt(III) compounds.

In solution, most organocobalt(III) compounds are unstable to visible light. Secondary Co-C bonds are less stable than primary Co-C bonds. There are few reported examples of tertiary Co-C bonds. The electronic spectra of alkylcobaloximes are complex and in some instances ill-defined. Equatorial ligand transitions occur in regions where they are indistinguishable from transitions associated with the axial base ligand. The bands observed beween 400-500nm are probably a result of d-d transitions[133]. Infra-red spectroscopy has been used to give information on the *cis* and *trans* influences of equatorial and axial ligands on one another. The axial cyanide stretching frequency of alkylcobalamins[134], alkylcobaloximes[135] and alkylpentacyanocobaltates[136] have been studied and show some correlation[135]. N.m.r spectroscopy has proved to be a useful tool in the study of organocobalt(III) compounds. These compounds are diamagnetic. The chemical shift of the organic group is dependent upon a number of factors which include the electronic effects of the equatorial and axial ligands. An example of this is the small changes observed in the methyl resonance of methylcobaloximes on changing the axial base[137,138].

Reactions of organocobalt(III) compounds.

The compounds undergo four basic types of reaction, which are as follows:

(1) Co-C bond cleavage

(2) Insertion into Co-C bonds

(3) Reactions of the coordinated ligand

(4) ligand displacement.

The two types of relevance are (1) and (2).

3.1.1.3.1. Co-C bond cleavage reactions.

(a): Cleavage by nucleophiles: several β-substituted ethylcobaloximes react with base to give an alkene and Co(I) species.

Electron attracting β-substituents increase the tendency of organocobalt(III) compounds to undergo elimination reactions. Generally, the ability of a nucleophile to cause dealkylation of an organocobalt(III) compound is dependent on the electron density at cobalt. Several nucleophilic reagents (thiols, BH_4^-) are capable of acting as reducing agents towards organocobalt(III) compounds.

$$[(Co)(CHCCR_2)py] + BH_4^- \longrightarrow R_2CCCH_2 + [(Co)py]^- \qquad (3.7)$$

(b): Cleavage by electrophiles: A number of electrophilic reagents (metal ions, halogens *etc)* will induce cleavage of the Co-C bond. Hg(II) species are effective reagents for the cleavage of Co-C bonds by attack at carbon. This was first demonstrated by Halpern and Maher[139] who isolated methylchloromercury(II) by reaction of mercury(II) chloride with methylpentacyanocobaltate(III).

$$MeCo(CN)_5^{3-} + HgCl_2 \longrightarrow MeHgCl + Cl^- + Co(CN)_5^{2-} \qquad (3.8)$$

Other electrophiles, such as nitrosyl chloride, will attack at carbon. Reaction of nitrosyl chloride with benzylpentacyanocobaltate(III) gives the corresponding aldoxime[140].

$$PhCHCo(CN)_5^{3-} + NOCl \longrightarrow Co(CN)_5^{3-} + Cl^- + PhCH_2NO \longrightarrow PhCHNOH \qquad (3.9)$$

(c): Homolytic cleavage of Co-C bonds: Homolytic cleavage of Co-C bonds occurs under several conditions including on heating and on irradiation. The photochemical reactions of organocobalt(III) compounds

are efficient and absorption of visible light leads to homolysis of the Co-C bond to give Co(II) and free radical[141, 142].

$$RCo(III) \xrightarrow{h\upsilon} R + Co(II) \qquad (3.10)$$

The Co-C bond is relatively weak(85-125kJmol^{-1})[143]. A study of the aerobic photodecomposition of alkylcobalamins show that the quantum yields are dependent on the pH of the solution and the wavelength of the incident light (250-570nm). Alkylaquocobaloximes in aqueous solution under anaerobic conditions are very photosensitive. The ease of homolytic cleavage is dependent upon the inductive and steric effects of the alkyl ligand. Most organocobalt(III) compounds decompose on heating without melting. This involves homolytic cleavage or β-hydride elimination. The thermal stability of organocobalt(III) compounds decreases from primary alkyl substituents through secondary to tertiary alkyl substituents.

3.1.1.3.2. Insertion reactions.

SO_2 reacts with organocobalt(III) compounds to give the corresponding alkanesulphonylcobalt(III) compound[142,143].

$$RCo(dmgH)_2py + SO_2 \longrightarrow R(SO_2)Co(dmgH)_2py \quad (3.11)$$

Organocobalt(III) compounds undergo thermal insertion of oxygen. The mechanism for the photochemical reaction is not fully understood, but it is believed that the axial base is labilised in the excited state and the resulting five coordinate species rapidly reacts wih oxygen. Thermal insertion of oxygen has been of special interest as the thermal reaction is only observed with less stable organocobaloximes[145].

3.2. Azamacrocyclic organocobalt(III) complexes as living free radical polymerisation catalysts.

3.2.1. Introduction.

The homolytic cleavage of Co-C bonds yields alkyl radicals and Co(II). This process leaves a vacant coordination site on Co(II) to which a suitable substrate (e.g. activated alkene) can be added. This process can initiate carbon-carbon bond formation and polymerisations.

The work presented is an extension of research carried out by a Postdoctoral Research Assistant at Warwick, Dr. H.A.A.Omar. This introduction will briefly review his findings

3.2.1.1. Synthesis of azamacrocyclic organocobalt(III) compounds.

The majority of existing organocobalt(III) compounds have Co coordinated to unsaturated or partially saturated ligands such as porphyrins or Schiff's-base macrocycles. Very few organocobalt(III) complexes of fully saturated azamacrocycles have been prepared[148].

Organocobalt(III) compounds of saturated azamacrocycles were prepared following the method of Espensen[148]. In this reaction, the anaerobic photolysis of an alkylcobaloximes $[RCo(dmgH)_2py]$ at low pH in the presence of $[Co(mac)]^{2+}$ ions (mac= saturated azamacrocycles) gives the corresponding organocobalt(III) azamacrocyclic compound. This method takes advantage of the acid lability of the bis(dimethylglyoximate)cobalt(II) complex and the acid inertness of many $[Co(mac)]^{2+}$ ions. The reaction is illustrated below.

$$trans[py(dmgH)_2Co(III)R] \longrightarrow [(H_2O)(dmgH)_2Co(II)] + py + R$$

$$[(H_2O)(dmgH)_2Co(II)] + 2H \longrightarrow [Co(H_2O)_6]^{2+} + dmgH_2$$

$$[Co(mac)(H_2O)]^{2+} + R \longrightarrow trans[CoR(mac)(H_2O)]^{2+}$$

The yield of azamacrocyclic organocobalt(III) compounds prepared by this route is approximately 30%. The *trans* geometry of these compounds was established by x-ray crystallography.

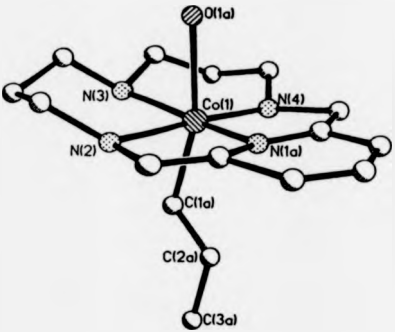

Figure 3.1 The crystal structure of *trans*- $[RCo(L)OH_2]^{2+}$.

R=Propyl

L=3,7,11,17-tetraaza-bicyclo[11.3.1]heptadeca-1(17),13,15-triene.

A range of azamacrocyclic organocobalt(III) compounds were prepared by this method and their ability to catalyse the polymerization of alkenes in different media investigated.

3.2.1.2. Polymerization of alkenes in aqueous media.

Polymerization of alkenes was carried out in aqueous media using emulsion polymerization conditons. A small quantity (typically 1mg) of azamacrocyclic organocobalt(III) catalyst was used in the polymerisation of 2 grams of alkene. The catalyst, disolved in the aqueous phase, was photolysed using a 300W sun lamp.There was a quantitative yield of polymer. The molecular weight of the polymer, determined by Gel Permeation Chromatograghy (G.P.C.) was approximately $1x10^6$. This indicates that polymerisation is occurring *via* a free radical pathway. On photolysis, the catalyst yields alkyl radicals which initiate polymerisation. This is confirmed by the addition of a free radical scavenger (2,6-(t-butyl)phenol) to the system which inhibits polymerization.

3.2.1.3. Polymerization of alkenes in organic media.

Polymerization of alkenes was carried out in tetrahydrofuran (thf) solution. The solubility of the catalysts in thf is low; 1 mg of catalyst was used to polymerise 2g of alkene. On photolysis of the solution over 18 hours a number of observations were made:

(a). The catalyst slowly dissolves in the solution with time.

(b). The viscosity of the solution increases with time. This was indicated by the speed of rotation of the magnetic stirrer bar which was noticed to decrease with time. In some cases the viscosity of the solution was such that the magnetic stirrer bar would not rotate.

(c). Further addition of alkene to the system followed by photolysis gives further polymerization.

(d). Addition of a free radical scavenger to this system does not inhibit polymerization.

These results show that polymerization occurs by a different mechanism. The molecular weight of the polymer was determined by G.P.C. to be of the order 2×10^4.

3.2.1.4. Copolymerization of styrene and ethylacrylate in thf.

The copolymerisation of styrene and ethylacrylate was attempted by the method previously decribed in section 3.2.1.3. The copolymer was characterised by ^{13}C n.m.r. and found to contain no styrene units. This observation, coupled with those presented in 3.2.1.3. indicate that in thf solution, polymerization must occur *via* a metal based mechanism. This evidence also supports the view that only activated alkenes (alkenes with electron-withdrawing substituents) will polymerize by a metal based mechanism.

3.2.1.5. Spectulative mechanism for the polymerization of activated alkenes in thf.

The proposed mechanism of polymerization in thf is shown in scheme 3.1. The postulated mechanism indicates that the initial step involves the loss of the axial water ligand and isomerisation from a *trans*-geometry to a *cis*-geometry. This leaves the vacant site in a *cis*-position to the alkyl group. This is followed by the coordination of alkene at the vacant site. On photolysis, homolysis of the Co-C bond is followed by *cis*-migration of the radical to the alkene, leaving a new vacant site on Co which coordinates another molecule of alkene. Hence propagation proceeds.

The proposed mechanism for termination is shown in scheme 3.2. Termination could occur by β-hydride elimination which produces a stable hydridocobalt species. It has been reported that hydridocobalt species are capable of the addition of alkenes. The observed "living" polymerisation of alkenes in thf could be the result of the presence of the hydridocobalt species.

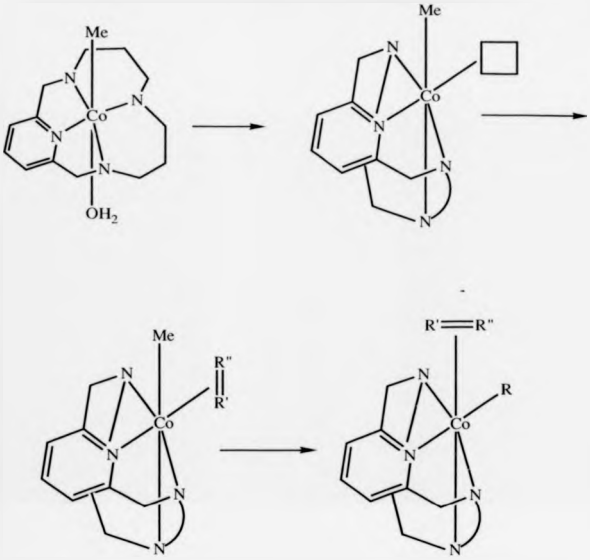

PROPAGATION

Scheme 3.1 Speculative mechanism for the polymerisation of alkenes by azamacrocylic organocobalt(III) complexes in thf. The macrocyclic N functionality is omitted for clarity.
R= growing polymer chain.

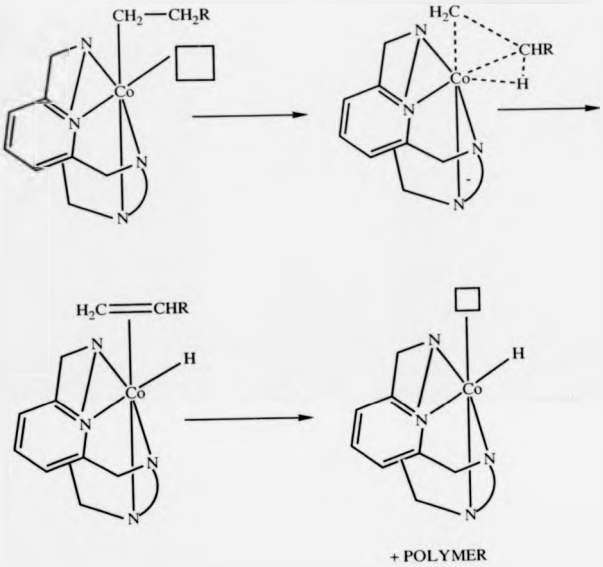

Scheme 3.2 Termination by β-hydride elimination. The macrocycle N functionality is omitted for clarity.

In this section, the mechanism of polymerization of activated alkenes by azamacrocyclic organocobalt(III) compounds was investigated by

(1). Isolation and characterisation of azamacrocyclic hydridocobalt(III) compounds by the reaction of hydrogen with cobalt(II) azamacrocyclic complexes.

(2). determination of the polymer tacticity.

(3). Diode Array Gel Permeation Chromatography of polymer samples taken at regular intervals during photopolymerisation.

A second area was to develop an azamacrocyclic ligand which would increase the solubility of the macrocyclic organocobalt(III) complexes in organic media

3.2.2. Experimental.

Materials, solvents and spectroscopy were used as detailed in section 2.2.1.2. Gel Permeation Chromatography(G.P.C.) and Diode Array G.P.C. were carried out at I.C.I plc (Paints). G.P.C. was carried out using the following equipment: Perkin Elmer series 2 pump, Perkin Elmer LC420 auto injector, Perkin Elmer LC100 column oven, ERMA ERC 7510 refractive index detector interfaced to a Digital NEC 380 computer. Three PL gel columns of length 30cm were used with particle size 10μm with pore size $1x10^{-4}m$, $1x10^{-6}m$ and $5x10^{-8}m$. The molecular weight and polydispersity of the polymers was determined from a calibration curve obtained by g.p.c. using polystyrene standards. The solvent used was thf at a flow rate of $1cm^3min^{-1}$. The solvent was degassed on line using a ERMA 3RC 3310 vacuum degasser.

The apparatus used for Diode Array G.P.C. was as follows:- Waters 510 pump, Waters 712 wisp auto injector, Waters 990 photodiode array detector, three Waters ultrstryragel columns-30cm in length, particle size 10μm. The three columns had the following internal pore diameters: 10^3-$10^5x10^{-10}m$, $500x10^{-10}m$ and $100x10^{-10}m$. The solvent used was u.v. grade

unstabilised thf. A NEC APC(III) computer was used with Waters Revision 3 software.

Synthesis of Ligands L^7 and L^8.

Synthesis of L^7, 3,7,11-trimethyl-3,7,11,17-tetraazabicyclo[11.3.1]heptadeca-1(17)13,15-triene.

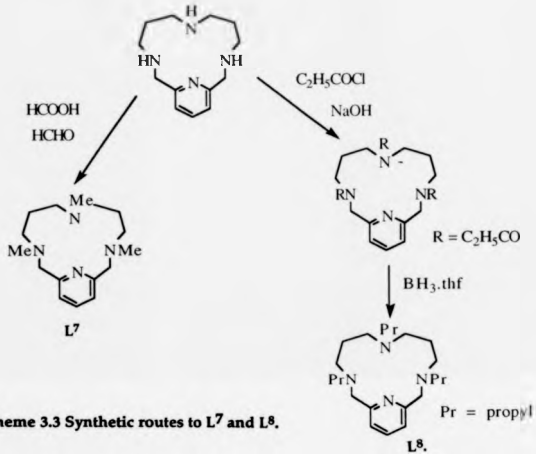

Scheme 3.3 Synthetic routes to L^7 and L^8.

3,7,11,17-tetraazabicyclo[11.3.1]heptadeca-1(17)13,15-triene (1) was prepared by a template reaction with Cu^{2+} as previously reported[152]. L^7 was prepared using the route shown in scheme 3.3 by the method published by Omar[153].

Synthesis of 3,7,11-triethylamide-3,7,11,17-tetraazabicyclo[11.3.1]heptadeca-1(17)13,15-triene, 2.

The ligand (1) (5.81g, 0.025 moles) is dissolved in water (100cm^3) and NaOH (3g, 0.075 moles) added. Propanoyl chloride (7.40g, 0.08 moles) is

dissolved in dichloromethane (100cm^3) and placed in an addition funnel. The dichloromethane solution is added slowly to the aqueous solution under N_2 with vigorous stirring. Stirring is continued overnight. The two phases are separated and the aqueous layer extracted with dichloromethane (3x50cm^3). The combined extracts and organic layer were dried (anhydrous $MgSO_4$) and solvent removed to give a pale yellow oil. The oil is passed down a silica column(2 x 20cm length) eluted with 2% methanol in dichloromethane to give a colourless oil. Repeated column chromatography failed to give a spectroscopically pure compound, although an electron impact mass spectrum gave the molecular ion peak at m/z 402 (calc 402). Crude yield 8.67g.

Synthesis of L[8], 3,7,11-tripropyl-3,7,11,17-tetraazabicyclo[11.3.1]heptadeca-1(17)13,15-triene.

The crude product, compound 2, is dissolved in dry thf (150cm^3) and placed in a 1dm^3 round-bottomed flask fitted with a condenser, N_2 inlet and tightly fitting subaseal stoppers. 200cm^3 of borane-tetrahydrofuran adduct in thf (approximately 1moldm^{-3}) is added carefully under N_2 by syringe. The resulting solution is heated at reflux for 48 hours. Methanol (100cm^3) is added to destroy unreacted BH_3-thf adduct. The solvent is removed by rotary evaporation to give a white solid. The solid is dissolved in dilute (1 moldm^{-3}) HCl (250cm^3) and heated at reflux for 12 hours. The resulting solution is cooled, basified to pH>12 using NaOH and extracted using dichloromethane (6x100cm^3). The organic washings were combined and dried (anhydrous $MgSO_4$). After fitration, the solvent is removed and the resulting yellow oil passed down a neutral alumina colunn (2x20cm long) and eluted with 5% methanol in dichloromethane to give the product (5.42g; 60% yield based on compound (1)). Electron impact mass spectrum m/z 360 (calc 360). ^{1}H n.m.r. ($CDCl_3$, relative populations in parentheses): δ 7.58 (1H, t), 7.19 (2H, d), 3,78 (4H, s), 2.53 (8H, mult), 2.23 (4H, t), 2.14 (2H, t), 1.57 (4H, sx), 1.35 (4H,q), 1.22

(2H,sx), 0.88 (6H, t), 0.65 (3H, t) ppm. ^{13}C n.m.r. ($CDCl_3$): δ 157.26(2), 136.52(1), 122.53(2), 60.62(2), 58.19(2), 57.24(1), 52.21(2), 51.95(2), 29.75(2), 24.30(1), 20.35(2), 11.97(2), 11.80(1) ppm

Preparation of the Co(II) complexes of L^7 and L^8.

$[Co(dmso)_6][BF_4]_2$ and $[Co(dmso)_6][CF_3SO_3]_2$ were prepared by a published method[100]. Solid complexes of the tetrafluoroborate and triflate salts of L^7 were prepared by mixing ethanolic solutions of the ligand and Co dmso solvates in a 1:1 molar ratio. The red precipitates were collected by suction filtration under N_2 and recrystallised from nitromethane/ethanol/diethylether (1:2:2) in 80% yield(BF_4 salt) and 72% yield (triflate salt).

The Co(II) complex of L^8 was obtained by mixing ethanolic solutions of $[Co(dmso)_6][ClO_4]_2$[100] and L^8 in a 1:1 molar ratio. The complex was obtained as a purple solid by precipitation with diethylether Purification of the complex was achieved by passing down a Sephadex C25 ion exchange column (2 x 10cm long) eluted with 0.2 $moldm^{-3}$ $NaClO_4$. After removal of water and exhaustive recrystallisation from nitromethane/diethylether (1:2) to remove $NaClO_4$ gave the product as a purple solid in 72% yield.

Hydrogenation of the Co(II) complexes of L^7 and L^8.

The Co(II) complexes (1 mmol) are placed in a 200cm^3 autoclave bomb and methanol (50cm^3) added. The bomb is subjected to treatment with H_2 (100 atmospheres) for 4 days at 75°C. The cooled solution is recovered and solvent removed to give a solid product.

X-ray crystallography of $[Co(L^7)][CF_3SO_3]_2$, 3,7,11-trimethyl-3,7,11,17-tetraazabicyclo[11.3.1]heptadeca-1(17)13,15-triene-cobalt(II) triflate.

A deep red crystal of 3,7,11-trimethyl-3,7,11,17-tetraazabicyclo[11.3.1]heptadeca-1(17),13,15-triene-cobalt(II)triflate $C_{18}H_{31}CoF_6N_4O_6S_2$ M=635.51, orthorhombic, space group Pnma,

a=17.308(8), b=10.182(3), c=14.081(6)Å, U=2552.4Å^3, Z=4, T=290K, Mo-K radiation, λ=0.71069Å, μ(Mo-K)=9.2 cm^{-1}. Data were collected with a Siemens P3R3 four-circle diffractometer in ω -2ϑ mode. Maximum 2ϑ was 50^o with scan range 1.3^o(2ϑ) around the $K_{\alpha1}$-$K_{\alpha2}$ angles, scan speed 4-29 min^{-1}, depending on the intensity of the 2s pre-scan; backgrounds were measured at the end of the scan for 0.25 of the time. *hkl* ranges were 0/12, 0/16, 0/21. Three standard reflections were monitored every 200 reflections, and showed slight changes during data collection. Unit cell dimensions and standard deviations were obtained by least squares fit to 15 reflections (20<2ϑ<22). Reflections were processed using profile analysis to give 2403 unique reflections; 1725 were considered observed ($I/\sigma(I)>2.0$) and used in refinement; they were corrected for Lorentz, polarisation and absorption effects, the last by the Gaussian method. Crystal dimensions were 0.15 x 0.34 x 0.44 mm. Systematic reflection conditions:0*kl*, *l*+*k* =2n, *hk* 0, *h*=2n; *h* 00, *h*=2n, 0*k* 0, *k* =2n; 00*l*, *l* =2n, indicate space group Pnma. Heavy atoms were located by the Patterson interpretation section of SHELXTL and the light atoms found on successive Fourier syntheses.

Anisotropic temperature factors were used for all non hydrogen atoms. Hydrogen atoms were given fixed isotropic temperature factors U=0.08Å^2. Those defined by molecular geometry were inserted at calculated positions and not refined; methyl groups were treated as rigid CH_3 units, with their initial orientation taken from the strongest H atom peaks on a difference Fourier synthesis.

The anticipated location of the S(2) atom on the mirror plane did not produce a good solution. A disordered arrangement was evident and the solution involved placing the sulphur atoms on either side of the plane with a site occupation factor of 0.5; two sets of O(22) and O(23) atoms were also required. The final diagrams were drawn to show only a single S(2) atom in an approximately tetrahedral environment.

Final refinement was on F by cascaded least squares methods refining 200 parameters. Largest positive and negative peaks on a final difference Fourier synthesis were of height 0.59el$Å^{-3}$. A weighting scheme of the form $W=1/(\sigma^2(F)+gF^2)$ with g =0.008573 was used and shown to be satisfactory by a weight analysis. Final R =0.06, R_w =0.074 and S =0.92. Maximum shift/error in the final cycle was 0.05. Computing with SHELXTL PLUS[27] on a DEC Microvax-II. Scattering factors in the analytical form and anomalous dispersion factors were taken from reference 28. Final atomic coordinates are given in the appendix.

Photopolymerisation studies.

The azamacrocyclic organocobalt(III) compound used in this study was prepared by Dr. H.A.A. Omar and is the compound illustrated in figure 3.1 $[RCo(L)(OH_2)][ClO_4]_2$ where R is propyl and L is 3,7,11,17 tetraazabicyclo[11.3.1]-1(17),13,15-triene. Thf (20g) is placed in a 50cm flask fitted with a condenser and N_2 inlet and methyl methacrylate added(2g). The solution is degassed to remove O_2 impurities and the catalyst (1mg, 1.81×10^{-6} moles) added. The flask is placed in a glass water bath and the solution subjected to photolysis using a 300W sun lamp for 24 hours. During this time, 1 cm^3 aliquots of the solution were removed for analysis by G.P.C. and Diode Array G.P.C. After photolysis is complete, the solvent is removed and the polymer analysed by ^{13}C n.m.r.

3.2.3. Results and Discussion.

Ligand synthesis.

Ligand L^8 was obtained in good yield using the method of Benniston[56]. Reaction of the secondary amines with excess propanoyl chloride gives the triamide (2) which was reduced to give L^8 using BH_3-thf. This method demonstrates a facile two step synthetic route to fully N-alkylated azamacrocycles.

$$R_2NH + R'COCl \longrightarrow RNCOR'$$

$$R_2NCOR' \longrightarrow R_2NCH_2R'$$

Solubility of $[Co(L^8)][ClO_4]_2$.

This compound exhibits solubility in a range of organic solvents. These include methanol, ethanol, dichloromethane, chloroform, acetonitrile and nitromethane. The increased solubility in organic media can be directly attributed to the increased length of the alkyl substituents of the macrocycle.

Synthesis and characterisation of the Co(II) complexes of L^7 and L^8 after reaction with hydrogen.

The proposed mechanism for the metal-centred photopolymerisation was described in 3.2.1.5. This suggests the presence of a stable hydridocobalt species which is able to catalyse polymerization of alkenes after addition of alkene to the Co-H bond. In an attempt to prepare these compounds, the Co(II) complex of L^7 (BF_4 and CF_3SO_3 salts) were reacted with H_2 under pressure at elevated temperatures. The products of the reaction are a different colour from the starting material.

$$[Co(L^7)]^{2+} \xrightarrow[100\ atm.\ 75^oC]{H_2} \text{blue compound}$$

Comparison of the u.v.-visible spectra of $[Co(L^7)]^{2+}$ and the blue product of the reaction is shown in figure 3.2. A comparison of the extinction coefficients shows that there has been a ten-fold increase and a small shift to longer wavelengths. This observation could be a result of the formation of a Co(III) species (i.e. Co-H). This evidence is supported by the infra-red spectrum of the product of hydrogenation (figure 3.3). This shows an absorption at $2100cm^{-1}$. This absorption could correspond to the Co-H

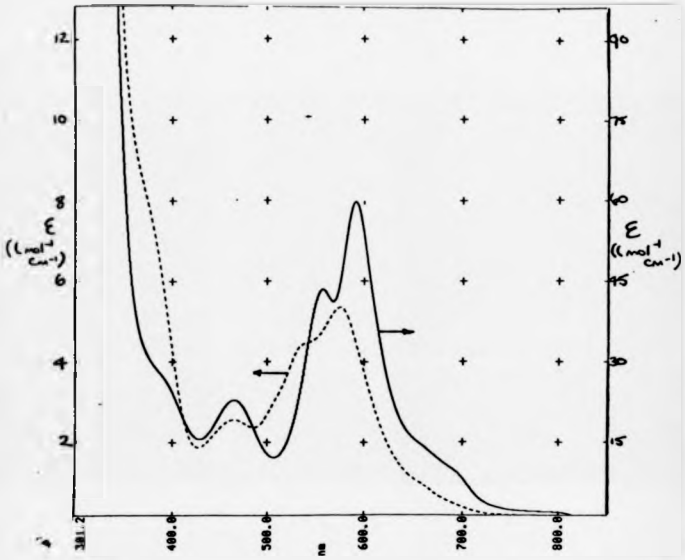

Figure 3.2 The u.v.-visible spectra of $[Co(L^7)](BF_4)_2$ (dashed line) and the product of the reaction of the reaction of $[Co(L^7)](BF_4)_2$ with H_2 (solid line).

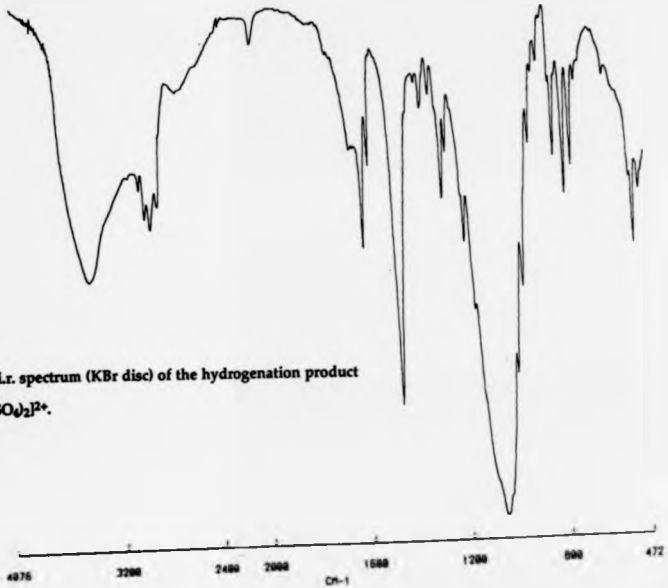

Figure 3. 3.The i.r. spectrum (KBr disc) of the hydrogenation product of $[Co(L^7)(CF_3SO_4)_2]^{2+}$.

stretching vibration[155]. Although this evidence suggests the presence of a Co-H bond another alternative explanation for the u.v. spectral changes could be an isomerisation. This possibility was investigated by x-ray crystallography. The bond lengths and bond angles of the Co(II) species should be markedly different to those of Co(III). The molecular structure would also show the presence of a different isomer. Crystals suitable for x-ray crystallography of $[Co(L^7)][BF_4]_2$ were grown but the stucture proved unobtainable. Figures 3.4 and 3.5 show the molecular geometry of $[Co(L^7)][CF_3SO_3]_2$. The macrocycle lies in a planar fashion about the five coordinate Co(II) ion. The methyl groups of the macrocycle lie above the macrocyclic plane, in a *trans* position to the coordinated triflate group. The bond lengths between Co and the pyridine donor is approximately 0.2Å shorter than the remaining Co-N and Co-O bond lengths (table 3.1). The coordination geometry about Co is best described as square pyramidal. Unfortunately a crystal of the hydrogenation product of $[Co(L^7)][CF_3SO_3]_2$ was not obtained. Further characterisation was carried out by measurement of the magnetic susceptibility of $[Co(L^7)][BF_4]_2$ and the hydrogenation product in D_2O solution by the Evans method[156], and in the solid state using a Johnson Mathey balance. The results are given in table 3.2. This result suggests that reductive elimination of hydrogen occurs in solution. Solution i.r. spectroscopy of the hydrogenation product of $[Co(L^7)][BF_4]_2$ support this view as no absorption at 2100cm^{-1} was observed.

Table 3.2 Magnetic susceptibility of $[Co(L^7)](BF_4)_2$ and $[Co(L^7)](BF_4)_2 + H_2$.

Complex	Magnetic Susceptibility (B.M)	
	Solid	Solution (H_2O)
$[Co(L^7)](BF_4)_2$	2.2	4.24
$[Co(L^7)](BF_4)_2 + H_2$	dia	4.31

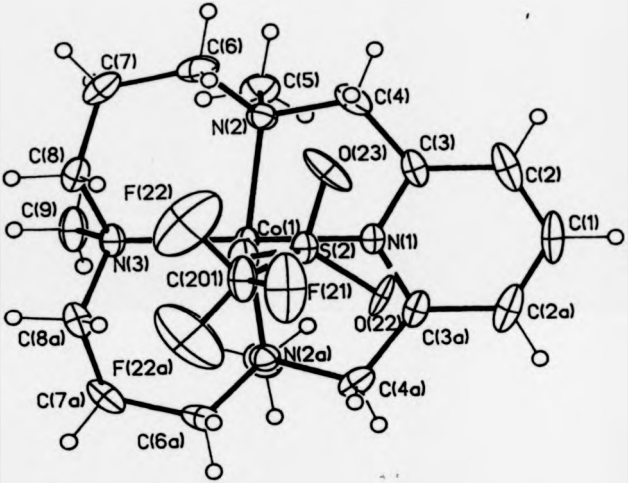

Figure 3.4 The crystal structure of $[Co(L^7)(CF_3SO_4)_2]^{2+}$

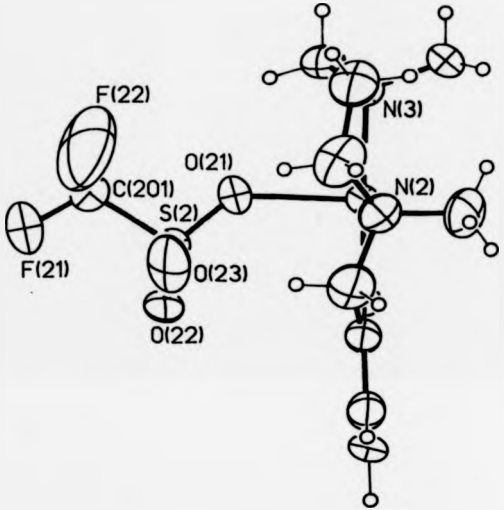

Figure 3.5 The crystal structure of $[Co(L^7)(CF_3SO_4)_2]^{2+}$ showing the planar nature of the macrocycle.

The hydrogenation reaction was repeated with $[Co(L^8)][ClO_4]_2$, as the increased steric bulk of the ligand was expected to increase the stability of the proposed hydridocobalt species and reduce the tendency for reductive elimination of hydrogen.

The magnetic susceptibility of $[Co(L^8)][ClO_4]_2$ and the product of its hydrogenation were measured in solution (water) and in the solid state (table 3.3). The measurements show that the hydrogenation product was diamagmetic. Hydrogenation has caused a large change in the u.v.-visible spectrum (figure 3.6). The ^1H n.m.r. of the hydrogenation product in D_2O (figure 3.7) shows, by consideration of the pyridyl proton resonances, the product to exist as two isomeric species in the ratio 3:1. The propyl groups of the macrocycle can protrude above or below the plane of the macrocycle. This gives three possible isomers for this complex. As two isomers have been identified in solution, the presence of a Co-Co bond can be discounted. A chemical test was used to establish the presence of a Co-H bond.

Table 3.3 Magnetic susceptibility of $[Co(L^8)](ClO_4)_2$ and $[Co(L^8)](ClO_4)_2 + H_2$.

Complex	Magnetic Susceptibility (B.M)	
	Solid	Solution (H_2O)
$[Co(L^8)](ClO_4)_2$	2.1	1.80
$[Co(L^8)](ClO_4)_2 + H_2$	dia	dia

The u.v.-visible spectrum of the dye, malachite green, is shown in figure 3.8. This dye can be reduced which results in a blue to colourless colour change. The hydrogenation product of $[Co(L^8)][ClO_4]_2$ was added to an aqueous solution of malachite green and the u.v.-visible spectrum recorded (figure 3.9). The solution turned colourless indicating that reduction had occurred. This is chemical evidence for the presence of a Co-

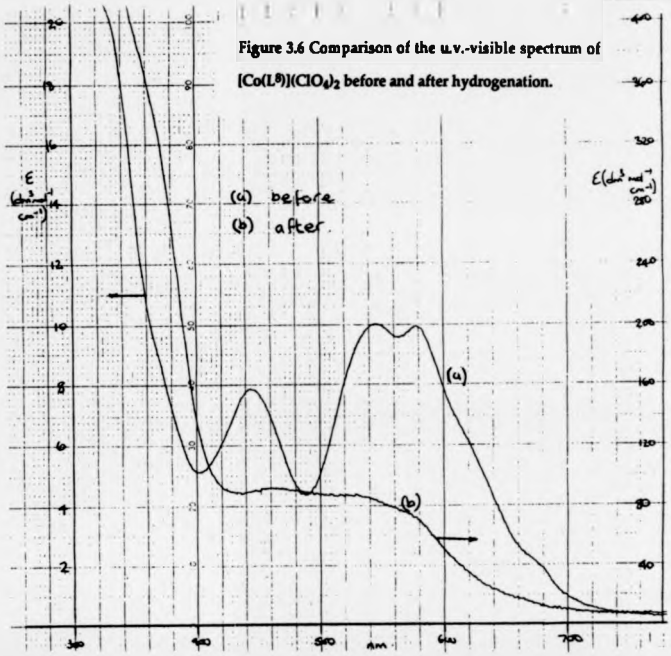

Figure 3.6 Comparison of the u.v.-visible spectrum of $[Co(L^8)](ClO_4)_2$ before and after hydrogenation.

Figure 3.7 The ^1H n.m.r. of the hydrogenation product of $[Co(L^9)](ClO_4)_2$.

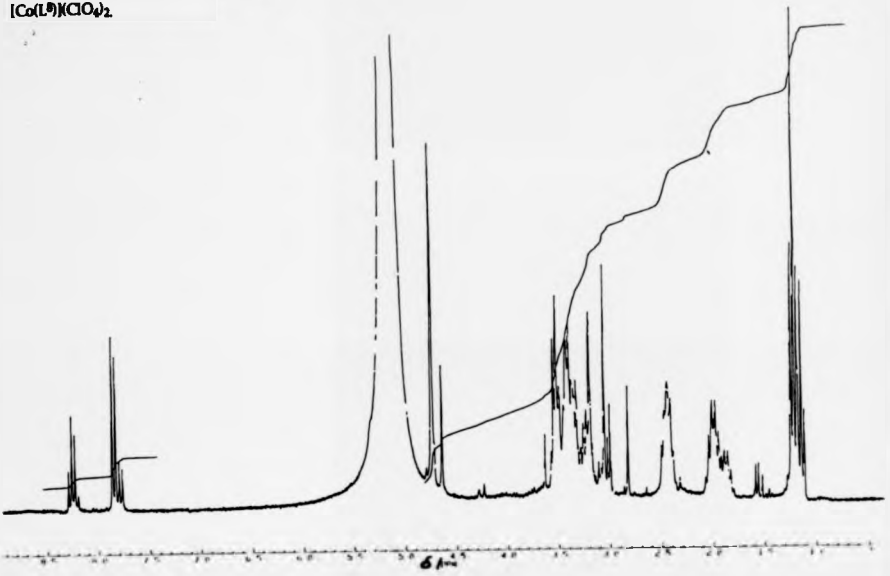

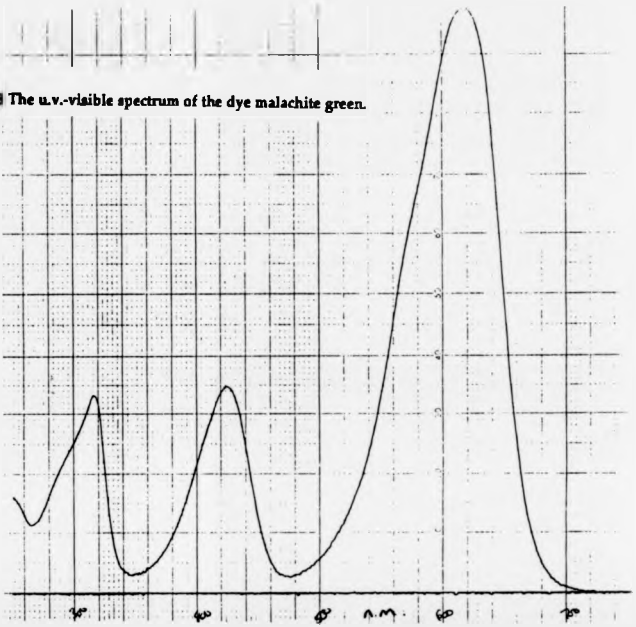

Figure 3.8 The u.v.-visible spectrum of the dye malachite green.

Figure 3.9 The u.v.-visible spectrum of malachite green after addition of the hydrogenation product of $[Co(L^9)](ClO_4)_2$.

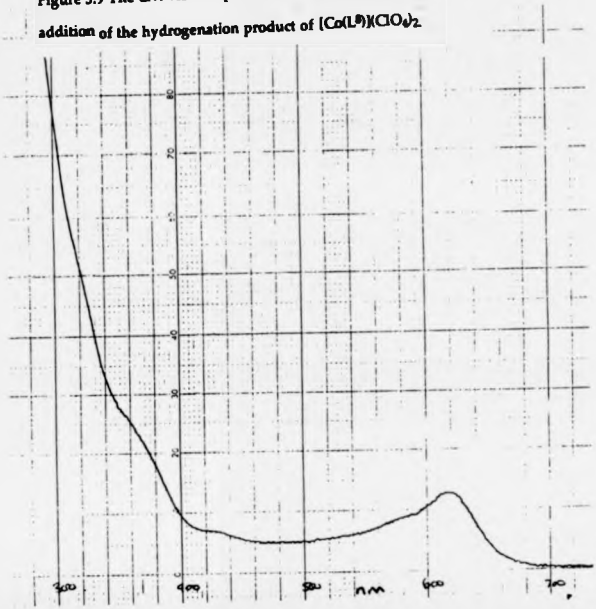

H bond. As a control experiment, $[Co(L^8)][ClO_4]_2$ was added to an aqueous solution of malachite green. No reduction was observed.

^{13}C. n.m.r. studies of polymers.

The determination of the tacticity of the polymers prepared by photopolymerisation of azamacrocyclic organocobalt(III) compounds will give information on the mechanism of polymerization. The proton decoupled ^{13}C n.m.r. spectrum of polymethylmethacrylate is shown in figure 3.10. The spectrum shows that the majority of the polymer produced is isotactic[157]. This result leads to the conclusion that alkene addition is stereospecific i.e. addition has occurred to give the minimum steric interaction between the substituents along the polymer chain. An attempt was made to prepare stereoregular polyacrylonitrile but this was unsuccessful as the steric interactions of the CN groups are not large enabling free rotation of C-C bonds to give atactic polymers.

G.P.C. analysis of the polymerization of methyl methacrylate.

G.P.C. was used to determine the variation in the molecular weight of the polymer during photopolymerization over 24 hours. A typical G.P.C. trace is shown in figure 3.11. A plot of M_w against time is shown in figure 3.12. There are two interesting features of the plot:-

(1) high molecular weight polymer is produced very quickly

(2) there is a two-fold increase in molecular weight between 23 and 24 hours.

This increase in molecular weight is an unusual result which could not be explained.

Diode Array G.P.C. analysis of the phoyopolymerization of methyl methacrylate.

Diode Array G.P.C. analysis can be visualised as two techniques in series: molecular weight determination by G.P.C. followed by u.v.-visible spectroscopy of the eluent. In this series of experiments, it was hoped to

Figure 3.10 ^{13}C n.m.r. spectrum of polymethlymethacrylate prepared by photopolymerisation.

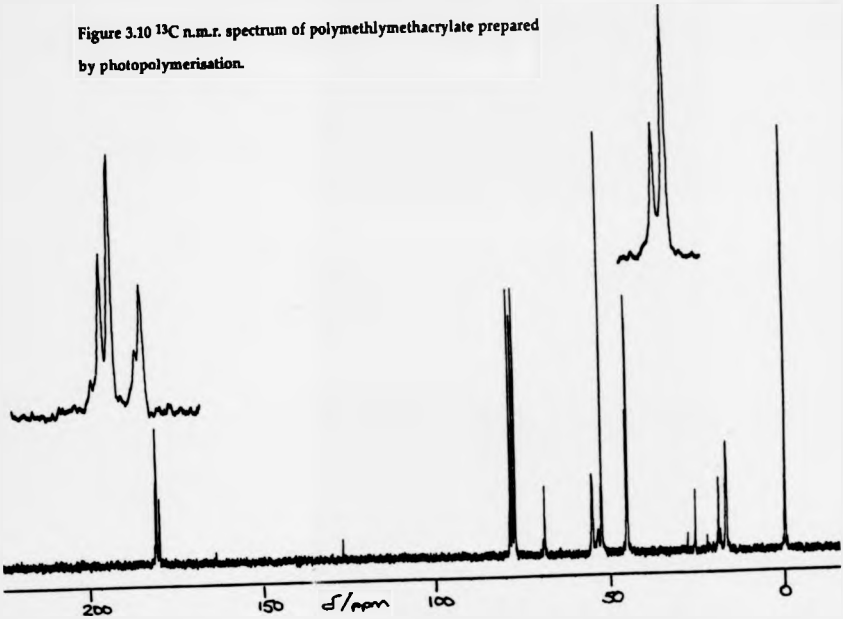

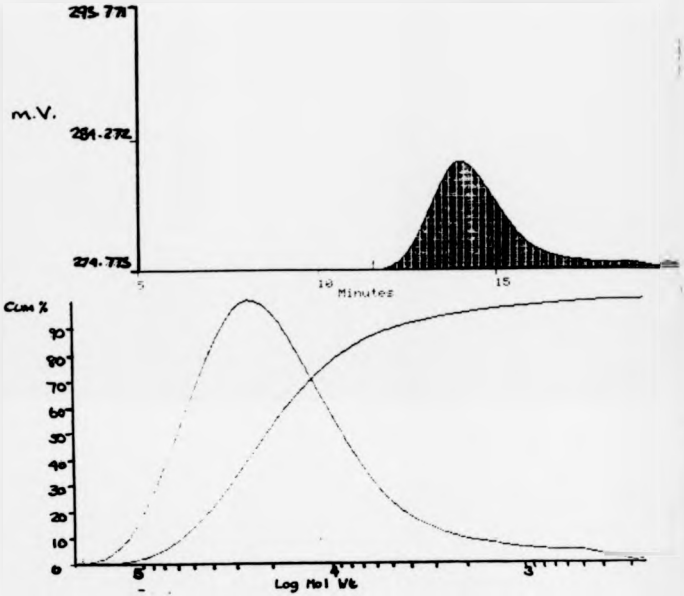

Figure 3.11 A typical set of results obtained from G.P.C. analysis.

Figure 3.12 The variation of molecular weight with time during the photopolymerisation of methyl methacrylate.

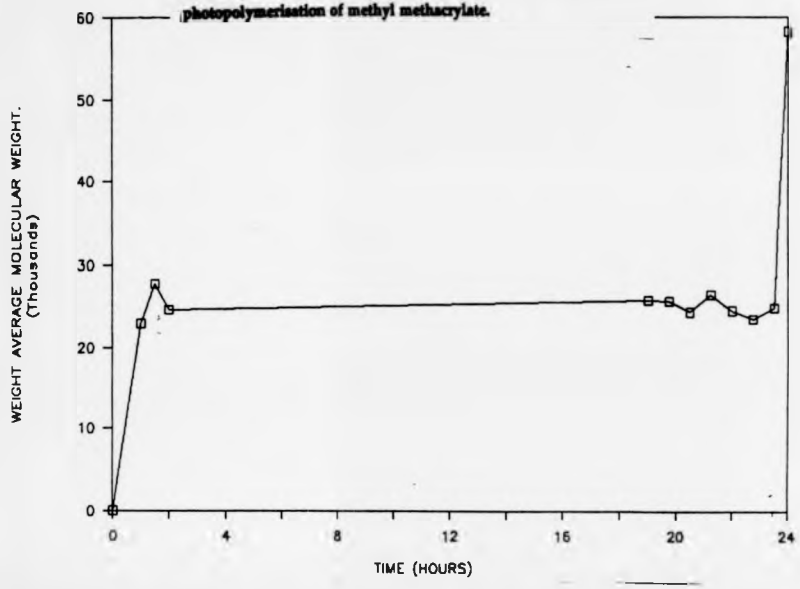

identify several species in solution, namely organocobalt species attached to high molecular weight polymer. The low molecular weight region was analysed for signs of dimer, trimer or oligomer formation. A typical three dimensional plot obtained by Diode Array G.P.C. is shown in figure 3.13. Attempts to locate Co by observation of the d-d transitions failed but the complex was identifiable by absorption from its pyridine moiety. The results indicate that at 19.1 minutes, species that have a molecular weight of 357 are detected. This could be the presence of trimeric species with attached Co. Dimeric species could have eluted after 19.73 minutes (molecular weight 210). The large absorption at 20.4 minutes is the presence of methyl methacrylate. Few oligomeric species were seen above the level of trimer. Polymer eluted after 10 minutes. These results give some indication of the mechanism of polymerisation. Polymerization probably occurs by the initial formation of dimeric and trimeric species which react further to give high molecular weight polymer.

Figure 3.13 A typical three-dimensional plot obtained from diode array G.P.C. analysis.

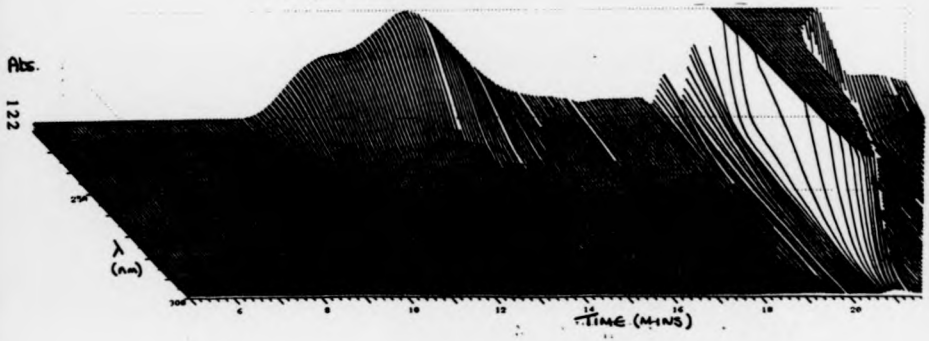

3.2.4. Conclusions.

The increased alkylation of L^8 leads to the increased solubility of the Co(II) complex of L^8 in organic media.

The reaction of hydrogen with the Co(II) complex of L^7 gives a colour change and a marked increase in the extinction coefficients observed in the u.v.-visible spectrum. The presence of the hydridocobalt(III) species could be inferred in the solid state from the i.r. spectrum. In solution, this compound reductively eliminates hydrogen.

The increased steric bulk of L^8 enabled the isolation and chemical identification of the Co-H bond.

The results of the polymerisation studies was that polymer formation in thf solution probably involves the initial formation of dimeric and trimeric species which react further to give high molecular weight species

3.3 Synthesis and coordination chemistry of two oxygen containing macrocyclic ligands.

3.3.1. Introduction.

The oxygen containing macrocycles were prepared to establish a proposed mechanism of the photopolymerisation of alkenes by azamacrocyclic organocobalt(III) compounds. The mechanism proposed the initial breaking of a tertiary N-Co bond in the position *trans* to the coordinated pyridyl moiety The idea was to incorporate a weak oxygen donor in this position which would readily break under the photopolymerization conditions which would lead to an increase in the rate of photopolymerisation. It was subsequently shown that this mechanism did not occur but the coordination chemistry of the ligands were investigated in any case.

3.3.2 Experimental.

Materials, solvents and spectroscopy were used as detailed in section 2.2.1.2.

Synthesis of ligands L^9 and L^{10}

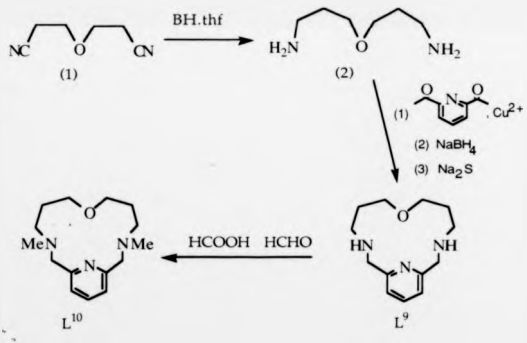

Synthesis of 5-oxa-1,9-diazanonane.

5-oxa-1,9-heptanedinitrile(1) (10g, 0.08 moles) is placed in a $1dm^3$ three-necked round bottomed flask fitted with a N_2 inlet, condenser and tight fitting subaseal stoppers. $200cm^3$ of BH_3-thf adduct in thf (approximately $1moldm^{-3}$) is added carefully under N_2 by syringe. The resulting solution is heated at reflux for 48 hours. Methanol ($100cm^3$) is added to the cooled solution to destroy unreacted BH_3-thf adduct. The solvent is removed by rotary evaporation to give a white solid. The white solid is dissolved in dilute HCl ($1moldm^{-3}$) ($250cm^3$) and heated at reflux for 12 hours. the resulting solution was cooled, basified to pH>12 and extracted using dichloromethane (6 x $50cm^3$). The organic washings were combined and dried (anhydrous $MgSO_4$). After filtration the solvent was removed. The resulting yellow oil was Kugelrohr distilled to yield a colourless liquid, bpt 80°C at 0.2mmHg in 52% yield (5.49g). Electron impact mass spectrum $(M+1)^+$ 133 (calc 133) ^1H n.m.r. ($CDCl_3$ relative populations in parentheses):δ 3.65 (4H,t), 2.85 (4H,t), 1.77 (4H, pent) 1.32 (4H, br) ppm. ^{13}C n.m.r. ($CDCl_3$):δ 67.85(2), 38.31(2), 32.36(2) ppm.

Synthesis of L^9, 7-oxa-3,11,17-triazabicyclo[11.3.1]heptadeca-1(17),13,15-triene.

$Cu(NO_3)_2.3H_2O$ (5,56g, 0.023 moles) is dissolved in 1:1 ethanol/water ($500cm^3$) in a $1dm^3$ round bottomed flask. The amine (2) (3g, 0.023 moles) is added to the solution which turns dark blue/green. Pyridine-2,6-dicarboxaldehyde[99] (3.11g, 0.023 moles) is added to the solution and the solution heated on a steam bath for 3 hours. The solution is transferred to a $2dm^3$ beaker and cooled to 0°C using an ice bath. $NaBH_4$ (3.8g, 0.1 moles) is added slowly over an hour and the resulting solution stirred at room temperature for 2 hours. After heating on a steam bath for 2 hours $Na_2S.9H_2O$ (29.81g, 0.12 moles) is added to the cooled solution and heating continued for a further hour. The black precipitate is removed by filtration through celite. The filtrate is extracted with dichloromethane

($6 \times 50 cm^3$), combined extracts dried (anhydrous Na_2SO_4), filtered and solvent removed to give a red oil. Kugelrohr distillation of the oil gave the product as a white solid (mpt 125°C, 0.01mmHg) 58% yield (3.135g). Electron impact mass spectrum $(M+1)^+$ 236 (calc 236). ^1H n.m.r. ($CDCl_3$): δ 7.52 (1H, t), 6.98 (2H, d), 3.82 (4H, s), 3.50 (4H, t), 3.14 (2H, br), 2.52 (4H, t), 1.75 (4H, pent) ppm. ^{13}C. n.m.r. ($CDCl_3$): δ 158.59(1), 136.63(2), 120.69(2), 68.31(2), 53.88(2), 45.43(2), 29.32(2) ppm.

Synthesis of L^{10}, 7-oxa-3,11-dimethyl-3,11,17-triazabicyclo[11.3.1]heptadeca-1(17),13,15 triene.

The ligand L^9 (0.78g, 3.32mmol) is dissolved in 98% formic acid (0.46g, 0.01 moles)in a $50cm^3$ round bottomed flask and cooled to 0°C in an ice bath. Formaldehyde solution (37%, 0.1g, 3.17mmol) is added and the resulting solution heated to 90°C for 24 hours. The solvent is removed and the residue co-evaporated twice with concentrated HCl. The residue is basified to pH > 12 using NaOH and extracted with dichloromethane ($6 \times 50 cm^3$). The combined extracts are dried (anhydrous $MgSO_4$), filtered and solvent removed to give a yellow oil. The oil is Kugelrohr distilled to give the pure product as a pale yellow liquid (bp 120°C, 0.04mmHg), yield 72% (0.628g). Electron impact mass spectrum $(M+1)^+$ 264 (calc 264). ^1H. n.m.r. ($CDCl_3$): δ 7.54 (1H, t), 7.12 (2H, d), 3.66 (4H, s), 3.41 (4H, t), 2.36 (6H, s), 2.26 (4H, t), 1.62 (4H, pent) ppm. ^{13}C. n.m.r. ($CDCl_3$): δ 158.01(1), 136.20(2), 122.61 (2), 66.99(2), 64.29(2), 50.83(2), 43.14(2), 26.44(2) ppm.

Preparation of the metal complexes of L^9 and L^{10}.

Solid complexes of L^9 and L^{10} were obtained in good yields (>70%) by mixing ethanolic solutions of the ligands with $[M(dmso)_n][BF_4]_2$ (100) (M=Ni, Cu n=6. M=Zn, n=4) in a 1:1 molar ratio. The precipitates were isolated by suction filtration under N_2 and recrystallised from nitromethane/ethanol/diethylether (1:2:2)

Preparation of the red Ni(II) isomer of L^9.

$[Ni(H_2O)_6][BF_4]_2$ (0.17g, 0.5 mmol) is placed in a dry Schlenk tube and fresh triethylorthoformate ($10cm^3$) added. The resulting solution is stirred overnight under dry N_2 to prepare $[Ni(EtOH)_6][BF_4]_2$ which is not isolated. L^9 (0.117g, 0.5 mmol) dissolved in ethanol ($2cm^3$) is added to the Schlenk tube. Immediately a red solid precipitates. The solid is collected by suction filtration under dry N_2 and recrystallised from nitromethane/diethylether (1:2) to give the product (yield 75%)

3.3.3 Results and Discussion.

Ligand Synthesis.

Preparation of the amine (2) utilised the reduction of the dinitrile (1) by BH_3-thf adduct. This reagent proved superior to the literature procedure[158]. The literature method used $LiAlH_4$ as the reductant in dry diethylether. The method had an unwanted side reaction which contaminated the product with 3-aminopropan-1-ol by the following route (scheme 3.4). 3-aminopropan-1-ol proved difficult to separate from the desired product.

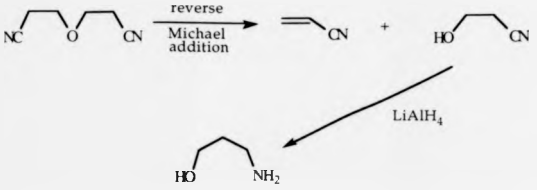

Scheme 3.4. Production of 3-aminopropan-1-ol impurity during the reduction of 5-oxa-1,9-heptanedinitrile by $LiAlH_4$ in diethylether.

The target macrocycles were prepared in good yield using the template technique used to prepare ligands L^5 and L^6.

Metal complexes of L^9.

The metal complexes of L^9 have the general formula $[M(L^9)(solvent)_3][BF_4]_2$ where M is Ni, Cu or Zn and the solvent is dmso or water. The formulae were confirmed by elemental analysis. The evidence indicates that in these complexes, the macrocyclic oxygen donor does not coordinate to the metal ion. In an attempt to acheive oxygen coordination, L^9 was added to the ethanol solvate of Ni(II) in triethylorthoformate. This

produced a red solid. The u.v.-visible spectra of the red solid and blue $[Ni(L^9)(dmso)_2][BF_4]_2.3H_2O$ were compared (figure 3.14).

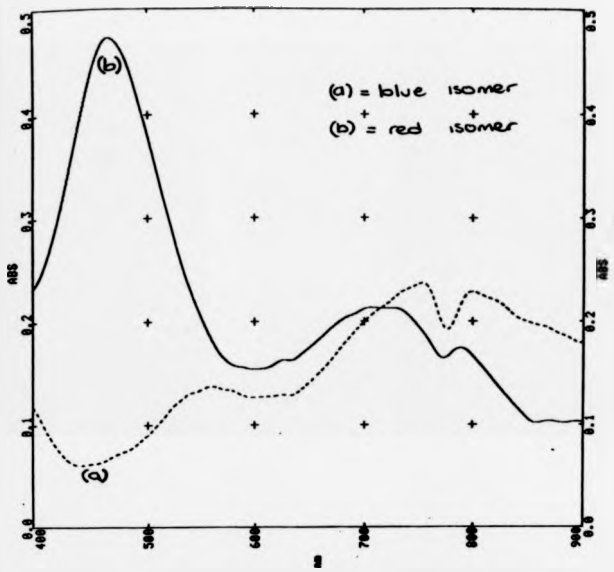

Figure 3.14 Comparison of the u.v.-visible spectra of the red and blue isomers of Ni(II) complex of L^9.

The difference in the spectra could be a result of coordination of the macrocyclic oxygen donor. The macrocyclic oxygen donor is very weak and it does not compete for donor sites occupied by comparatively strongly bound dmso molecules. This occurs despite of the macrocyclic effect. The macrocyclic effect combined with the low strength of ethanol coordination to Ni(II) allows the macrocyclic oxygen donor to coordinate in the red isomer. Elemental analysis of this isomer gives the formula as $[Ni(L^9)(OH_2)][BF_4]_2$, a five coordinate species.

Dissolution of the red isomer will produce a blue solution with the breaking of the Ni-O bond. Conversion of the blue isomer to the red isomer proved unsuccessful, i.e.

Figure 3.14 also indicates complex kinetic processes occuring in the region 650-850nm. This could be a result of equilibria between different macrocyclic conformations.

Metal complexes of L^{10}.

The metal complexes of L^{10} have the formula $[M(L^{10})(dmso)][BF_4]_2$ (M=Cu, Zn) and $[M(L^{10})(dmso)_2][BF_4]_2$ (M=Ni) confirmed by elemental analysis. The u.v.-visible spectrum of $[Ni(L^{10})(dmso)_2][BF_4]_2$ is shown in figure 3.15. The unusual profile could be a result of a five coordinate species in solution with a loosely bound donor (either dmso or macrcyclic oxygen) dissociating on solvation.

Figure 3.15 The u.v.-visible spectrum of $[NiL^{10}(DMSO)_2](BF_4)_2$.

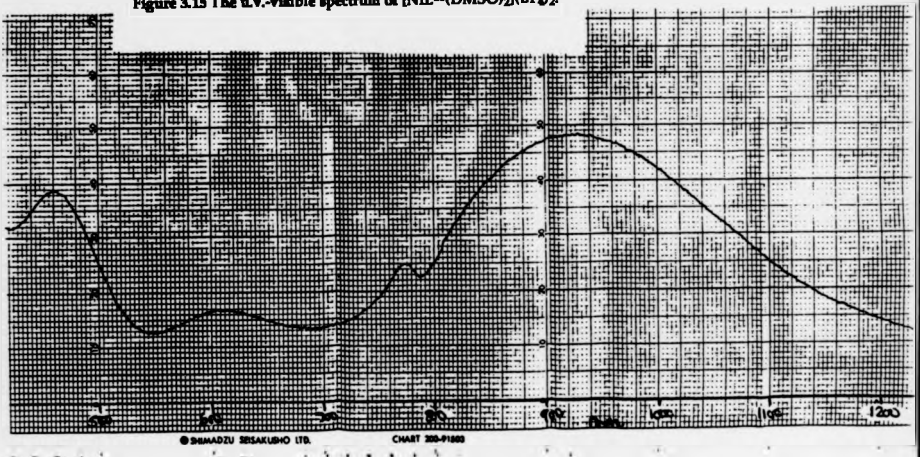

Analyses indicate coordination of the macrocyclic oxygen donor. This could be a weak interaction which occurs through the adoption of a folded macrocyclic geometry.

3.3.4 Conclusions.

The macrocyclic oxygen donors of ligands L^9 and L^{10} are weak donors. This is illustrated by the synthesis of the two isomers of the Ni(II) complex of L^9.

3.3.5. Further Work.

The research presented in part three could be extended by:

(1). The reaction of hydrogen with Co(II) complexes of azamacrocycles could be investigated to determine whether this reaction can be applied to a wide range of macrocycles.

(2). Polymerisation studies of the hydridocobalt(III) complex of L^8 would establish the presence of a hydride in the termination mechanism.

Table 3.5 Characterisation of the metal complexes of L^9 and L^{10}.

Complex	Colour	U.V. Visible (CH_3NO_2) λ_{max} /e / $dm^3mol^{-1}cm^{-1}$)	Analysis			Conductivity $\Omega^{-1}cm^{-1}mol^{-1}$ (CH_3NO_2)	Magnetic suscept. μeff/BM
			% C	% H	% N		
$[NiL^9(DMSO)_3](BF_4)_2$ $CH_3NO_2.H_2O$	Blue	799 (19.2) 751 (20.3) 539 (11.6)	36.13 (30.25)	5.56 (4.93)	7.02 (6.20)	156.77	3.15
$[NiL^9(OH_2)](BF_4)_2$	Red	790 (17.5) 714 (21.3) 466 (47.3)	32.15 (32.73)	4.77 (4.54)	8.65 (8.81)	148.95	3.39
$[CuL^9(DMSO)_2](BF_4)_2$	Blue	581 (239.3)	31.34 (31.31)	5.26 (4.35)	8.12 (8.25)	162.57	1.99
$[ZnL^9(DMSO)_2](BF_4)_2$	White		32.38 (32.21)	5.27 (5.19)	6.66 (6.79)	149.77	
$[NiL^{10}(DMSO)_2](BF_4)_2$	Green	932 (23.3) 774 (12.1) 612 (8.2) 460 (18.9)	35.00 (35.17)	5.72 (5.85)	6.44 (6.63)	165.71	3.276
$[CuL^{10}](DMSO)](BF_4)_2$	Purple	609 (393)	35.28 (34.92)	5.40 (5.25)	7.26 (7.42)	157.50	2.07
$[ZnL^{10}](DMSO)](BF_4)_2$	White		35.17 (35.41)	5.38 (4.64)	7.24 (7.31)	148.72	

Magnetic susceptibilities determined using a Johnson Mathey balance.

4. References.

1. Tabushi, I., Okino, H. and Kurunda, Y., *Tetrahedron Letters*, 1976, 4339.
2. Tabushi, I., Tanigushi, Y. and Kato, H., *Tetrahedron Letters*, 1977, 1049.
3. Richman, J. E. and Atkins, T. J., *J. Amer. Chem. Soc.*, 1974, **96**, 2268.
4. Thompson, M. C. and Busch, D. H., *J. Amer. Chem. Soc*, 1964, **86**, 3651.
5. Lever, A. B. P., *Adv. Inorg. Chem.*, 1965, 27.
6. Curtis, N. F., *Coord. Chem. Rev.*, 1968, 3.
7. Curtis, N. F., Curtis, Y. M. and Powell, H. J. K., *J. Amer. Chem. Soc.*, 1966, 1815.
8. Schrauzer, G. N., *Chem. Ber*, 1962, **95**, 1438.
9. Ansell, W. R., Cooper, M. K., Dancey, K. P., Duckworth, P. A., Henrick, K., McPartlin, M. and Tasker, P. A., *J. Chem. Soc. Chem. Commun.*, 1985, 439.
10. Busch, D. D. H. and Cairns, C., in *Progress in Macrocyclic Chemistry* R. M. Izatt and J. J. Christensen, Eds. (J. Wiley and Sons., New York., 1987), vol. 3,.
11. Nelson, S. M., *Pure. Appl. Chem.*, 1980, **52**, 461.
12. Popov, A. I. and Lehn, J. M., in *Coordination Chemistry of Macrocyclic Compounds* G. A. Melson, Eds. (Plenum Press, New York, 1979) pp. 560.
13. Ng, F. T., Zaw, K. and Henry, P. M., *J. Mol. Catal.*, 1990, **1**, 127.
14. Cabbiness, D. K. and Margerum, D. W., *J. Amer. Chem. Soc.*, 1969, **91**, 6540.
15. Cabbiness, D. K. and Margerum, D. W., *J. Amer.Chem. Soc*, 1970, **92**, 2151.
16. Kodama, M. and Kimura, E., *J. Chem Soc. Dalton. Trans.*, 1976, 2341.
17. Hinz, F. D. and Margerum, D. W., *Inorg Chem*, 1974, **13**, 2941.
18. Pedersen, C. J., *J. Amer. Chem. Soc.*, 1967, **89**, 2459.
19. Lehn, J. M., *Acc. Chem. Res*, 1978, **11**, 49.
20. Hancock, R. D., *Prog. Inorg. Chem.*, 1989, **37**, 187.

20a. Hancock, R. D., *Acc. Chem. Res*, 1990, **23**, 253.

21. Olsen, D. C. and Valsilevkis, J., *Inorg. Chem.*, 1969, **8**, 1611.

22. Olsen,. J. and Valsilevkis, D. C. , *Inorg Chem*, 1971, **10**, 463.

23. Lovecchio, F. V., Gore, E. S. and Busch, D. H., *J. Amer. Chem. Soc.*, 1974, **96**, 3109.

24. Fabrizzi, L., *Comments in Inorg Chem*, 1985, **4**, 33.

25. Palmer, J. M., Papaconstantinou, E. and Endicott, J. F., *Inorg. Chem.*, 1969, **8**, 1516.

26. Friedburg, M., Meyerstein, D. and Yamamoto, Y., *J. Chem. Soc. Dalton Trans.*, 1982, 1137.

27. Jubran, N., Cohen, H., Konesh, Y. and Meyerstein, D., *J. Chem. Soc. Chem. Commun.*, 1984, 1683.

28. Rorabacher, D. B., Martin, M. J., Koenigbauer, M. J., Maluk, M., Schroder, R. R., L.F.Schroder, Endicott, J. F. and Ochrymowcz, L. A., in *Copper Coordination Chemistry: Boichemical and Inorganic Perspectives* K. D. Karlin and J. Zubieta, Eds. (Adenine, New York, 1983) pp. 167.

29. Pedersen, C. J., *J. Amer. Chem. Soc.*, 1967, **89**, 7017.

30. Streitweiser, A. and Heathcock, C. H., *Introduction to Organic Chemistry*. (Macmillian, New York, 1981).

31. Green, N., *Tetrahedron Letters*, 1972, 1793.

32. Newcome, G. R., Sauer, J. P., Roper, J. M. and Hager, D. C., *Chemical Rev.*, 1977, **77**, 513.

33. McDaniel, C. W., Bradshaw, J. S., Krakowak, K. E., Izatt, R. M., P.B.Savage, Tarbet, B. J. and Bruening, R. L., *J. Heterocyclic Chem.*, 1989, **26**, 413.

34. Bright, D. and Truter, M. R., *Nature*, 1970, **225**, 176.

35. Busch, M. A. and Truter, M. R., *J. Chem. Soc. Perkin Trans. II*, 1972, 341.

36. Fenton, D. E., Mercer, M., Poonia, N. S. and Truter, M. R., *J. Chem. Soc. Chem. Commun.*, 1972, 66.

37. Mallinson, P. R. and Truter, M. R., *J. Chem. Soc. Perkin Trans II*, 1972, 1818.

38. Lamb, R. D., Izatt, R. M., Christensen, J. J. and Eatough, D. J., in *Coordination Chemistry of Macrocyclic Compounds* G. A. Melson, Eds. (Plenum Press, New York, 1979)

39. Izatt, R. M., Bradshaw, J. S., Nielsen, S. A., Lamb, J. D. and Christensen, J. J., *Chem. Rev.*, 1985, **85**, 271.

40. Chaudhuri, P. and Wieghardt, K., *Prog. Inorg. Chem.*, 1987, **35**, 329.

41. Trofimenco, S., *Acc. Chem. Res.*, 1979, **4**, 17.

42. Kaden, T. A., *Top. Curr.Chem.*, 1984, **121**, 157.

43. Bernhardt, P. V. and Lawrence, G. A., *Aust. J. Chem.*, 1990, 297

44. Wieghardt, K., Kliene-Boymann, M., Nuber, B. and Weiss, J., *Z. Anorg. Allg. Chem.*, 1986, **536**, 179.

45. Weighardt, K., Kleine-Boymann, M., Nuber, B. and Weiss, J., *Inorg. Chem.*, 1986, **25**, 1654.

46. Wieghardt, K., Kleine-Boymann, M., Nuber, B. and Weiss, J., *Inorg. Chem.*, 1986, **25**, 1309.

47. Nonoyana, M., *J. Inorg. Nucl. Chem.*, 1977, **39**, 550.

48. Nonoyana, M., *Inorg. Chem. Acta.*, 1976, **20**, 53.

49. Bounsall, E. J. and Koprich, S. R., *Can. J. Chem.*, 1970, **48**, 1481.

50. Isied, S. S., *Inorg. Chem.*, 1980, **19**, 911.

51. Yamashita, M., Ito, H., Toriumi, K. and Ito, T., *Inorg. Chem.*, 1983, **22**, 1566.

52. Volkert, W. A., Holmes, R. A., Derveer, D. G. V., Barefield, E. K., Zuckman, S. A., Freeman, G. M. and Troutner, D. E., *Inorg. Chem.*, 1981, **20**, 2386.

53. Lai, T. F. and Poon, C. K., *Inorg. Chem.*, 1976, **15**, 1562.

54. Stetter, H. and Frank, W., *Angew. Chem. Int. Ed. Eng.*, 1976, **15**, 686.

55. Madeysk, C. M., Michael, J. P. and Hancock, R. D., *Inorg. Chem.*, 1984, **23**, 1487.

56. Alcock, N. W., Benniston, A. C., Grant, S. J., Omar, H. A. A. and Moore, P., *J. Chem. Soc. Chem. Commun.*, in press.

57. Cooper, S. R., *Acc. Chem. Res.*, 1988, **21**, 141.

58. Beinert, H., *Coord. Chem. Rev.*, 1980, **33**, 55.

59. DeSimone, R. E. and Glick, M. D., *J. Amer. Chem. Soc.*, 1976, **98**, 762.

60. Alcock, N. W., Herron, N. and Moore, P., *J. Chem. Soc. Chem. Commun.*, 1976, 886.

61. Herron, N. and Moore, P., *J. Chem. Soc. Dalton Trans.*, 1978, 394.

62. Gerber, D., Chongsorwangvirod, P., Leung, A. K. and Ochrymovycz, L. A., *J. Org. Chem.*, 1977, **42**, 2644.

63. Setzer, W. N., Ogle, C. A., Wilson, G. S. and Glass, R. S., *Inorg. Chem.*, 1983, **22**, 266.

64. Blake, A. J., Gould, R. O., Lavery, A. J. and Schroder, M., *Angew. Chem.*, 1986, **98**, 282.

65. Sellman, D. and Zapf, L., *J. Organomet. Chem.*, 1985, **289**, 57,71.

66. Ochrymowycz, L. A., Mak, C.-K. and Mincha, J. D., *J. Org. Chem.*, 1974, **14**, 2079.

67. Buter, J. and Kellog, R. M., *J. Chem. Soc. Chem. Commun.*, 1980, 466.

69. Wieghardt, K., Kuppers, H.-J. and Weiss, J., *Inorg. Chem.*, 1985, **24**, 3067.

70. Hartman, J. R. and Cooper, S. R., *J. Amer. Chem. Soc.*, 1986, **108**, 4481.

71. Osvath, P., Sargeson, A. M., Skelton, B. W. and White, A. H., *J. Chem. Soc. Chem. Commun.*, 1991, 1036.

72. Dietrich, B., Lehn, J.-M. and Sauvage, J. P., *Tetrahedron Letters*, 1969, **34**, 2885.

73. Lehn, J.-M., *Structure and Bonding*, 1973, **16**, 1.

74. Moras, D., Metz, B. and Weiss, R., *Acta Crystallographica*, 1973, **B29**, 388.

75. Lehn, J.-M. and Sauvage, J. P., *J. Amer. Chem. Soc.*, 1975, **97**, 6700.

76. Lehn, J.-M., Pine, S. H., Watanabe, E. and Willard, A. K., *J. Amer. Chem. Soc.*, 1977, **99**, 6766.

77. Lehn, J.-M., *Pure and Appl. Chem.*, 1980, **52**, 2441.

78. Deitrich-Buchecker, C. O., Sauvage, J. P. and Kern, J.-M., *J. Amer. Chem. Soc.*, 1984, **106**, 3043.

79. Ciampolini, M., Dapporto, P., Nardi, N. and Zanubini, F., *Inorg. Chem.*, 1983, **22**, 13.

80. Ciampolini, M., Dapporto, P., Innocenti, P. and Zanubini, F., *J. Chem. Soc. Dalton Trans.*, 1984, 575 and 995.

81. Kyba, E. P., C, W. H., McPHaul, J. M. and John, A. M., *J. Amer. Chem. Soc.*, 1977, **99**, 8053.

82. Deldonno, T. A. and Rosen, W., *J. Amer. Chem. Soc.*, 1977, **99**, 8051.

83. Barclay, G. A. and Barnard, A. K., *J. Chem. Soc.*, 1961, **Part 4**, 4269.

84. Kauffmann, T. and Ennen, J., *Chem. Ber.*, 1985, **118**, 2692.

85. Kauffman, T. and Ennen, J., *Chem. Ber.*, 1985, **118**, 2702.

86. Kauffman, T. and Ennen, J., *Chem. Ber.*, 1985, **118**, 2714.

87. Turner, G. P. A., *Introduction to Paint Chemistry and Principles of Paint Technology*. (Chapman and Hall) 1987.

88. *Metal Ion Activation of Dioxygen*. T. G. Spiro, Eds., (Wiley, New York).

89. Hoffman, B. M., Diemente, D. L. and Bassolo, F., *J. Amer. Chem. Soc.*, 1970, **92**, 61.

90. Getz, D., Melamud, E., Silver, B. L. and Dori, Z., *J. Amer. Chem. Soc.*, 1975, **97**, 3846.

91. Martell, A. E., in *Oxygen Complexes and Oxygen Activation by Transition Metals*. A. E. Martell and D. T. Sawyer, Eds. (Plenum Press, New York, 1988).

92. Motekaitis, R. J. and Martell, A. E., *J. Chem. Soc. Chem. Commun.*, 1988, 1020.

93. Motekaitis, R. J. and Maretell, A. E., *J. Amer. Chem. Soc.*, 1988, **110**, 7715.

94. Motekaitis, R. J. and Martell, A. E., *Inorg. Chem.*, 1991, **30**, 694.

95. Dietrich, B., Lehn, J.-M. and Sauvage, J. P., *Tetrahedron Letters*, 1969, 2885.

96. Dietrich, B., Hosseini, M. W., Lehn, J.-M. and Sessions, R. B., *Helv. Chim. Acta.*, 1985, **68**, 289.

97. Jazwinnski, J., Lehn, J.-M., Lilienbaum, D., Ziessel, R., Guillheim, J. and Pascard, C., *J. Chem. Soc. Chem.Commun.*, 1987, 1691

98. McDowell, D. and Nelson, J., *Tetrahedron Letters*, 1988, 385.

99. Alcock, N. W., Kingston, R. G., Moore, P. and Pierpoint, C., *J. Chem. Soc. Dalton Trans.*, 1984, 1937.

100. Selbin, J., Bull, W. E. and Holmes, L. H., *J. Inorg. Nucl. Chem.*, 1961, **16**, 219.

101. Hunter, J., Nelson, J., Harding, C., McCann, M. and McKee, V., *J. Chem. Soc. Chem. Commun.*, 1990, 1148.

102. Ngwenya, M. P., Martell, A. E. and Rubenspies, J., *J. Chem. Soc. Chem. Commun.*, 1990, 120.

103. McKee, V., Robinson, W. T., McDowell, D. and Nelson, J., *Tetrahedron Letters*, 1989, **30**, 7453.

104. Karlin, K. D., Hayes, J. C., Gultneh, Y., Cruse, R. W., McKown, J. W., Hutchinson, J. P. and Zubieta, J., *J. Amer. Chem. Soc.*, 1984, **106**, 2121.

105. Ciampolini, M. and Nardi, N., *Inorg. Chem.*, 1966, **5**, 41.

106. Hay, R. W., Basak, A. K. and Pujari, M. P., *J. Chem. Soc. Dalton Trans.*, 1989, 197.

107. Chin, J. and Jubian, V., *J. Chem. Soc. Chem. Commun.*, 1989, 839.

108. Kimura, E., Shiota, T., Koike, T., Shiro, M. and Kodama, M., *J. Amer. Chem. Soc.*, 1990, **112**, 5805.

109. Jones, R. D., Summerville, D. A. and Basolo, F., *Chem. Rev*, 1979, **79**, 139.

110. Egli, R. A., *Helv. Chim. Acta.*, 1970, **53**, 47.

112. Sheldrick, G. M., in *SHELXTL User Manual* (Nicolet XRD Corporation, Madison, Wisconsin) 1987.

113. *International Tables for X-ray Crystallography*. (Kynoch Press, Birmingham, 1974), vol. 4.

114. H. A. A. Omar (personal communication).

115. Alcock, N. W., Balakrishnan, K. P., Moore, P. and Pike, G. A., *J. Chem. Soc. Dalton Trans.*, 1986, 985.

116. Alcock, N. W., Balakrishnan, K. P., Berry, A., Moore, P. and Reader, C. J., *J. Chem. Soc. Dalton Trans.*, 1988, 1089.

117. Alcock, N. W., Balakrishnan, K. P., Moore, P. and Omar, H. A. A., *J. Chem. Soc. Dalton Trans.*, 1987, 545.

119. Motekaitis, R. J., Martell, A. E., Lehn, J. and Watanabe, E., *Inorg. Chem.*, 1982, **21**, 4253.

120. Martell, A. E., *Acc. Chem. Res.*, 1982, **15**, 155.

121. I. Abrahams (personal communication).

122. Taylor, P. L. and Evans, I. C. I. plc (Paints), 1987.

123. M. S. French (personal communication).

124. Takeuchi, K., Busch, D. H. and Alcock, N. W., *J. Amer. Chem. Soc.*, 1983, **105**, 4261.

125. Lehert, P. G. and Hodgkins, D. C., *Nature*, 1961, **192**, 937.

126. Schrauzer, G. N. and Kohnle, J., *Chem. Ber.*, 1964, **97**, 3656.

127. Halpern, J. and Maher, J. P., *J. Amer. Chem. Soc.*, 1964, **86**, 2311.

128. Schrauzer, G. N., Ribeiro, A., Lee, L. P. and Ho, R. K. Y., *Angew. Chem. Int. Ed. Eng.*, 1971, **10**, 807.

129. Johnson, A. W., Mervyn, L., Shaw, N. and Smith, E. L., *J. Chem. Soc.*, 1963, 4146.

130. Richrock, M. N., Bied-Charreton, C. and Gaudener, A., *Tetrahedron Letters*, 1971, 2859.

131. Schrauzer, G. N. and Holland, R. J., *J. Amer. Chem. Soc.*, 1971, **93**, 4060.

132. Schrauzer, G. N. and Holland, R. J., *J. Amer. Chem. Soc.*, 1971, **93**, 1505.

133. Ochiai, E., Long, K. M., Sperati, R. and Busch, D. H., *J. Amer. Chem. Soc.*, 1969, **91**, 3201.

134. Firth, R. A., Hill, H. A. O., Pratt, J. M., Thorpe, R. G. and Williams, R. J. P., *J. Chem. Soc.*, 1968, **A**, 2428.

135. Dodd, D. and Johnson, M. D., *J. Organomet. Chem.*, 1973, **52**, 1.

136. Halpern, J. and Maher, J. P., *J. Amer. Chem. Soc.*, 1965, **87**, 5361.

137. Schrauzer, G. N. and Windgassen, R. J., *J. Amer. Chem. Soc*, 1966, **88**, 3738.

138. Schrauzer, G. N. and Windgassen, R. J., *J. Amer. Chem. Soc.*, 1967, **89**, 6391.

139. Halpern, J. and Maher, J. P., *J. Amer. Chem. Soc.*, 1964, **86**, 2311.

140. Bartlett, E. H. and Johnson, M. D., *J. Chem. Soc.*, 1970, **A**, 523.

141. Gupta, B. D. and Roy, S., *Inorg. Chem. Acta*, 1988, **146**, 209.

142. Toscano, P. J. and Marzilli, L. G., *Prog. Inorg. Chem.*, 1984, **31**, 105.

143. Comprehensive Organometallic Chemistry , vol. 5.

144. Cozens, R. J., Deacon, G. B., Felder, P. W., Murray, K. S. and West, B. O., *Aust. J. Chem.*, 1970, **23**, 481.

145. Yamano, Y , Masuda, I. and Shinra, K., *Inorg. Nucl. Chem Lett.*, 1969, **5**, 729.

147. Duong, K. N. V., Fontaine, C., Giannotti, C. and Gaudemer, A., *Tetrahedron Letters*, 1971, 1187.

146. Giannotti, C., Septe, B. and Benlian, D., *J. Organomet. Chem*, 1972, **39**, C5.

148. Bakac, A. and Espensen, J. H., *Inorg. Chem.*, 1987, **26**, 4353.

149. Johnson, M. D. and Meeks, B. S., *J. Chem. Soc.*, 1971, **B**, 185.

150. Schrauzer, G. N. and Holland, R. J., *J. Amer. Chem. Soc*, 1971, **93**, 1505.

151. Schrauzer, G. N. and Windgassen, R. J., *J. Amer. Chem. Soc.*, 1967, **89**, 1999.

152. Balakrishnan, K. P., Omar, H. A. A., Moore, P., Alcock, N. W. and Pike, G. A., *J. Chem. Soc. Dalton Trans.*, 1990, 2965.

153. H.A.A. Omar Synthesis and studies of metal complexes of new azamacrocyclic ligands. (PhD Thesis, Warwick University, 1987).

155. Moore, D. S. and Robinson, S. D., *Chem. Soc. Rev.*, 1983, **12**, 415.

156. Evans, D., *J. Phys. Chem.*, 1959, **28**, 2003.

157. Peat, I. R. and Reynolds, W. F., *Tetrahedron Letters*, 1972, **14**, 1359.
158. Boge, E. M., Freyburg, D. P., Kokot, E., Mockler, G. M. and Sim, E., *Inorg. Chem.*, 1977, **16**, 1655.

Appendix.

X-ray Data from crystals $[Zn(L^5)](BF_4)$ and $[Co(L^7)](CF_3SO_3)_2$

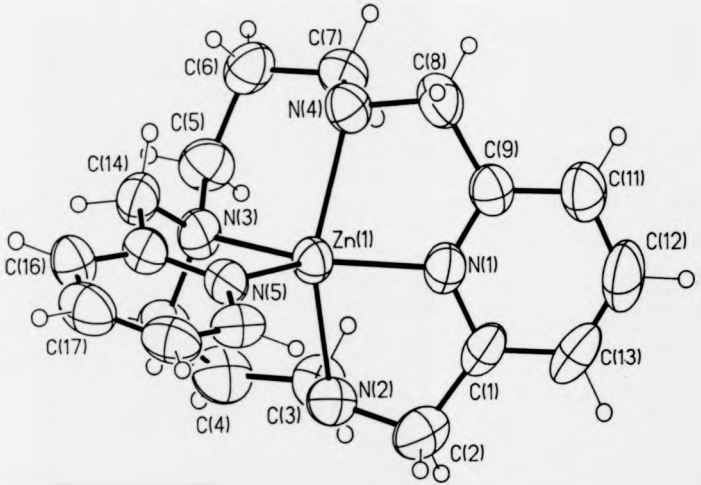
C(7)
C(6)
C(8)
N(4)
C(5)
C(9)
C(14)
C(11)
N(3)
Zn(1)
C(12)
C(16)
N(1)
N(5)
C(17)
C(13)
N(2)
C(1)
C(4)
C(3)
C(2)

TABLE 1. Atom coordinates ($\times 10^4$) and isotropic thermal parameters ($A^2 \times 10^3$)

Atom	x	y	z	U
Zn(1)	9558.7(7)	-299.4(5)	2065.9(5)	43(1)*
B(1)	10559(9)	1164(6)	5020(6)	54(3)*
F(11)	10315(5)	325(4)	5405(4)	82(2)*
F(12)	11403(8)	1612(4)	5507(6)	148(4)*
F(13)	9560(6)	1667(5)	4889(5)	110(3)*
F(14)	11050(9)	1037(5)	4205(5)	138(4)*
B(2)	8631(9)	1919(7)	9417(6)	56(3)*
F(21)	9382(8)	1703(4)	10108(5)	117(3)*
F(22)	8431(7)	1176(5)	8908(5)	111(3)*
F(23)	7542(7)	2203(7)	9693(6)	150(4)*
F(24)	9106(9)	2607(7)	8958(7)	173(5)*
N(1)	11245(5)	-453(5)	2572(4)	49(2)*
N(2)	9221(6)	-1288(5)	3142(4)	55(2)*
N(3)	8241(5)	-871(4)	1225(4)	48(2)*
N(4)	10676(6)	107(4)	912(4)	51(2)*
N(5)	8319(5)	696(4)	2270(4)	46(2)*
C(1)	11405(8)	-936(6)	3326(5)	56(3)*
C(2)	10241(9)	-1246(7)	3767(6)	71(3)*
C(3)	9173(8)	-2178(5)	2633(6)	59(3)*
C(4)	7968(9)	-2305(6)	2168(6)	71(3)*
C(5)	7406(8)	-1454(6)	1761(6)	63(3)*
C(5)	8662(9)	-1404(7)	428(5)	64(3)*
C(6)	9610(9)	-941(6)	-149(5)	61(3)*
C(7)	10793(7)	-700(6)	324(6)	60(3)*
C(8)	11886(7)	408(6)	1275(6)	59(3)*
C(9)	12181(6)	-119(5)	2118(5)	53(2)*
C(11)	13360(7)	-244(8)	2432(6)	70(3)*
C(12)	13520(9)	-728(8)	3210(7)	80(4)*
C(13)	12573(10)	-1076(7)	3651(6)	74(4)*
C(14)	7575(8)	-37(6)	935(6)	58(3)*
C(15)	7409(7)	643(6)	1671(5)	50(2)*
C(16)	6409(7)	1228(6)	1707(6)	62(3)*
C(17)	6367(9)	1877(6)	2395(6)	70(3)*
C(18)	7304(8)	1919(6)	3012(6)	64(3)*
C(19)	8249(8)	1322(5)	2926(5)	55(2)*

* Equivalent isotropic U defined as one third of the trace of the orthogonalised U_{ij} tensor

TABLE 2. Bond lengths (A)

Zn(1)-N(1)	2.018(8)	Zn(1)-N(2)	2.188(9)
Zn(1)-N(3)	2.091(8)	Zn(1)-N(4)	2.198(9)
Zn(1)-N(5)	2.013(8)	B(1)-F(11)	1.375(11)
B(1)-F(12)	1.348(13)	B(1)-F(13)	1.336(12)
B(1)-F(14)	1.344(13)	B(2)-F(21)	1.360(13)
B(2)-F(22)	1.339(13)	B(2)-F(23)	1.333(13)
B(2)-F(24)	1.320(15)	N(1)-C(1)	1.338(11)
N(1)-C(9)	1.326(10)	N(2)-C(2)	1.462(12)
N(2)-C(3)	1.501(11)	N(3)-C(5)	1.485(12)
N(3)-C(5)	1.495(11)	N(3)-C(14)	1.481(11)
N(4)-C(7)	1.471(11)	N(4)-C(8)	1.505(11)
N(5)-C(15)	1.345(10)	N(5)-C(19)	1.339(10)
C(1)-C(2)	1.510(13)	C(1)-C(13)	1.390(14)
C(3)-C(4)	1.510(14)	C(4)-C(5)	1.511(13)
C(5)-C(6)	1.512(13)	C(6)-C(7)	1.522(13)
C(8)-C(9)	1.509(12)	C(9)-C(11)	1.392(12)
C(11)-C(12)	1.371(15)	C(12)-C(13)	1.333(15)
C(14)-C(15)	1.490(12)	C(15)-C(16)	1.393(12)
C(16)-C(17)	1.396(14)	C(17)-C(18)	1.385(14)
C(18)-C(19)	1.361(12)		

TABLE 3. Bond angles (deg.)

N(1)-Zn(1)-N(2)	79.0(3)	N(1)-Zn(1)-N(3)	145.1(3)
N(2)-Zn(1)-N(3)	93.5(3)	N(1)-Zn(1)-N(4)	79.0(3)
N(2)-Zn(1)-N(4)	147.9(3)	N(3)-Zn(1)-N(4)	91.4(3)
N(1)-Zn(1)-N(5)	130.3(3)	N(2)-Zn(1)-N(5)	104.2(3)
N(3)-Zn(1)-N(5)	84.6(3)	N(4)-Zn(1)-N(5)	107.8(3)
F(11)-B(1)-F(12)	109.7(8)	F(11)-B(1)-F(13)	112.7(8)
F(12)-B(1)-F(13)	112.5(8)	F(11)-B(1)-F(14)	109.6(7)
F(12)-B(1)-F(14)	106.1(9)	F(13)-B(1)-F(14)	105.9(8)
F(21)-B(2)-F(22)	110.1(8)	F(21)-B(2)-F(23)	112.6(9)
F(22)-B(2)-F(23)	106.1(9)	F(21)-B(2)-F(24)	109.2(9)
F(22)-B(2)-F(24)	112.4(9)	F(23)-B(2)-F(24)	106.4(9)
Zn(1)-N(1)-C(1)	119.7(5)	Zn(1)-N(1)-C(9)	118.9(5)
C(1)-N(1)-C(9)	121.3(7)	Zn(1)-N(2)-C(2)	108.1(5)
Zn(1)-N(2)-C(3)	101.5(5)	C(2)-N(2)-C(3)	112.7(7)
Zn(1)-N(3)-C(5)	109.5(5)	Zn(1)-N(3)-C(5)	118.0(5)
C(5)-N(3)-C(5)	109.0(7)	Zn(1)-N(3)-C(14)	101.2(5)
C(5)-N(3)-C(14)	108.6(6)	C(5)-N(3)-C(14)	110.2(6)
Zn(1)-N(4)-C(7)	107.6(5)	Zn(1)-N(4)-C(8)	106.9(5)
C(7)-N(4)-C(8)	111.7(6)	Zn(1)-N(5)-C(15)	111.3(5)
Zn(1)-N(5)-C(19)	129.7(5)	C(15)-N(5)-C(19)	118.8(7)
N(1)-C(1)-C(2)	114.3(7)	N(1)-C(1)-C(13)	119.5(8)
C(2)-C(1)-C(13)	126.2(8)	N(2)-C(2)-C(1)	112.8(7)
N(2)-C(3)-C(4)	111.7(7)	C(3)-C(4)-C(5)	116.4(7)
N(3)-C(5)-C(4)	115.5(7)	N(3)-C(5)-C(6)	115.9(7)
C(5)-C(6)-C(7)	115.5(7)	N(4)-C(7)-C(6)	112.7(7)
N(4)-C(8)-C(9)	110.1(7)	N(1)-C(9)-C(8)	116.5(7)
N(1)-C(9)-C(11)	120.3(8)	C(8)-C(9)-C(11)	123.2(7)
C(9)-C(11)-C(12)	118.2(8)	C(11)-C(12)-C(13)	120.9(9)
C(1)-C(13)-C(12)	119.7(9)	N(3)-C(14)-C(15)	112.8(7)
N(5)-C(15)-C(14)	115.9(7)	N(5)-C(15)-C(16)	121.9(7)
C(14)-C(15)-C(16)	122.1(7)	C(15)-C(16)-C(17)	117.9(8)
C(16)-C(17)-C(18)	119.6(8)	C(17)-C(18)-C(19)	118.6(8)
N(5)-C(19)-C(18)	123.2(8)		

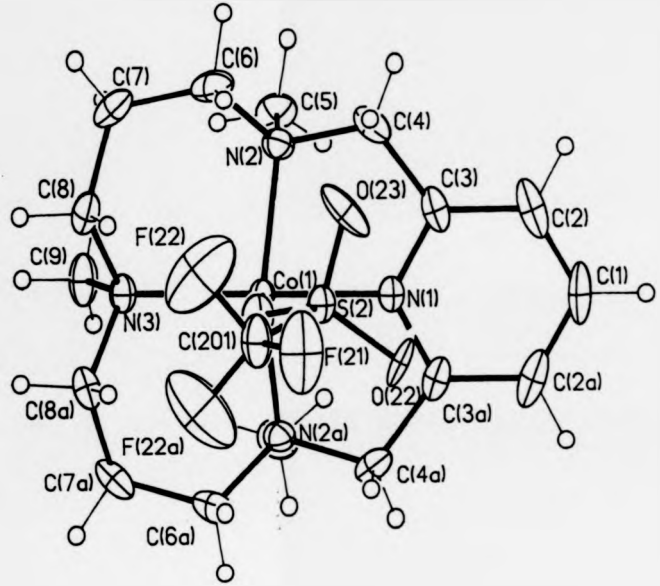
C(7)
C(6)
C(5)
C(4)
N(2)
C(8)
O(23)
C(3)
C(2)
F(22)
C(9)
Co(1)
S(2)
N(1)
C(1)
N(3)
C(201)
F(21)
O(22)
C(2a)
C(8a)
C(3a)
N(2a)
F(22a)
C(4a)
C(7a)
C(6a)

TABLE 1. Atom coordinates ($x10^4$) and isotropic thermal parameters (A^2x10^3)

Atom	x	y	z	U
Co(1)	2773.2(5)	7500.0	-3421.3(6)	35(1)*
S(1)	-71(2)	7500	3217(2)	71(1)*
S(2)	1722.9(12)	7804.9(29)	-1455.8(15)	46(1)*
O(11)	695(4)	7500	2995(9)	117(4)*
O(12)	-327(5)	8668(7)	3644(5)	134(3)*
O(21)	1821(3)	7500	-2439(4)	57(2)*
O(22)	2077(6)	7045(15)	-769(8)	64(6)*
O(23)	1819(6)	9071(13)	-1233(8)	96(4)*
F(11)	-328(5)	8539(8)	1594(5)	179(4)*
F(12)	-1237(5)	7500	2138(8)	161(5)*
F(21)	529(4)	7500	-427(5)	153(5)*
F(22)	432(4)	8413(9)	-1700(7)	212(5)*
N(1)	3480(3)	7500	-2424(4)	42(2)*
N(2)	2990(3)	9445(5)	-3425(3)	51(1)*
N(3)	2043(3)	7500	-4523(5)	47(2)*
C(1)	4534(5)	7500	-1004(6)	84(5)*
C(2)	4264(3)	8641(10)	-1356(5)	82(3)*
C(3)	3720(3)	8638(7)	-2077(4)	55(2)*
C(4)	3291(3)	9774(6)	-2469(5)	65(2)*
C(5)	3601(3)	9683(7)	-4119(5)	70(2)*
C(6)	2343(4)	10317(7)	-3618(6)	73(3)*
C(7)	1910(4)	9984(7)	-4496(5)	73(2)*
C(8)	1534(3)	8676(6)	-4462(4)	59(2)*
C(9)	2410(5)	7500	-5459(6)	71(4)*
C(101)	-507(7)	7500	2082(9)	90(5)*
C(201)	760(5)	7500	-1295(7)	76(4)*

* Equivalent isotropic U defined as one third of the trace of the orthogonalised U_{ij} tensor

TABLE 2. Bond lengths (A)

Co(1)-O(21)	2.188(5)	Co(1)-N(1)	1.885(6)
Co(1)-N(2)	2.018(5)	Co(1)-N(3)	2.024(6)
Co(1)-N(2a)	2.018(5)	S(1)-O(11)	1.399(8)
S(1)-O(12)	1.409(7)	S(1)-C(101)	1.776(13)
S(1)-O(12a)	1.409(7)	S(2)-O(21)	1.430(5)
S(2)-O(22)	1.389(12)	S(2)-O(23)	1.337(13)
S(2)-C(201)	1.757(9)	S(2)-S(2a)	0.621(6)
S(2)-O(22a)	1.164(11)	S(2)-O(23a)	1.943(13)
O(21)-S(2a)	1.430(5)	O(22)-S(2a)	1.164(11)
O(22)-O(22a)	0.927(30)	O(22)-O(23a)	1.388(19)
O(23)-S(2a)	1.943(13)	O(23)-O(22a)	1.388(19)
F(11)-C(101)	1.301(11)	F(12)-C(101)	1.303(15)
F(21)-C(201)	1.290(12)	F(22)-C(201)	1.237(11)
N(1)-C(3)	1.328(7)	N(1)-C(3a)	1.328(7)
N(2)-C(4)	1.487(8)	N(2)-C(5)	1.482(8)
N(2)-C(6)	1.480(8)	N(3)-C(8)	1.504(7)
N(3)-C(9)	1.470(10)	N(3)-C(8a)	1.504(7)
C(1)-C(2)	1.351(10)	C(1)-C(2a)	1.351(10)
C(2)-C(3)	1.404(8)	C(3)-C(4)	1.493(9)
C(6)-C(7)	1.497(10)	C(7)-C(8)	1.490(9)
C(101)-F(11a)	1.301(11)	C(201)-S(2a)	1.757(9)
C(201)-F(22a)	1.237(11)		

TABLE 3. Bond angles (deg.)

O(21)-Co(1)-N(1)	92.7(2)	O(21)-Co(1)-N(2)	98.6(1)
N(1)-Co(1)-N(2)	82.8(1)	O(21)-Co(1)-N(3)	89.3(2)
N(1)-Co(1)-N(3)	178.1(2)	N(2)-Co(1)-N(3)	96.9(1)
O(21)-Co(1)-N(2a)	98.6(1)	N(1)-Co(1)-N(2a)	82.8(1)
N(2)-Co(1)-N(2a)	157.9(3)	N(3)-Co(1)-N(2a)	96.9(1)
O(11)-S(1)-O(12)	114.3(4)	O(11)-S(1)-C(101)	103.0(6)
O(12)-S(1)-C(101)	104.1(4)	O(11)-S(1)-O(12a)	114.3(4)
O(12)-S(1)-O(12a)	115.2(6)	C(101)-S(1)-O(12a)	104.1(4)
O(21)-S(2)-O(22)	119.8(6)	O(21)-S(2)-O(23)	114.9(5)
O(22)-S(2)-O(23)	108.4(8)	O(21)-S(2)-C(201)	101.8(4)
O(22)-S(2)-C(201)	104.8(6)	O(23)-S(2)-C(201)	105.4(5)
O(21)-S(2)-S(2a)	77.5(1)	O(22)-S(2)-S(2a)	56.1(6)
O(23)-S(2)-S(2a)	164.5(5)	C(201)-S(2)-S(2a)	79.8(1)
O(21)-S(2)-O(22a)	140.1(6)	O(22)-S(2)-O(22a)	41.4(13)
O(23)-S(2)-O(22a)	67.0(9)	C(201)-S(2)-O(22a)	116.4(6)
S(2a)-S(2)-O(22a)	97.6(7)	O(21)-S(2)-O(23a)	86.1(4)
O(22)-S(2)-O(23a)	45.6(7)	O(23)-S(2)-O(23a)	153.9(9)
C(201)-S(2)-O(23a)	83.8(4)	S(2a)-S(2)-O(23a)	10.6(4)
O(22a)-S(2)-O(23a)	87.0(8)	Co(1)-O(21)-S(2)	135.0(3)
Co(1)-O(21)-S(2a)	135.0(3)	S(2)-O(21)-S(2a)	25.1(2)
S(2)-O(22)-S(2a)	26.3(4)	S(2)-O(22)-O(22a)	56.1(6)
S(2a)-O(22)-O(22a)	82.4(7)	S(2)-O(22)-O(23a)	88.8(8)
S(2a)-O(22)-O(23a)	62.5(8)	O(22a)-O(22)-O(23a)	144.9(7)
S(2)-O(23)-S(2a)	4.9(2)	S(2)-O(23)-O(22a)	50.5(7)
S(2a)-O(23)-O(22a)	45.6(6)	Co(1)-N(1)-C(3)	119.3(3)
Co(1)-N(1)-C(3a)	119.3(3)	C(3)-N(1)-C(3a)	121.5(6)
Co(1)-N(2)-C(4)	106.7(4)	Co(1)-N(2)-C(5)	107.6(4)
C(4)-N(2)-C(5)	107.2(5)	Co(1)-N(2)-C(6)	116.1(4)
C(4)-N(2)-C(6)	108.1(5)	C(5)-N(2)-C(6)	110.7(5)
Co(1)-N(3)-C(8)	110.1(3)	Co(1)-N(3)-C(9)	113.7(5)
C(8)-N(3)-C(9)	108.6(4)	Co(1)-N(3)-C(8a)	110.1(3)
C(8)-N(3)-C(8a)	105.5(6)	C(9)-N(3)-C(8a)	108.6(4)
C(2)-C(1)-C(2a)	118.6(9)	C(1)-C(2)-C(3)	120.6(8)
N(1)-C(3)-C(2)	119.4(6)	N(1)-C(3)-C(4)	112.1(5)
C(2)-C(3)-C(4)	128.3(7)	N(2)-C(4)-C(3)	110.1(5)
N(2)-C(6)-C(7)	114.6(6)	C(6)-C(7)-C(8)	114.0(6)
N(3)-C(8)-C(7)	116.0(5)	S(1)-C(101)-F(11)	111.6(7)
S(1)-C(101)-F(12)	112.4(10)	F(11)-C(101)-F(12)	106.0(8)
S(1)-C(101)-F(11a)	111.6(7)	F(11)-C(101)-F(11a)	108.8(11
F(12)-C(101)-F(11a)	106.0(8)	S(2)-C(201)-F(21)	115.6(7)
S(2)-C(201)-F(22)	105.6(5)	F(21)-C(201)-F(22)	106.7(7)
S(2)-C(201)-S(2a)	20.3(2)	F(21)-C(201)-S(2a)	115.6(7)
F(22)-C(201)-S(2a)	122.3(7)	S(2)-C(201)-F(22a)	122.3(7)
F(21)-C(201)-F(22a)	106.7(7)	F(22)-C(201)-F(22a)	97.5(10
S(2a)-C(201)-F(22a)	105.6(5)		